Republic of Iraq

Ministry of Higher Education

and Scientific Research

University of Babylon

College of Science/Department of Physics

Study of Nonlinear Optical Properties for PMMA Polymer Doped with MG Dye and Cu Nanoparticles

A Thesis

Submitted to the Council of Physics Department /College of Science, University of Babylon in Partial Fulfillment of the Requirements for the Degree of Master of Science in Physics

By

Israa Kadhim Abdulridha Nasir

B.Sc. in Physics 2006

Supervised by

Prof . Dr.
Ban Ali Naser Ghalib

2022 A.D. **1444 A.H.**

جمهورية العراق

وزارة التعليم العالي والبحث العلمي

جامعة بابل

كلية العلوم / قسم الفيزياء

دراسة الخواص البصرية اللاخطية لبوليمر PMMA المشوب بصبغة ميليكات الخضراء وجسيمات النحاس النانوية

رسالة مقدمة إلى

مجلس قسم الفيزياء – كلية العلوم – جامعة بابل وهي جزء من متطلبات

نيل درجة الماجستير في العلوم/ الفيزياء

من قبل

اسراء كاظم عبد الرضا ناصر

بكالوريوس علوم فيزياء/ ٢٠٠٦

بإشراف

الأستاذ الدكتورة

بان علي ناصر غالب

١٤٤٤ هـ

٢٠٢٢ م

﴿اللَّهُ نُورُ السَّمَاوَاتِ وَالْأَرْضِ مَثَلُ نُورِهِ كَمِشْكَاةٍ فِيهَا مِصْبَاحٌ الْمِصْبَاحُ
فِي زُجَاجَةٍ الزُّجَاجَةُ كَأَنَّهَا كَوْكَبٌ دُرِّيٌّ يُوقَدُ مِن شَجَرَةٍ
مُّبَارَكَةٍ زَيْتُونِةٍ لَّا شَرْقِيَّةٍ وَلَا غَرْبِيَّةٍ يَكَادُ زَيْتُهَا يُضِيءُ وَلَوْ لَمْ تَمْسَسْهُ نَارٌ
نُّورٌ عَلَى نُورٍ يَهْدِي اللَّهُ لِنُورِهِ مَن يَشَاءُ وَيَضْرِبُ اللَّهُ الْأَمْثَالَ
لِلنَّاسِ وَاللَّهُ بِكُلِّ شَيْءٍ عَلِيمٌ﴾

صدق الله العلي العظيم

سورة النور: الآية (٣٥)

Supervisor Certification

I certify that this thesis is titled (**Study of Nonlinear Optical Properties for PMMA Polymer Doped with MG Dye and Cu Nanoparticles**) was prepared by (**Israa Kadhim Abdulridha Nasir**) under my supervision at Department of Physics, College of Science, University of Babylon, as a partial fulfillment of the requirements for Master Degree in Physics.

Signature:

Supervisor: **Dr. Ban Ali Naser Ghalib**

Title: Professor

Address: Department of Physics - College of Science -

University of Babylon

Date: / / 2022

Certification of the Head of the Department

In view of the available recommendation, I forward this thesis for debate by the examination committee.

Signature:

Name: Dr. Samira Adnan Mahdi

Title: Assistant Professor

Address: Head of Department of Physics - College of Science -

University of Babylon

Date: / / 2022

Dedications

To

Whom absent from my world and present in my heart my father and my brothers

(may God have mercy on them)

My Family

With my love and respect

My Professor

With my grateful for her teaching

My Friends

For their kindness, Attention and encouragement

ISRAA

Acknowledgments

First of all, I should thank my **God (Allah)** for helping me in completing my thesis, prayer and peace be upon the best of his creation **Mohammed** and his progeny and companions.

I would like to express my thanks and gratitude to supervisor ***Prof. Dr. Ban Ali Naser*** for suggesting the topic of the thesis, continuous advice and her guidance throughout this work. I am grateful to the department of physics for providing the necessary facilities and help. Special thanks to ***Prof. Dr. Abdulazeez O. Mousa*** for providing the necessary facilities and help.

. I would like to express my great and special thanks to ***Prof. Dr. Talib Mohsin*** in Physics Department / College of Education for Pure Sciences / University of Babylon, for his assistance.

Finally, my great thanks and respect to all who help me.

ISRAA

Summary

The present research includes studied the spectral, linear and nonlinear optical properties for Malachite green (MG) organic laser dye doped with PMMA polymer and Cu nanoparticles for used its application as a nonlinear optics.

In this work, solutions of Malachite green organic laser dye dissolved in chloroform solvent have been prepared, at concentrations (2, 4, 6 and 8) $\times 10^{-5}$ M at room temperature, also thin films have accomplished. The effect of laser power on the nonlinear optical properties for all prepared samples have studied. MG laser dye have been characterized using Fourier Transform Infrared (FT-IR).

The linear optical properties for all prepared samples have been studied as well as the absorption and transmission spectra using UV-Vis spectrophotometer for different concentrations of dye dissolved in chloroform solvent. The results showed when the concentrations increased the absorbance also increased for the same wavelength. The opposite relationship was observed for transmittance. The spectral optical properties of all the prepared samples have been studied using fluorescence spectrometer.

The nonlinear tests measurements have used (Z- scan) technique in two configuration (Close aperture) and (Open aperture) in order to determine the nonlinear refractive index (n_2) and nonlinear absorption coefficient (β) respectively. The measurements were performed using (CW) diode pumped solid state laser (457 nm) wavelength, at different laser powers (70,84 and 102) mW.

The results have showed increasing in nonlinear refractive index and decreasing in nonlinear absorption coefficient with increasing laser powers, for all prepared samples.

The results also have showed increasing of nonlinear refractive index while decreasing of nonlinear absorption coefficient with increasing concentrations for all samples of organic laser dye .

Thin films have better spectral, linear and nonlinear optical properties than solutions. The samples prepared from dye doped with polymer and nanoparticles have better spectral, linear and nonlinear optical properties compared to samples prepared from pure dye.

The results indicate that the optical power limiting threshold is inversely related to the solution concentration. The prepared thin films of laser dye doped with PMMA polymer and Cu nanoparticles give spectral, linear and nonlinear optical parameters high than pure dye. The highest value of the quantum efficiency (95%) and the highest value of the nonlinear refractive index and the nonlinear absorption coefficient (13.997×10^{-3} cm^2/mW) and (3.583 cm/mW) were obtained respectively.

The results indicate that all samples of pure and doped dye (solutions and thin films) could be employed as a suitable medium for a variety of optoelectronic applications, including optical power limiting and active laser medium in liquid lasers.

Contents

List of Symbols

Symbol	Description
A	Absorbance
a_{RB}	The area under the fluorescence curve of Rhodamine B
a	The area under the fluorescence curve of the chemical
α	Absorption coefficient
α_o	Linear absorption coefficient
B	Magnetic field
β	Nonlinear absorption coefficient
C	Concentration
C_1	Primary concentration
C_2	New concentration
D	Donor
d	The distance from focal plane to the aperture plane
E	Electric field
f	Focal length of lens
$F(\bar{v})$	Molecular florescence spectrum
$h\upsilon$	The photon energy
h	Plank's constant
I_o	The intensity at the focal spot
I_A	Intensity of the absorbed beam
I_F	Fluorescence intensity
I_R	Intensity of the reflected beam
I_T	Intensity of the transmitted beam
K_{ET}	The energy transfer rate constant
k	wave number
K_{FM}	probability of radiation transition

Symbol	Description
K_F	Total probability of transition
K_d	Rate constants for non-radioactive processes
K_{IC}	The rate of inter conversion
K_{ISC}	The rate of intersystem crossing
L_{eff}	The effective length of the sample
L	The sample length
M_W	Molecular weight
n_o	Linear refractive index
n_2	The nonlinear refractive coefficient
p	Polarization
$P^{(1)}$	The linear polarization
$P^{(2)}$	The second nonlinear polarization
$P^{(3)}$	The third order nonlinear polarization
P(I)	The power of the transmitted laser beam
$P(I)_{ref}$	Power of the reference laser beam
P_{peak}	The peak power of the laser pulse
R(z)	Radius of curvature of the beam
S_{00}	Ground state
S_{1n}	Higher vibrational level
S_{2n}	Second excited singlet state
S_1	First excited state
S_2	Second excited state
T	Transmittance
T_1	Triplet excited state
T_n	Triplet state
T(z)	The minimum value of normalized transmittance

Symbol	Description
T_g	Glass transition temperature
t	Thickness of Samples
τ	Lifetime
V	Volume of the solvent
V_1	Volume before dilution
V_2	Volume after dilution
$\bar{\nu}^2 max$	The dye solution's highest wave number
$\bar{\nu}$	Wave number
w	Spot size
W	Weight
χ	The electric susceptibility
$\chi^{(1)}$	The linear susceptibility
$\chi^{(2}$	The second order nonlinear susceptibility
$\chi^{(3)}$	The third order nonlinear susceptibility
Z	The distance between the focal plane in free space and the center of the sample
Φ_F	Quantum yield of fluorescence
$\Delta\Phi_o$	The nonlinear phase shift,
$\theta_\circ$	The laser beam's divergence angle
w_o	The beam radius at the focal point
λ	Wavelength

List of Abbreviations

Abbreviation	Full Name
AL_2O_3	Aluminum oxide
Cu	Copper
CW	Continuous wave
DFDL	Distributed feedback dye laser
DPSS	Diode pump solid state laser
DMSO	Dimethyl sulfoxide
FT-IR	Fourier transforms infrared spectrometer
HeNe	Helium-Neon
IR	Infrared
MG	Malachite green dye
Na Fl	Fluorescein Sodium
Nd:YAG	Neodymium-doped Yttrium Aluminum Garnet
NLA	Nonlinear absorption
NLO	Nonlinear optics
NLR	Nonlinear refraction
O_2	Di oxygen
O_3	Tri oxygen
SA	Saturation of absorption
PAA	polyacrylamide hydrogel
PD	Photo Detector
PLA	polylactide
PMMA	Poly methyl methacrylate
Ps	Porous silica
PVA	poly polyvinyl alcohol
PVP	polyvinylpyrrolidone

Abbreviation	Full Name
RB	Rhodamine B
RSA	Reverse saturable absorption
SiO_2	Silicon dioxide
SSL	Solid – state laser
TiO_2	Titanium dioxide
TPA	Two Photons Absorption
UV	Ultra violet

List of Figures

List of Tables

Chapter One

General Introduction

1.1 Introduction

Nonlinear optics (NLO) have been the subject of many investigations theoretically and experimentally during recent years due to their applications in many branches. The nonlinear optical properties are important parameters in characterizing and determining the applicability of any material to nonlinear optical device. There are several techniques for measuring these parameters like Z-scan technique, degenerate four waves mixing and third harmonic generation [1]. Nonlinear optics are "nonlinear" in the sense that they occur when the response of a material to an applied optical field depends in a nonlinear manner upon the strength of the optical field [2].

Organic dyes are large molecular weight fluorescent chemicals having a strong absorption band in the visible range of the electromagnetic spectrum. Only organic molecules with an extended system of conjugated bonds alternating single and double bonds have this property [3]. These molecules are dissolved in an organic solvent or combined into a solid matrix in a dye laser. Although dyes get shown to laser in the solid, liquid, and gas phases, dyes have made one of most impact as laser media in the liquid and solid phases [4].

Dye lasers are active sources of coherent tunable radiation because of their unique operational flexibility. The important characteristics of dye lasers are their tunability, with emission from near ultraviolet to the near infrared [5]. Because of the big nonlinear characteristics for this organic dyes, fast response, and excellent stability into optical devices. Organic

dyes are one of the materials that play an essential role in the nonlinear optics area [6].

Dye doped polymers have applications in many fields of modern photonic technology, optical amplifiers, fiber optics, and optical limiting which is used for protecting the human eye and the sensors by handling the laser output [7]. Polymers have also contributed to the advancement of solid state dye laser systems. Polymeric composites have been discovered to exhibit optical characteristics that make them suitable as laser hosts for organic dyes [8].

Poly methyl methacrylate (PMMA) is the most frequently used host for laser dye due to its excellent optical transparency and its relatively high laser damage resistances [9]. Nanotechnology represents one of the greatest inventions of modern science, enabling materials of distinctive size, structure and composition to be formed. For the smaller particles the percentage of surface atoms increases, leading to changes in physical and chemical properties of the materials. PMMA composite thin films are modulated and improved by addition of Cu nanoparticles and those properties can be applied in the fields of optics and electronics [10].

The nonlinear properties of dyes solutions, dyes doped polymer thin films and Cu nanoparticles composite can be studied by Z-scan technique [11]. It is a sensitive and popular experimental method to measure intensity dependent of NLO properties of materials which can rapidly measure both nonlinear absorption (NLA) and nonlinear refraction (NLR) in solids, liquids and then studying the optical limiting behavior [12].

Optical limiters are devices that make use of organic materials. They are used to protect the eyes and sensors. An optical limiter, in an ideal world, would transmit light linearly at low incident light but become opaque at high incident light [13].

1.2 Literature Survey

Several researches of spectral, linear and nonlinear properties by using Z-scan for study nonlinear properties in organic dyes.

In (2012) **H. Shaaker *et al.*** [14], have studied optical properties and spectral behavior for pure and doping thin films of Malachite green dye. The result showed that the refractive index and absorption index are independent of film thickness and the nonlinear optical properties and nonlinear refractive index are sensitive to the wavelength of light and doping materials.

In (2012) **R. Manshad and Q. Hassan** [15], have studied nonlinear optical properties to determine the nonlinear optical properties of the Orcein dye in chloroform solvent and a dye doped PMMA polymer film. The experiments were performed using continuous wave (CW) laser with a wavelength of (532) nm. This material exhibits negative optical nonlinearity. The open aperture Z-scan data of nonlinear optics materials in solution and thin film sample displayed two photon absorption and saturable absorption, respectively.

In (2013) **V. Sukumarana and A. Ramalingamb** [16], have investigated the spectral characteristics and the nonlinear optical properties of Malachite green dye doped in PMMA polymer. The experiments were performed using CW (He-Ne) laser at (632.8) nm. Analysis of nonlinearity of Malachite green dye showed (self-defocusing) nonlinearity in the Z-scan experiment is a signature of negative nonlinearity

In (2013) **M. Rusal *et al*** [17], have studied nonlinear properties of PMMA films before and after the addition of the filler by using Z-scan. The results show that increase the nonlinear optical properties in the PMMA/copper matrix more than in the unmodified PMMA/copper matrix. The nonlinear refractive index is directly proportional to the input

intensity while the nonlinear absorption coefficient is inversely proportional to the input power.

In (2014) **H. Kitching *et al.*** [18], have studied the interaction of gold and silver nanoparticles with Malachite green (MG) dye. The result of UV-Vis spectrum have showed only a small peak at (685) nm of Malachite green dye doped with gold nanoparticles while for pure MG dye was found at (617) nm in relative proximity to the aggregate peak ,these effects were not observed with silver nanoparticles .

In (2015) **L. Guru** [19], researched the nonlinear optical applications for Malachite green dye doped with polymer (PVA) as a film. FT-IR spectra were recorded in a range of (4000 - 400) cm^{-1}. In this study (C=N) bond vibrations show a peak near to (1173) cm^{-1} but single bond (C-N) show a peak in the range of (1120-1140) cm^{-1}. This vibrational band appears at (1155 and 1070) cm^{-1} and confirms the presence of single bond (C-N) group. Similarly, stretching vibration of (C-NH_2) bond sketches the peak at (1300) cm^{-1} and in this study, the vibrational peak is observed at (1335) cm^{-1}.

In (2015) **J. Worood** [20], have used Z-scan method to study optical properties of Acridine dye doped in PMMA polymer and alumina nanoparticles, using a pulsed Nd:YAG laser with a wavelength of (532) nm. The results indicates the samples show high nonlinear optical properties, negative nonlinear refractive index (self-defocusing) and two photon absorption for nonlinear absorption coefficient and it was found out that the Acridine dye doped with PMMA and Al_2O_3 nanoparticles could best be active medium as dye lasers.

In (2016) **I. Hussein and S. Abdulkareem [**21], have studied the nonlinear optical characteristics of Giemsa dye in chloroform solvent at various concentrations, a continuous wave (CW) low power solid-state

laser (SSL) operating at a wavelength of (532 nm) as an excitation source as well as dye mixed with PMMA as a dye-doped polymer film. The obtained results indicate that in addition to negative nonlinear refraction, Giems dye exhibits positive nonlinear saturable absorption (SA) and negative nonlinear refraction.

In (2017) **K. Lamyaa** [22], have been prepared thin film of Rhodamine B dye and TiO_2 nanoparticles doped in PMMA polymer by a casting method. The nonlinear optical properties were measured by Z-scan technique using Nd:YAG laser with (1064 nm) wavelength. The nonlinear refractive index (n_2) and nonlinear absorption coefficient (β) were estimated for the thin film for different energies of the laser, (n_2) and (β) were decreased with increasing intensity of incident laser beam. Also, the type of (β) was two-photon absorption and (n_2) negative nonlinear reflective.

In (2018) **H. Imad Al-Deen *et al*.** [23], have prepared Celestin blue B dye doped PMMA polymer film at different concentrations were using casting technique. The nonlinear optical properties and optical power limiting behavior of Celestin blue B dye-doped polymer films have been studied using the Z-scan technique with a continuous wave laser beam at wavelength (532) nm. The experimental results showed that the dye - doped polymer film has a large optical nonlinearities. It is found that the optical power limiting depends on the dye concentration and possesses low optical power limiting threshold.

In (2019) **R. Mohammad *et al*.** [24], have studied spectral and linear optical properties of Malachite green dye. The values of absorption and refraction coefficient decrease as the concentration of the solution decreases and the decreasing in concentration of the dye solution leads to

decrease in the intensity of the fluorescence spectra and the shift of its top spectra to short wavelengths (blue shift) in different solvent.

In (2019) **T. Noor Al-huda** [25], have prepared organic laser dye doped with PMMA polymer and silver nanoparticle. The structural, spectral ,linear and nonlinear optical properties were studied. The measurements performed using diode pump solid state laser operating at (457) nm wavelength. The results showed that increasing of the nonlinear refractive index when increasing concentrations but decreasing of nonlinear absorption coefficient, when increasing concentrations for all prepared samples

In (2020) **A. Jassim *et al*.** [26], have studied the optical properties of Malachite green dye as solution and films prepared by casting method. Were found two transitions wavelengths (428,622) nm when dye is dissolved in ethanol and (435,646) nm when preparing films. Linear optical properties were studied for the three concentrations and it was found increased absorption coefficients and refractive index by rising concentration.

In (2020) **S. Bashair** [27], have investigated organic dyes as liquid , pure dyes as thin films, pure dyes doped with Poly methyl methacrylate (PMMA) and pure dyes doped PMMA with titanium dioxide nanoparticles (TiO_2) to study the linear and nonlinear optical properties. The result show possibility of using the dyes (solution and thin films) as good optical limiting. The best result is achieved from pure dye as thin film for nonlinear parameters n_2 and (β) and optical limiting , it can be seen that all samples have a good nonlinear properties and can be used as photo device or as optical limiting. The properties of optical limiting for thin films of dyes are better than of dyes as solutions.

In (2021) **J. Shymaa** [28], have researched Rhodamine B dye as a laser active medium. The result show increasing the linear optical parameters (α_o and n_o) of the dye solution with increasing concentration. The experimental data of nonlinear optical properties of dye solution at different concentrations show self-defocusing phenomena and a negative nonlinear refractive index, as well as a two-photon absorption coefficient, indicating that the sample could be useful in nonlinear optical devices.

In (2022) **O. Muller *et al.*** [29], have studied the optical limiting behavior of a series of polymer-dye nonlinear nanocomposites, combined azophloxine, a red azo dye, with two polymer hosts, namely poly methyl methacrylate (PMMA) and polylactide (PLA).Investigation the nonlinear absorption coefficients and refractive indices were measured by the Z-scan method. Optical measurements in the nonlinear method were performed at the wavelength of (1064 nm) with nanosecond pulses at a low pulse repetition rate.

1.3 Aims of the Work

The main aims of this research are as the following steps :

1. Study spectral , linear and nonlinear optical properties for Malachite green dye organic laser dye dissolved in chloroform solvent at different concentrations .
2. Preparing thin films of Malachite green dye doped with PMMA polymer and Cu nanoparticles using drop casting method .
3. Study the effect of adding PMMA polymer and Cu nanoparticles on spectral, linear and nonlinear optical properties of Malachite green dye.
4. Possibility of using all samples of organic dye as active laser medium and optical limiting.

Chapter Two

Theoretical Part

2.1 Introduction

This chapter defines laser dyes, dyes calssification, applications of organic laser dyes, organic hosts (Polymers), nanoparticles, fluorescence spectra characteristics, fluorescence quantum efficiency, laser beam characteristics, laser light interaction with matter, optical properties, linear and nonlinear optical properties, Z-scan technique and optical limiting.

2.2 Laser Dyes

Laser dyes are large molecules with molecular weights of few hundred mu. When one of these molecules is dissolved in a suitable liquid solvent (such as ethanol, methanol or water) it can be used as laser medium in a dye laser. Generally, laser dyes are complex molecules containing a number of ring structures, which lead to complex absorption and emission spectra. The laser dyes can be classified into different classes by virtue of their structures that are chemically similar. Common examples are the coumarins, xanthenes and poly methenes as in Figure (2.1) [30].

Laser dyes can be used to span continuously the emission spectrum from the near ultraviolet to the near infrared. Laser dyes, either as solutions or solid, are the active medium in pulsed and CW dye lasers as well as ultra-shorter pulse with passive mode-locking. Thus a variety of dyes is necessary to cover the entire spectral range [31]. Dye molecules are used mostly to generate tunable laser. The basic absorption processes in laser dyes could be divided into linear and nonlinear absorption, the nonlinear have two parts:saturation of absorption (SA) and reverse saturable absorption (RSA). Saturation of absorption is vital for use of the dyes in mode locking [32].

The most important application of (RSA) is for optical limiting devices that protect sensitive optical components, including human eye from laser induced damage. Laser dyes are promising compounds for nonlinear optical applications because they exhibit strong nonlinear optical behavior**.** For effective performance, laser dyes molecules should have the following characteristics [33]:

1. Strong absorption at excitation wavelength and minimal absorption at lasing wavelength.
2. High quantum yield (0.5-1.0) .
3. Good photochemical stability.
4. A short fluorescence lifetime (5-10) ns.
5. Low probability of intersystem crossing to the triplet state.
6. Laser dyes have to be very pure since impurities frequently quench the laser output.

By appropriate dye selection it is possible to produce coherent light of any wavelength from (320 to 1200) nm. The approximate working ranges of various laser dyes are shown schematically as in Figure (2.1).

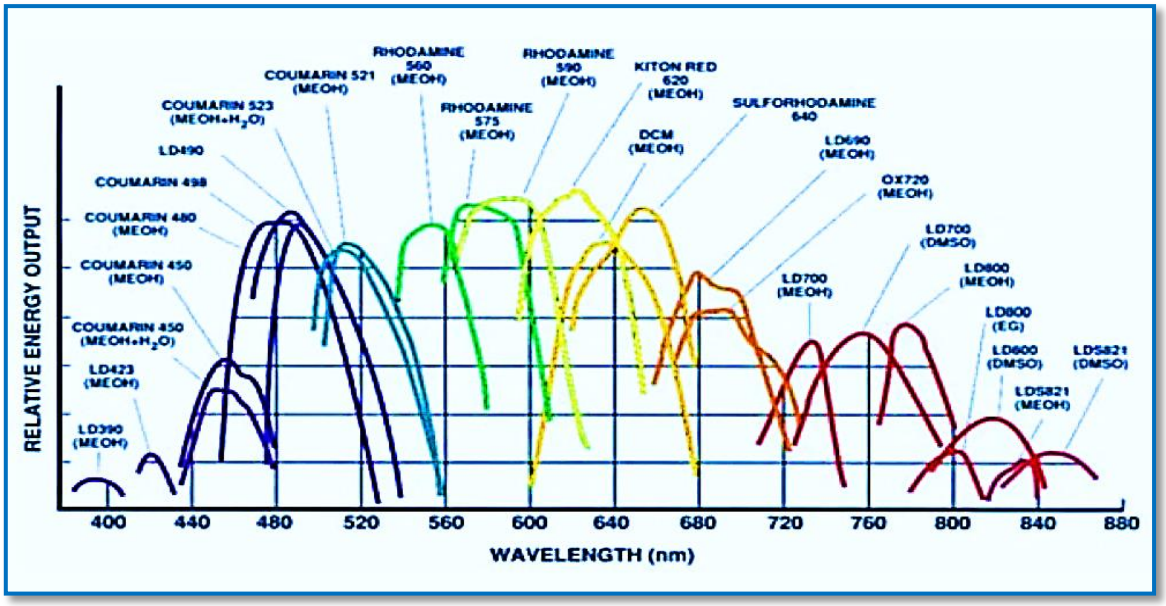

Figure (2.1) : Laser Dyes [34].

2.3 Dyes Classification

Normally, dyes are classified in two separate ways, either accordance to their chemical structure or according to the method of application. Around thirty different groups of dyes can be discerned based on chemical structure. Organic dyes are one of most used in dye laser and classified according to their chemical structure into [35]:

1. Poly methane dyes: gives a laser action in near IR (0.7-1.5) μm.
2. Xanthene dyes: gives a laser action in visible region (500-700) nm.
3. Coumarin dyes: gives a laser action in blue – green region (400- 500) nm.
4. Scintillator dyes: gives a laser action in UV-region ($\lambda <$ 400 nm).

Xanthene dyes are important dyes because of having strong optical absorption, long phosphorescence life time and number of double bonds, It is cover the wavelength region from (500 to 700) nm. Xanthene dyes divided into two main classes (rhodamines, fluorescein). Another important advantage is actually that they are comparatively easy for manufacture, without complicated purifications, not like most other dyes [36].

2.4 Applications of Organic Laser Dyes

There are many applications of laser organic dyes [37]:

1- Industrial applications of laser dyes include separation of isotopes of important radioactive elements such as uranium. Uranium is used as fuel in the nuclear power reactors to generate electricity.

2- Medical applications of laser dyes include skin treatments, including tattoo removal, diagnostic measurements, activation of photosensitive drugs for photodynamic therapy; etc. In the field of medical applications, dye lasers have potential advantages over other lasers. Dye lasers are unique sources of tunable

coherent radiation, from the ultraviolet to the near infrared. The medical applications of dye lasers are some of the most important clinical applications.

3- Optical communications.

4- Image processing.

5- Switching.

6- 3D data storage and optical limiting.

2.5 Organic Laser Dye (Malachite Green)

Malachite green is an organic compound that classified in the dyestuff industry as a triarylmethane dye and also using in pigment industry , this dye is used as a direct dye for silk, wool, and to dye cotton that has been mordanted with tannin. Prepared from benzaldehyde and dimethylaniline, the dye occurs as lustrous green crystals soluble in water and in alcohol [38]. Malachite green refers to the chloride salt, although the term malachite green is used loosely and often just refers to the colored cation. There was another type of Malaghite green (oxalate salt) is also marketed. The anions have no effect on the color, the intense green color of the cation results from a strong absorption band at (621) nm. Malachite green is a xanthine dye. The intense color of this ion is caused by the extended conjugated system its used medicinally in solution as a local antiseptic. Malachite green is used as an active laser medium, effective against fungi and bacteria. Malachite green has frequently been used to catch thieves and pilferers [39].

2.6 Organic Hosts (Polymers)

The name polymer is derived from the Greek word, in which the first word "Poly" means multiple and the second one "mer" means part. The polymer has a synonym word "macromolecule". The building block unit of the polymer is the monomer. Polymers are macromolecules composed of repeated units (monomer), and sometimes these units are repeated linearly and the chain is formed by

connecting these units or the chains to form branches or they are interconnected [40]. The polymer chain length is determined by the number of the repeated unites (monomer) in the chain and it is called the degree of polymerization. Its molecular weight is equal to the product of the molecular weight of the monomer by the degree of polymerization. One of the important characteristics of polymers is their high molecular weight. Atoms are bonded together in the polymer chain by strong covalent bonds, and are attracted by very weak internal forces [41]. The polymer is called "homopolymer" if the repeated units are the same whereas the polymer formed of different units is called "co-polymer" or "mixed polymer". The polymer is said to be "ordered" if its monomers repetition is constant. However if any reduction occurs to the arrangement of the monomers, the polymer becomes "Amorphous" [42].

2.6.1 Classification of Polymer

Polymers can be classified according to molecular structure to four types as shown in Figure (2.2) [43]:

a- Linear polymers. b- Branched polymers.

c- Cross linked polymers. d- Network polymers.

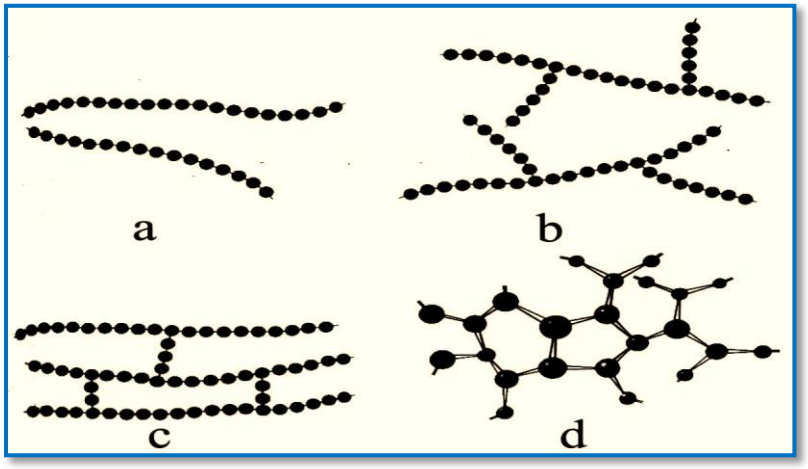

Figure (2.2) Types of polymers :- (a) Linear (b) Branched (c) Cross linked (d) Network [46].

2.6.2 Poly Methyl Methacrylate (PMMA)

This polymer, whose name is often abbreviated to PMMA, is the most important of the commercial acrylic polymers. These polymers are formally derived from poly (acrylic acid), [—$CH_2CH(CO_2H)$—]n. In the case of PMMA, this derivation can be thought of as coming about by replacement of the tertiary hydrogen atom by a methyl group, CH_3, and by esterification of the carboxylic acid group with methanol, CH_3OH [44]. At room temperature, PMMA is a hard, fairly rigid material. When heated above its glass transition temperature (T_g=105) $^{\circ}$C, it is a tough, pliable, and extensible material that is easily bent of formed into complex shapes and that can be molded or extruded [45]. The optical properties of poly methyl methacrylate are particularly important. PMMA absorbs very little light but there is about 4% reflection at each polymer air interface for normal incident light through a parallel sheet of acrylic material is about 92%. It can also serve as a conduct for light. The main applications for PMMA arise from the combination of its transparency and its good outdoor weathering properties [46].

2.7 Nanoparticles

Nanoparticle has a size range between (1 to 100) nm. Unexpected physical and chemical behavior of matter occurs at the nanometer scale, paving the way for a number of scientific exploitations, making nanoparticles a great area of scientific research. The transition from microparticles to nanoparticles yields dramatic changes in all properties. Nanoscale materials have a large surface area for a given volume. Many important chemical and physical interactions are governed by surfaces and surface properties. Nanostructures material can have substantially different properties from a larger-dimensional material of the same composition [47].

In nanomaterial, the surface area per unit volume is inversely proportional to the material's diameter, thus, the smaller diameter, the greater surface area per unit volume, change in particle diameter, layer thickness, or fibrous material diameter from the micrometer to nanometer range, will affect the surface area to the volume ratio by three orders of magnitude generally, there are different approaches for a classification of nanomaterials, the main classes of nanoscale structures can be classified by dimensions, some of which are summarized in Table (2.1) [48]. Also can be shown in Figure (2.3).

Table (2.1) Classification of Nanomaterials by Dimension [49].

Dimension	Example
0 dimension <100 nm	Particles , quantum dots
1 dimension <100 nm	Nanotubes, Nanowire, Nanorods
2 dimension <100 nm	Thin films,Coatings, Multilayers
3 dimension <100 nm	Nanometar-sized cluster

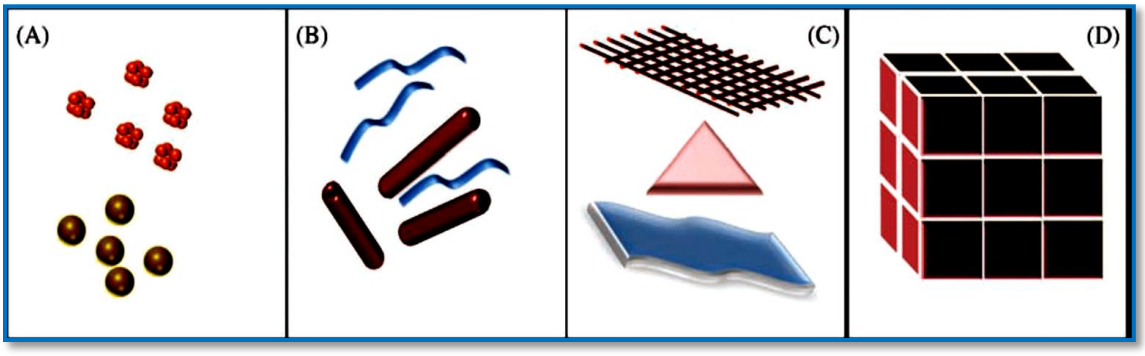

Figure (2.3) : Various Kinds of Nanomaterials. (A) 0D spheres and clusters.(B) 1D nanofibers, wires, and rods. (C) 2D films, plates, and networks. (D) 3D nanomaterials [49].

2.7.1 Copper Nanoparticle (Cu NPs)

Copper nanoparticles (Cu NPs) are very attractive due to their heat transfer properties such as high thermal conductivity. Cu NPs also have high surface area to volume ratio, low production cost, antibacterial potency, catalytic activity, optical and magnetic properties as compared to precision metals such as gold, silver or palladium. The main difficulty lies in their preparation and preservation as they oxidized immediately when exposed in air. Scientists are using different inert media such as Argon, Nitrogen [50].

2.7.2 Applications of Copper Nanoparticle

Copper nanoparticles are being used in numerous technologies and incorporated into a wide array of consumer products the applications of copper nanoparticles are listed below [51]:

- Acts as an anti-biotic, anti-microbial, and anti-fungal agent when added to plastics, coatings, and textiles.
- Copper diet supplements with efficient delivery characteristics.
- High strength metals and alloys.
- Heat sinks and highly thermal conductive materials.
- Efficient catalyst for chemical reactions and for the synthesis of methanol and glycol.
- As sintering additives and capacitor materials.
- Conductive inks and pastes containing (Cu) nanoparticles can be used as a substitute for very expensive noble metals used in printed electronics, displays and transmissive conductive thin film applications.
- Superficial conductive coating processing of metal and non-ferrous metal.
- As nanometal lubricant additives.

2.8 Photophysical Process of Laser Dyes

Jablonski diagram is a very important diagram used to describe the most important processes as shown in Figure (2.4). Absorbed light excites dye molecules from the lowest levels of the ground state (S_{00}) to higher vibrational levels of the (S_{1n}) state, thermal redistribution of the populations among the continuum of sublevels takes place within a very short time (~ 10^{-11} s).

Boltzman distribution in the continuum is achieved, with most of the excited molecules decaying nonradiatively to level (S_{10}). Excitation of the (S_1) state can also be affected by direct absorption from the ground state to the second excited singlet state (S_{2n}). For most organic dye solutions, the decay from (S_2 to S_1) state is nonradtive and very rapid(~ 10^{-10} to 10^{-11} s) [52]. A molecule in (S_{10}) can return to (S_{00}) by emitting a photon of light whose energy is less than the absorbed light. This spontaneous radiative process (fluorescence) is thus shifted to longer wavelengths from the absorption. The intersystem crossing from single to triplet manifold is comparatively slow considering the small energy gap between (S_1 and T_1).

Frequently the highest energy fluorescence band is of lower energy than the lowest energy absorption band. The difference in wavelength observed between these two bands is called the Stokes shift. A Stokes shift is the most easily observed as the difference between the wavelength of maximum absorption and the wavelength of maximum fluorescence [53]. Phosphorescence is the emission of a photon involving a change of multiplicity, because the change in multiplicity is formally forbidden. The phosphorescence lifetimes are significantly longer than the fluorescence lifetimes. Phosphorescence is commonly observed from (T_1 to S_0). Because the lifetime of phosphorescence is so long, molecules in (T_1) may lose their energy by other transitions that are more efficient or by chemical reaction [54].

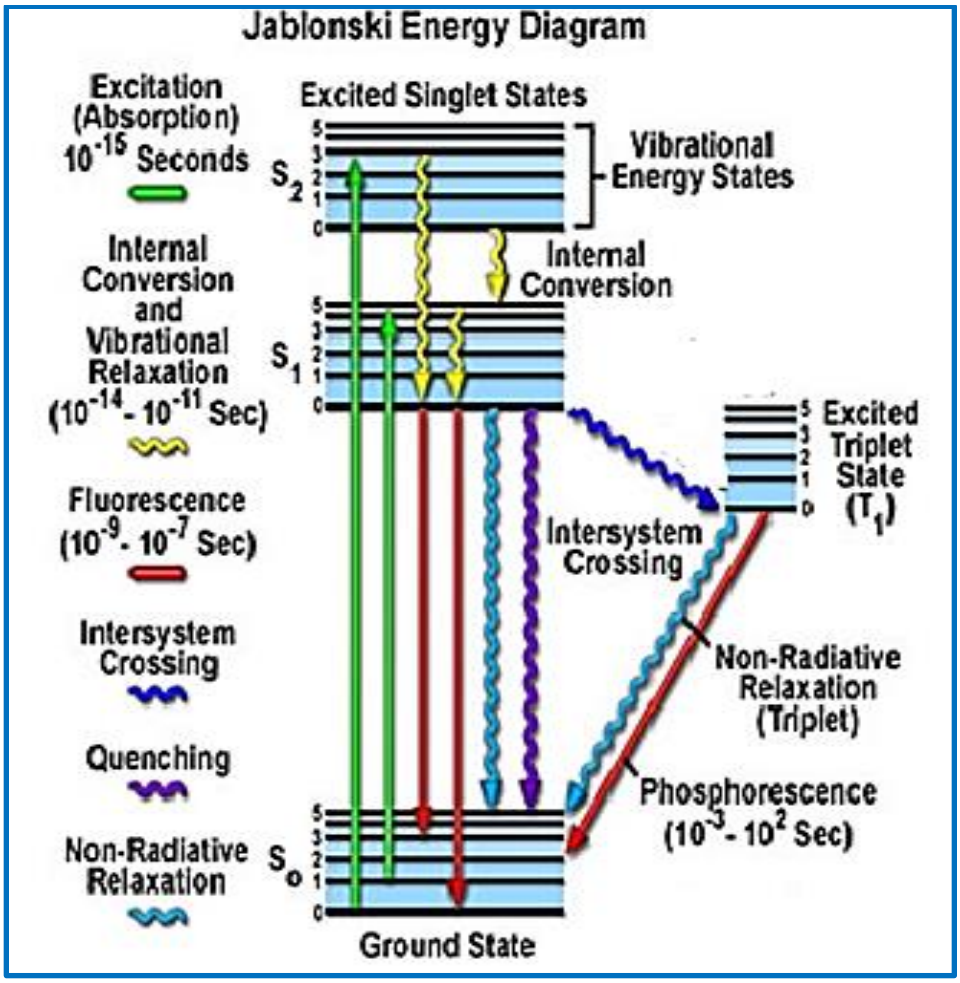

Figure (2.4) : Jablonski Diagram [54].

2.8.1 Radiative Processes

They are the processes which include emission of the photon as a result of the interaction between the atom and the photon of light. After absorbing the energy of the photon in the ground state, the excitation is from the lowest vibrational state in the S_o single band of the electronic ground state of the dye to any of the electronically excited singlet S_1, S_2, with the excitation S_0, S_1 being the strongest [55]. They are divided into:1-Flourescence. 2- Phosphorescence

2.8.1.1 Fluorescence

It is direct transition of molecule from the lowest vibrational level of the first excited state (S_1) to one of the vibrational levels of the ground state (S_0) ,emitting is energy in the form of fluorescence. This process occurs at a rate of time between (10^{-8} -10^{-9}) s. This time period differs from one sample to another and is known as the chronological age of the fluorescence sample and the wavelength longer than the wavelength that produced the excitation (energy loss), i.e., the stokes phenomenon [56].

2.8.1.2 Fluorescence Quantum Efficiency

The time of the radiative transition from the lower vibrational level to the excited electronic state then to a ground vibrational level and back to its first state after this period of time is called radiative lifetime (τ_{FM}), which is defined as the inverted rate of fluorescence emission (K_{FM}) in unit (sec^{-1}) [57]:

$$\tau_{FM} = \frac{1}{K_{FM}} \qquad (2.1)$$

Where: (K_{FM}) represents the probability of radiation transition.

Because of the presence of non-radiative processes competing with the possibility of radiation transition (K_{FM}), it will reduce the number of particles qualified for fluorescence emission, so the total probability of transition (K_F) will be the sum of the radiated and non-radioactive transition [58]:

$$\tau_F = \frac{1}{K_{FM} + \sum K_d} = \frac{1}{K_F} \qquad (2.2)$$

Where (ΣK_d) is the sum of constants (rate constants) for non-radioactive processes for the lowest vibratory state. The time of the fluorescence lifetime (τ_F) is the

actual time of the fluorescence, which is equal to the inverted total constants of all non-radiative and radioactive processes that cause energy loss [59].

$$\tau_F = \frac{1}{K_{FM} + K_{IC} + K_{ISC}} \qquad (2.3)$$

Where (K_{IC}) is the rate of inter conversion (s^{-1}) and (K_{ISC}) is the rate of intersystem crossing (s^{-1}). The lifetime of the fluorescence (τ_F) can be the main lifetime of the excited state. There is a relation between fluorescence intensity and fluorescence lifetime (τ_F) [60]:

$$I = I_\circ \exp(-t/\tau_F) \qquad (2.4)$$

Where (I) is the fluorescence intensity at time (t), ($I_\circ$) represents the highest fluorescence intensity and (t) time immediately after the cessation of excitation.

The lifetime of fluorescence (τ_F) can be calculated from a standard compound known as its chronological age, as well as the area under curve, as in the following relationship [61]:

$$\tau_F = \frac{a \times \tau_{fRB}}{a_{RB}} \qquad (2.5)$$

Where (τ_{fRB}) is the time-span of the standard compound, the Rhodamine B (3.230 ns) at concentration (10^{-4}) M and (a_{RB}) is the area under the fluorescence curve of Rhodamine B and its value (117.6 cm^{-1}), a is the area under the curve of the compound required in this research. The quantum efficiency (Φ_F) represents the quantum yield of fluorescence, which is the ratio between the probability of radiation transition (K_{FM}) and the sum of processes for the single states ($K_{FM}+K_{IC}+K_{ISC}$). This value is a physical constant of each type of excited

particles, or the ratio of total energy emitted to the amount of absorbed energy [62]:

$$\Phi_F = \frac{K_{FM}}{K_{FM} + K_{IC} + K_{ISC}} = \frac{K_{FM}}{K_{FM} + \sum K_d} \qquad (2.6)$$

$$\Phi_F = K_{FM}\tau_F = \frac{\tau_F}{\tau_{FM}} \qquad (2.7)$$

It is also possible to calculate the quantum yield of fluorescence (Φ_F) by calculating the ratio between the area of the fluorescence spectrum and the area of the absorbance spectrum, as shown in the following equation (2.8) [63]:

$$\Phi_F = \frac{\int F(v')dv'}{\int \varepsilon(v')dv'} \qquad (2.8)$$

It has been observed that the quantum yield of fluorescence for several compounds depends on the wavelength used in the excitation and the temperature. So, the quantum yield of fluorescence increases when non-radiative processes decrease and when the temperature is reduced, the relation between them is reversed. The values of fluorescence production are between (0-1), therefore, the lifetime of the fluorescence is far less than the radiation lifetime due to the non-radiative processes competing for the fluorescence process. Since values of the quantum efficiency are less than or equal to one, then **($\tau_{FM} > \tau_F$)** [64].

2.8.1.3 Phosphorescence

The phosphorescence process is the radiative transition which occurs from the excited triplet state (T_1) to the ground state (S_0). The phosphorescence is a spin-forbidden process. And also the phosphorescence lifetime is about (10^{-3} to 10^{-2} s) and this is longer than the lifetime of the fluorescence process [65].

2.8.2 Non-radiative Processes

Sometimes the electron can be relaxed without emission photon, where the photon energy can convert to kinetic energy or to the walls of the container. In the case of a solid, such as crystal and an ionic, the excited ion given energy them to lattice material, therefore the non-radiative processes do not emit the photons [66].

2.8.2.1 Intersystem Crossing

Intersystem crossing is a non-radiative transition, which occurs when singlet state (S_1) can be changed to the triplet (T_1) without emission radiation and the decay time of this translation about (5×10^{-8} s). This process involves a change in the spin multiplicity of the molecule [68]. Intersystem crossing occurs faster than the fluorescence, example, the benzophenone molecule, S_1 undergoes intersystem crossing to (T_1) with lifetime (10^{-10} s) and the fluorescence lifetime is (10^{-6} s), so, intersystem crossing at a rate that is (10^4) times faster than fluorescence. And because the excited triple state is lower in energy from the excited single state, the molecule cannot return to the excited single state, but, it can easily return to the ground state by phosphorescence processes [67].

2.8.2.2 Internal Conversion

If no spin-change occurs, the non-radiative process called internal conversion. This is the means by which higher excited singlet states decay rapidly to the lowest excited singlet before further photophysical change occurs. Similarly, higher triplet states decay rapidly to the lowest triplet state by this process, internal conversion can also occur from the lowest singlet state to the ground state [68].

2.9 Laser Beam Characteristics

Laser beam Characteristics will be explain in details in the following paragraphs.

2.9.1 Gaussian Beam

A Gaussian beam is a beam of electromagnetic radiation whose electric field intensity transverse is a Gaussian function. Many lasers emit beams with a Gaussian profile, in which case the laser is said to be operating on the fundamental transverse mode or "TEM_{00}". In TEM_{00} mode, the beam emitted from a laser is a perfect plane wave with a Gaussian transverse irradiance profile as shown in Figure (2.5) [69].

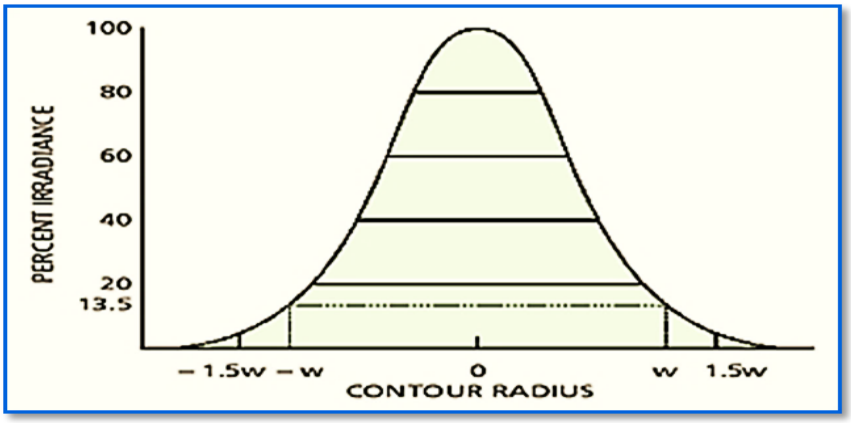

Figure (2.5): Irradiance profile of a Gaussian TEM_{00} mode [71].

2.9.2 Beam Waist and Divergence

For a Gaussian beam propagating in free space, the spot size (w) will be at minimum value (w_o) at one place along the beam, known as the beam waist. Figure (2.6) shows the Gaussian profile in free space. For a beam of wavelength (λ) at a distance (z) along the beam from the beam waist, the variation of the spot size is given by [70]:

$$w(z) = w_\circ[1 + (\frac{\lambda z}{\pi w_\circ^2})]^{1/2} \qquad (2.9)$$

R(z) is the radius of curvature of the beam; its variation is given by [71] :

$$R(z) = z[1 + (\frac{\pi w_o^2}{\lambda z})^2] \quad (2.10)$$

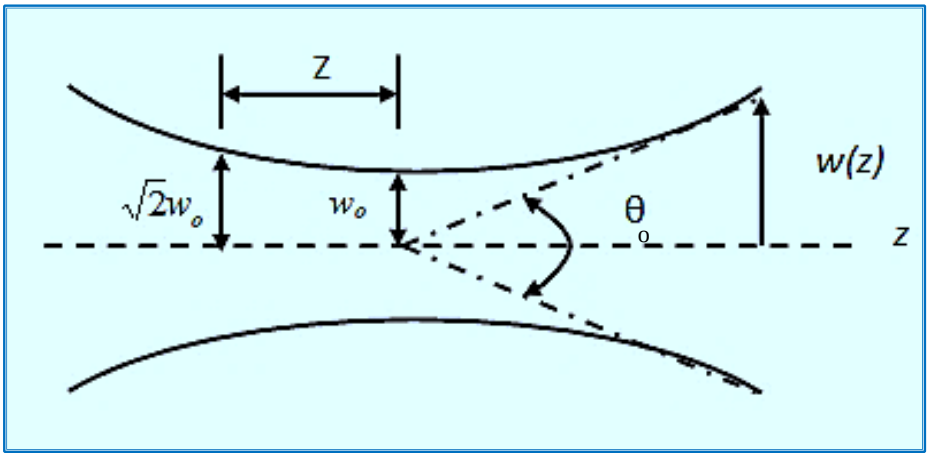

Figure (2.6): Gaussian profile in free space [72]

The divergence of a Gaussian beam, at a sufficient from the waist, tends to an angle [73] :

$$\theta_\circ \approx \tan\theta_\circ = \frac{\lambda}{\pi W_o} \quad (2.11)$$

It describes the spreading of the beam when propagating towards infinity. The above quantity means that larger values of the width mean lower values of the divergence and vice versa [74].

2.9. 3 Focusing Gaussian Beam with a Lens

A Gaussian beam can be imaged by lenses or mirrors. When a Gaussian beam passes through a focusing lens with focal length (f), the spot size (w_o) at the focal point is the same on both sides of the lens. The effect of focusing a Gaussian beam by a thin positive lens is shown in Figure (2.7) can be evaluated [75]:

$$W(z) = W_\circ[1 + \left(\frac{f}{Z_\circ}\right)^2]^{\frac{1}{2}} \quad (2.12)$$

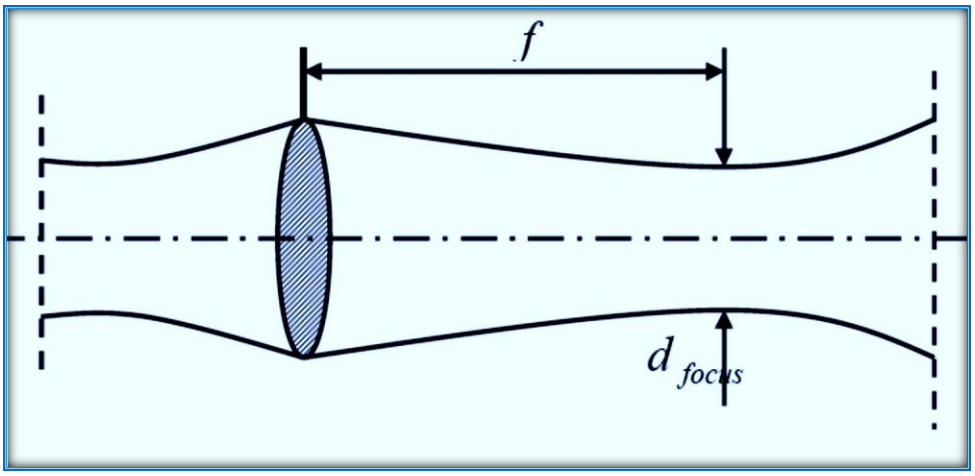

Figure (2.7): Lens focusing of a Gaussian beam [75]

In addition, the spot diameter (d_{focus}) at the focal point, at distance (f) from the lens, is now given by [76]:

$$d_{focus} = f\,\theta_{\circ} \qquad (2.13)$$

Where, (f) is focal length of a lens, and (θ_o) is the divergence angle of the laser beam as shown in Figure (2.7).

2.10 Interaction of Laser Light with Matter

When laser radiation strikes a material surface, part of it is absorbed and part is reflected. The energy that is absorbed begins to heat the surface. There are several regimes of parameters that should be considered, depending on the time scale and on the flounce. When laser beam acts on the material, laser energy is first absorbed by free electrons. The absorbed energy then propagates through the electron subsystem and then transferred to lattice therefore laser energy is transferred to material [77].

This process has a resonant feature because materials show different absorptions to lasers with different wavelengths, this dependence of absorption on wavelength is decided by the microstructure and electromagnetic properties of the material. The intensity of laser light produces a wide range of interaction.

The interaction of matter can be classified as linear interaction and nonlinear interaction. The advant of the laser as a coherent light with high intensity source gives birth of nonlinear optics, it plays an important role in many branches of science and technology [78]. The nonlinear optics effects are associated with light-induced changes in the optical constants of the material, either the absorption coefficient, the refractive index, or both. They are best treated by considering the interaction of the light beam with the atoms of the material as driving force acting on of oscillator group with natural resonance frequency [79].

2.11 Optical Properties

The study of the optical constants of a material is interesting for many reasons. Firstly, the use of materials in optical applications such as interference filters, optical fibers and reflective coating, requires accurate knowledge of their optical constants over a wide range of wavelengths. Secondly, the optical properties of all materials may be related to their atomic structure, electronic band structure and electrical properties [80]. The optical properties of organic dyes are divided into two types: linear optical properties and nonlinear optical properties.

2.11.1 Linear optical properties

When light interacts with matter the optical processes observed in solid state materials can be classified as reflection, refraction, absorption, and transmission [81]. The intensity (I_o) of the beam incident to the surface of the solid medium must equal the sum of the intensities of the transmitted, absorbed, and reflected beams, denoted as I_T, I_A, and I_R respectively[82]:

$$I_o = I_T + I_A + I_R \qquad (2.14)$$

$$T + A + R = 1 \qquad (2.15)$$

A number of parameters can be used to quantify the optical properties of materials, such as absorption coefficient, refractive index, extinction coefficient and real and imaginary dielectric constant.

2.11.1.1 Linear Optical Coefficients

A number of parameters can be used to quantify the optical properties of materials. In particular the refractive index, or refractivity, absorption coefficient, or absorbance, are defined as the ratio of refrected to incident intensity and absorbed to incident intensity respectively [83]. The liner absorption coefficient (α_o) and linear refractive index (n_o) can be found from transmittance spectrum according to the following equations [83]:

$$\alpha_o = \frac{1}{t} \ln(\frac{1}{T}) \qquad (2.16)$$

$$n_o = \frac{1}{T} + \left[\left(\frac{1}{T^2} - 1\right)\right]^{1/2} \qquad (2.17)$$

Where (t) is the thickness of sample and (T) is the transmittance.

2.11.2 Nonlinear Optical Properties

The study of events that develop as a result of changes in the optical properties of materials as a result of intense light contact is known as nonlinear optics. Nonlinear phenomena have received a lot of attention [84]. Positively charged particles travel in the direction of applied electric fields, while negatively charged particles go in the opposite direction. The displacement between positive and negative charged particles produces dipole moments, and the dipole moment per unit volume describes the induced polarization of the medium. Electric polarization is approximately linearly proportional to the applied electric field (E) when the applied electric fields are sufficiently minimal [85].

$$P = \chi . E \qquad (2.18)$$

Where (χ) is the electric susceptibility tensor in the case of linear optics.

When the applied electric fields are high enough, however, the induced polarization has a nonlinear dependence on them and may be described as a power series with respect to them [86]:

$$P = \chi^{(1)}.E + \chi^{(2)}.EE + \chi^{(3)}.EEE + \cdots \quad (2.19)$$

$$P = P(1) + P(2) + P(3) + \cdots \quad (2.20)$$

Where $\chi^{(1)}$ is the linear susceptibility, $\chi^{(2)}$ is the second order nonlinear susceptibility, and $\chi^{(3)}$ is the third order nonlinear susceptibility.

The term $\chi^{(1)}$ is responsible for linear absorption and refraction, and is the only term that reflects the linearity between the induced polarization and the incident electric field. The term $\chi^{(2)}$ is present only in non-centrosymmetric materials, i.e. materials that do not have inversion symmetry. The third order nonlinear optical interactions, which are described by the term $\chi^{(3)}$ [87]. The field of nonlinear optics (NLO) has been developing for a few decades as a promising field with important applications in the domain of photo electronics and photonics. Organic materials are considered as one of the important classes of third order NLO materials because they exhibit large and fast nonlinearities. To obtain materials with large third order nonlinearity, various types of organic compounds have been explored [88].

Third order nonlinearity has been measured using a variety of approaches, including degenerate four waves mixing, third harmonic production, and the Z-scan technique. Among these methods, Z-scan is the most straight forward for determining the nonlinear refractive index and nonlinear absorption coefficient. It gives not only the real and imaginary parts of the nonlinear susceptibility's magnitudes, but also the real part's sign. The Z-scan technique, which uses self-

focusing or self-defocusing events in optical nonlinear materials, may quickly quantify nonlinear refraction and nonlinear absorption in solid and liquid samples. The open-aperture and closed-aperture systems are the two approaches of Z-scan [89].

2.12 Nonlinear Optical Response of Organic Materials

Organic molecules have an isotropic nonlinear optical response (uniformity in all orientations). Carbons, for instance, may form two forms of covalent: s-bonds and π-bonds. Because π-bonds have a larger electronic density than s-bonds, they exhibit nonlinear optical properties[90]. (NLO) are dependent on the change in polarization of the electrons in the π-bonding. As a result, the nonlinear optical properties of organic materials containing π- bonds are more numerous than those seen in saturated compounds with the same amount of carbon atoms. Various types of organic compounds have been explored in order to develop materials that exhibit a high degree of third order nonlinearity[91].

2.13 Z-Scan Technique

Z-scan technique is a simple and direct method to characterize both the nonlinear refraction and nonlinear absorption. It is based on a single beam method. It refers to the process of inserting a sample in a focused Gaussian beam and translating it along beam axis through a focal region. The wave front distortion from self-focusing or self- defocusing will cause the Kerr nonlinearity. The beam power propagating through a small aperture at far field varies with a sample position. Measuring the output power versus position sample allows to determine nonlinearity. There are two methods of Z-scan, the closed-aperture and open-aperture system [92].

2.13.1 Closed-aperture Z-Scan

The change in intensity of a beam, focused by a lens (L) in Figure (2.8), as the sample passes through the focal plane is measured using a closed aperture Z-Scan. The light that travels through an axially centered aperture (A) in the far field is collected by the photo detector PD. The change in axis intensity is generated by the sample (S) self-focusing or self-defocusing, which results in a change in index of refraction, which forms a lens in a nonlinear sample, as shown in Figure (2.8) [93].

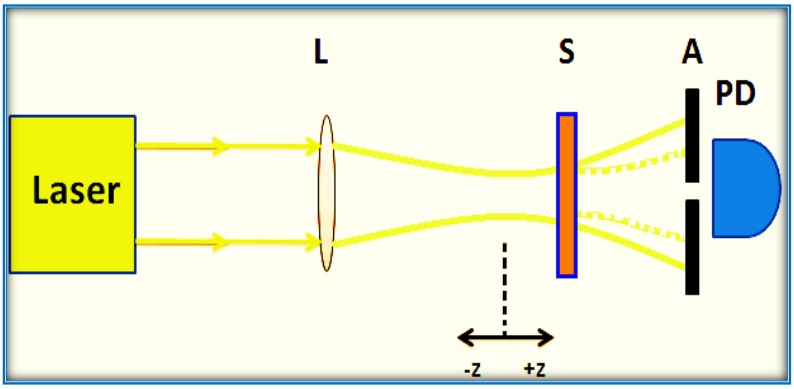

Figure (2.8): Closed aperture Z-scan [93].

If a material with a negative nonlinear refraction index and a thickness lower than the diffraction length of the focused beam is utilized, the Z-Scan transmittance as a function of (Z) is related to the sample's nonlinear refraction. This can be thought of as a narrow variable focal length lens. The beam irradiance is modest and nonlinear refraction is minimal distant from the focus (Z_o). The measured transmittance remains constant in this situation (i.e., Z-independent). Irradiance increases as the sample approaches the beam focus, causing self-lensing in the sample [94].

A negative self-lens in front of the focal plane will tend to collimate the beam on the aperture in the far field, increasing the aperture position transmittance. Following the focal plane, the same self-defocusing increases the beam divergence,

causing the beam to diverge at the aperture and lowering the measured transmittance. Far from focus (Z >0), nonlinear refraction is modest, resulting in a Z-independent transmittance. A negative nonlinearity's Z-Scan characteristic is a transmittance maximum (peak) followed by a transmittance minimum (valley). A positive nonlinearity is defined by an inverse Z-scan curve (i.e., a valley followed by a peak). These two cases are shown in Figure (2.9) [95].

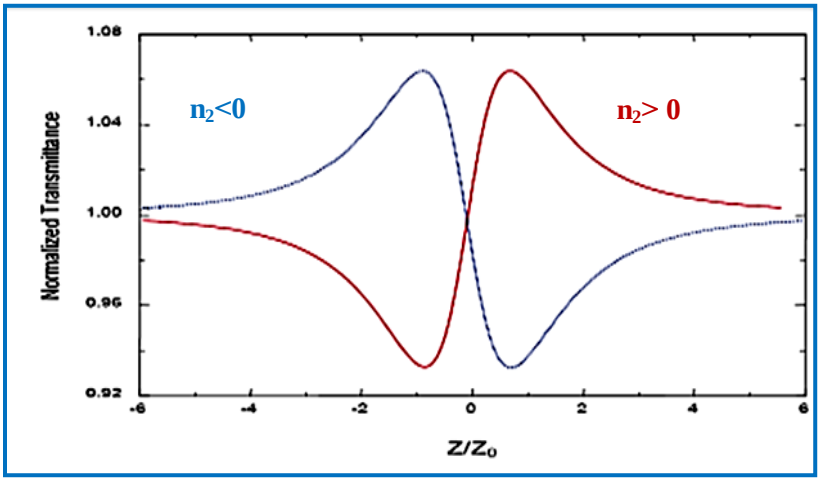

Figure (2.9): Calculated Z-Scan transmittance curves for a cubic nonlinearity [95].

The nonlinear refractive coefficient is calculated from the peak to valley difference of the normalized transmittance by the following formula [96]:

$$n_2 = \frac{\Delta\Phi_o}{I_o L_{eff} k} \qquad (2.21)$$

Where, (k = 2π/λ), (k) is wave number, (I_o) is the intensity at the focal spot and ($\Delta\Phi_o$) is the nonlinear phase shift [96]:

$$\Delta T_{p-v} = 0.406|\Delta\Phi_o| \qquad (2.22)$$

(ΔT_{p-v}) the difference between the normalized peak and valley transmittances, (L_{eff}) is the effective length of the sample, determined from [97]:

$$L_{eff} = \frac{(1-\exp^{-\alpha_o L})}{\alpha_o} \qquad (2.23)$$

Where (L) is the sample length. The intensity at the focal spot is given by [98]:

$$I_o = \frac{2P_{peak}}{\pi {\omega_o}^2} \qquad (2.24)$$

Which defined as the peak intensity within the sample at the focus, where (ω_o) is the beam radius at the focal point.

2.13.2 Open-aperture Z-Scan

An open-aperture Z-scan measures the variation in intensity of a beam in the far field at photo detector (PD), which captures the full beam, as focused by lens (L). Multiphoton absorption in the sample (S) as it travels through the beam waist causes the shift in intensity. Schematics of experimental setup used for the closed- and open-aperture Z-scan, is shown in Figure (2.10) [99].

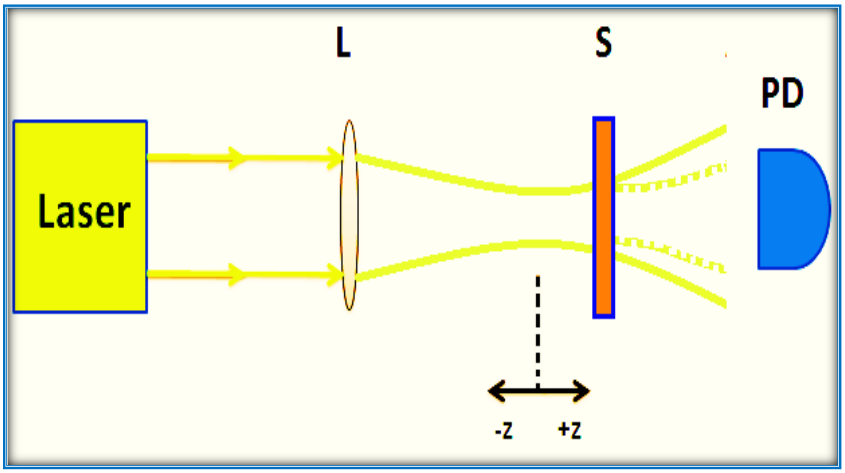

Figure (2.10): Open-aperture Z-scan [99].

Z-scan with a open aperture is clearly insensitive to nonlinear refraction, even with nonlinear absorption (thin sample approximation). With no aperture, the Z-scan signatures should be symmetric with regard to the focus (Z = 0), where they should have the lowest transmittance (e.g., two photon absorption) or maximum transmittance (e.g., saturation of absorption). In fact, the coefficients of nonlinear

absorption can be easily calculated from such transmittance curves. Nonlinear absorption coefficient (β), can be easily calculated by using the following equation [100] :

$$\beta = \frac{2\sqrt{2}\,T(z)}{I_o L_{eff}} \qquad (2.25)$$

Where T(z): the minimum value of normalized transmittance at the focal point, (Z=0). It should be clear that the transmittance versus position graph of sample in an open aperture Z-Scan should be symmetric around the focus as shown in Figure (2.11).

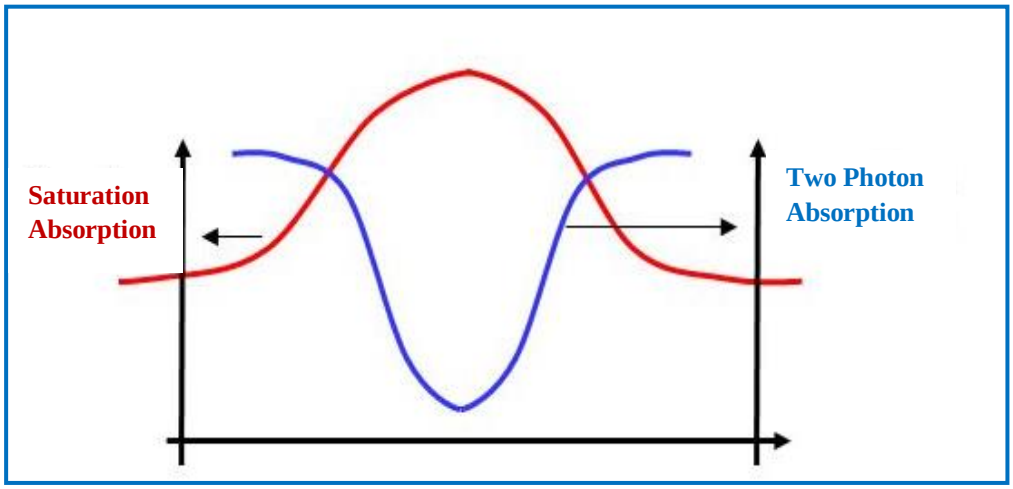

Figure (2.11): Open aperture Z-Scan curve [100].

2.14 Nonlinear Absorption and Nonlinear Refraction

The main optical properties involved in the light-matter interaction are absorption, which is defined by the nonlinear absorption coefficient (β), and nonlinear refractive index (n_2). These two parameters are depending on the electric field intensity of laser light. The energy of the absorbed photons allows the material to shift from the ground state to the excited state when it is irradiated.

When a substance is exposed to a high electric field, it changes its refractive index. In reality, the intensity of the electric field influences the index of refraction, gives the refractive index at high intensity [101]:

$$n = n_o + n_2 I \quad (2.26)$$

Where (n_o) is the linear refractive index and (n_2) is the nonlinear refractive coefficient related to the intensity.

The absorption of the material is also intensity dependent given by [102]:

$$\alpha = \alpha_o + \beta I \quad (2.27)$$

Where (α_o) is the linear absorption coefficient and (β) is the nonlinear absorption coefficient related to the intensity. The coefficients (n), and (α) are related to the intensity of laser.

2.15 Saturable Light Absorption

A nonlinear process that can be associated with real (rather than virtual) energy levels and population changes in those levels is that of saturable absorption. This process occurred when the nonlinear absorption coefficient ($\beta < 0$), which can be appeared when a strong light absorption between two levels causes saturation (bleaching) of the corresponding electronic transition. The two levels involved surface resonance ground and excited state. On the other hand, this is a process in which a material can be highly absorbing at a specific wavelength when a low-intensity beam is incident upon the material, yet an extremely intense beam (at that same wavelength) will pass through the medium with little change in intensity [103].

2.16 Two Photon Absorption (TPA)

Two-photon absorption (TPA) is the simultaneous absorption of two photons of identical or different frequencies in order to excite a molecule from one state (usually the ground state) to a higher energy electronic state. The energy difference between the involved lower and upper states of the molecule is equal to the sum of the energies of the two photons, as in the case of a saturable absorber. This process occurred when the nonlinear absorption coefficient $\beta > 0$. The two-photon transition rate can be significantly enhanced if an intermediate level (2) is located near the virtual level shown by the dashed line in Figure (2.12) [104].

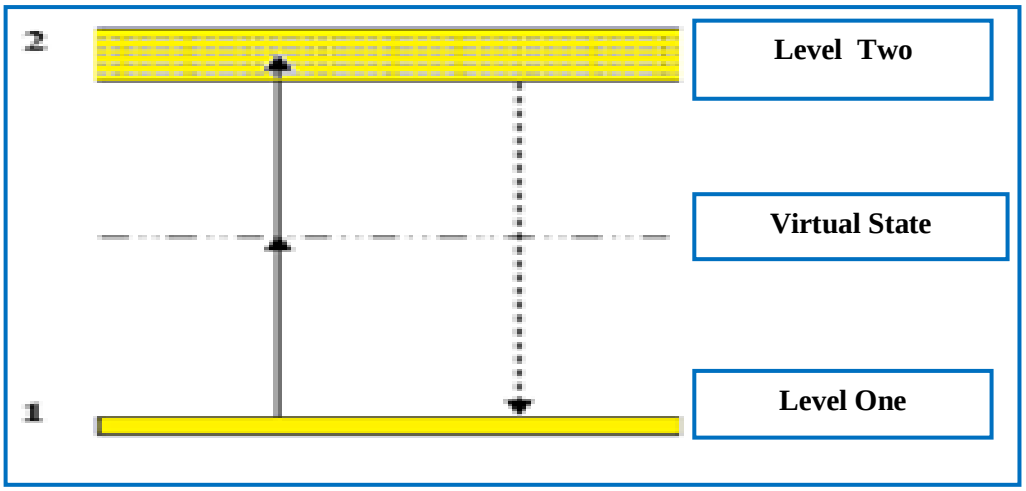

Figure (2.12): Energy levels for two-photon absorption process [104].

2.17 Kerr Effect

The nonlinear electronic polarization, which can be defined as altering the refractive index, is a nonlinear interaction of light in a material. The Kerr effect can produce a local change in the refractive index in high-intensity laser beams, causing the laser material to operate as a lens. This can cause laser beams to self-focus [105].

2.18 Optical Limiting

In a material with a strong nonlinear effect, the absorption of light increases with intensity such that beyond a certain input intensity the output intensity approaches a constant value. Such a material can be used to limit the amount of optical power entering a system. This can be used to protect expensive or sensitive equipment such as sensors, can be used in protective goggles, or can be used to control noise in laser beams. The ideal behavior of such a device is shown in Figure (2.13) [106].

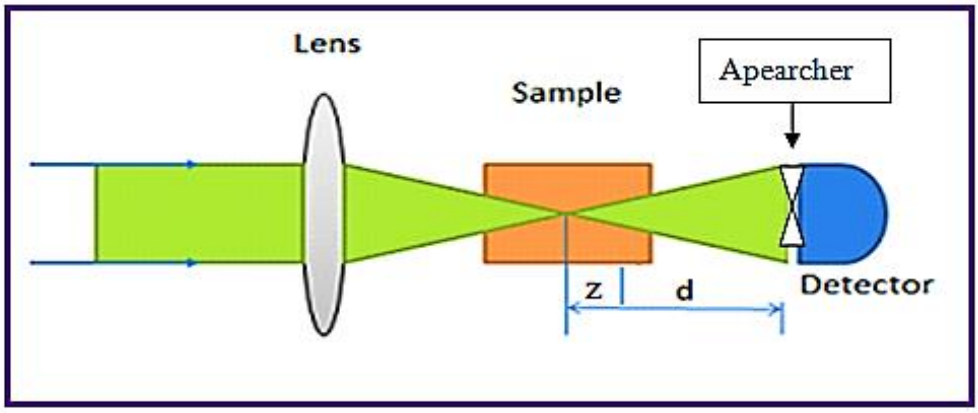

Figure (2.13): Schematic of theoptical Limiting Geometry [106].

The ideal optical limiter has the characteristics shown in Figure (2.14). It has a high transmittance for low input power or energy.

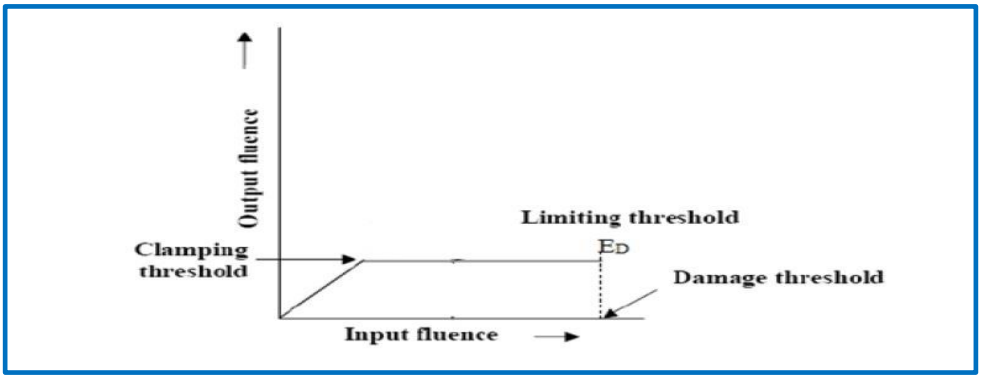

Figure (2.14): Schamatic Representation of the behaivor of an Ideal Optical Limiter [106].

Chapter Three

Experimental Part

3.1 Introduction

This chapter describes the preparation method of solutions and thin films of Malachite green organic dye doped with PMMA polymer and (Cu) nanoparticles and the instruments used for characterization the material. The Z-scan system was presented and a measurement was done using diode pumped solid state laser (DPSS) at wavelength (457 nm) and laser power (84 mW) and the procedure of these measurements with their photographic pictures.

3.2 Materials

3.2.1 Malachite Green Organic laser Dye

The dye used in this project is Malachite green (MG) due to its importance in many applications, especially because it functions as an active medium in dye lasers. Malachite green is an organic compound it is from Xanthene group. Malachite green is traditionally used as a dye for materials such as silk, leather and paper it is also used as a dyestuff and an antimicrobial in aquaculture. It is appears as green crystals with a metallic luster. [109]. Molecular structure of Malachite green shown in Figure (3.1) and the principle characteristics of this dye shown in Table (3.1) .

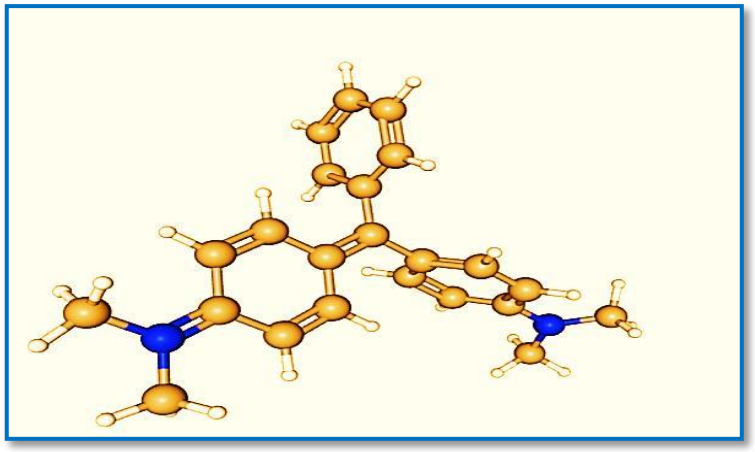

Figure (3.1): Molecular structure of Malachite green organic dye.

Table (3.1): The principle characteristics of Malachite green dye [107].

Properties	Malachite green
Molecular formula	$C_{23}H_{25}ClN_2$
Molecular weight	364.911 g/mol
Appearance	Green crystals with metallic luster.
Solvents	Methanol, Chloroform and Water
Other names	Aniline green, Basic green 4, Diamond green B, Victoria green B

3.2.2 The Solvent

Chloroform was utilized as a solvent. It is relatively unreactive, miscible with most organic liquids [108]. The molecular structure of chloroform solvent was shown in Figure (3.2) and the main characteristics of chloroform solvent are displayed in Table (3.2) .

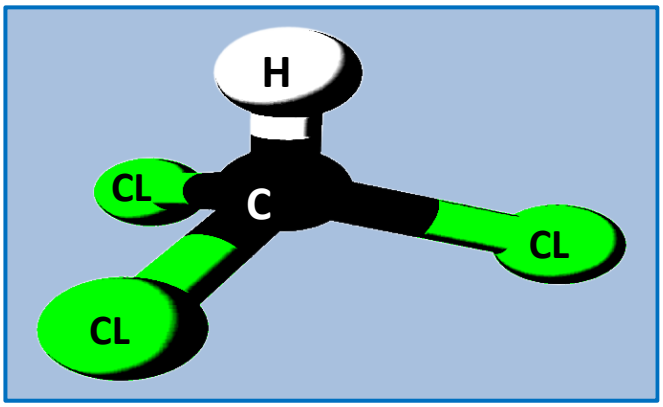

Figure (3.2): The molecular structure of chloroform solvent .

Table (3.2): The main characteristics of chloroform solvent [108].

Properties	Chloroform
Chemical formula	$CHCl_3$
Molar mass	46.07 (g/mol)
Refractive index	1.3614
Dielectric Constant	24.195
Polarity	0.5771
Density	0.7936 mg/ cm^3
Freezing Point	-114 ^oC
Boiling Point	78.3 ^oC

3.2.3 PMMA Polymer

PMMA or (Poly methyl methacrylate) polymer has named as acrylic or the acrylic glass and it has the trade names such as Plexiglas [109]. Molecular structure of PMMA polymer was shown in Figure (3.3) and the principle characteristics of this polymer was shown in Table (3.3).

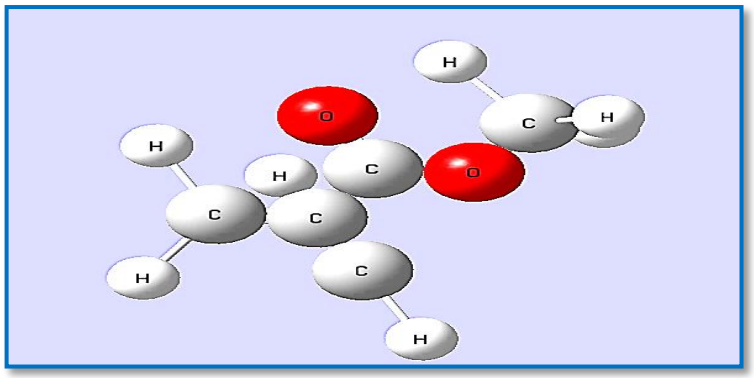

Figure (3.3): Structure of poly methyl methacrylate (PMMA).

Table (3.3): The main characteristics of PMMA polymer [109].

Material	Chemical formula	Molecular Weight M .Wt gm/mol	Melting Temperature T_m °C	Density g /cm^3
PMMA	$CH_2=C(CH_3)COOR$	84000	213	1.2

3.2.4 Cu Nanoparticles

Copper nanoparticles were supplied by laboratory Reagent LTD; the main characteristics are shown in Table (3.4). (Cu) nanoparticles are very attractive due to their heat transfer properties such as high thermal conductivity. (Cu NPs) also have high surface area to volume ratio, low production cost, antibacterial potency, catalytic activity, optical and magnetic properties as compared to precision metals such as gold, silver or palladium. The main difficulty lies in their preparation and preservation as they oxidized immediately when exposed in air [110].

Table (3.4): The main characteristics of Cu nanoparticles [110].

Cu nanoparticle	Description
Productive company	SIGMA-ALDRICH, Germany
Form	Nano powder
Surface area	40-70 m^2/g
Particle size	(10-100) nm

3.3 Work Scheme

Figure (3.4) shows the experimental procedure as a block diagram of the main steps followed in this work:

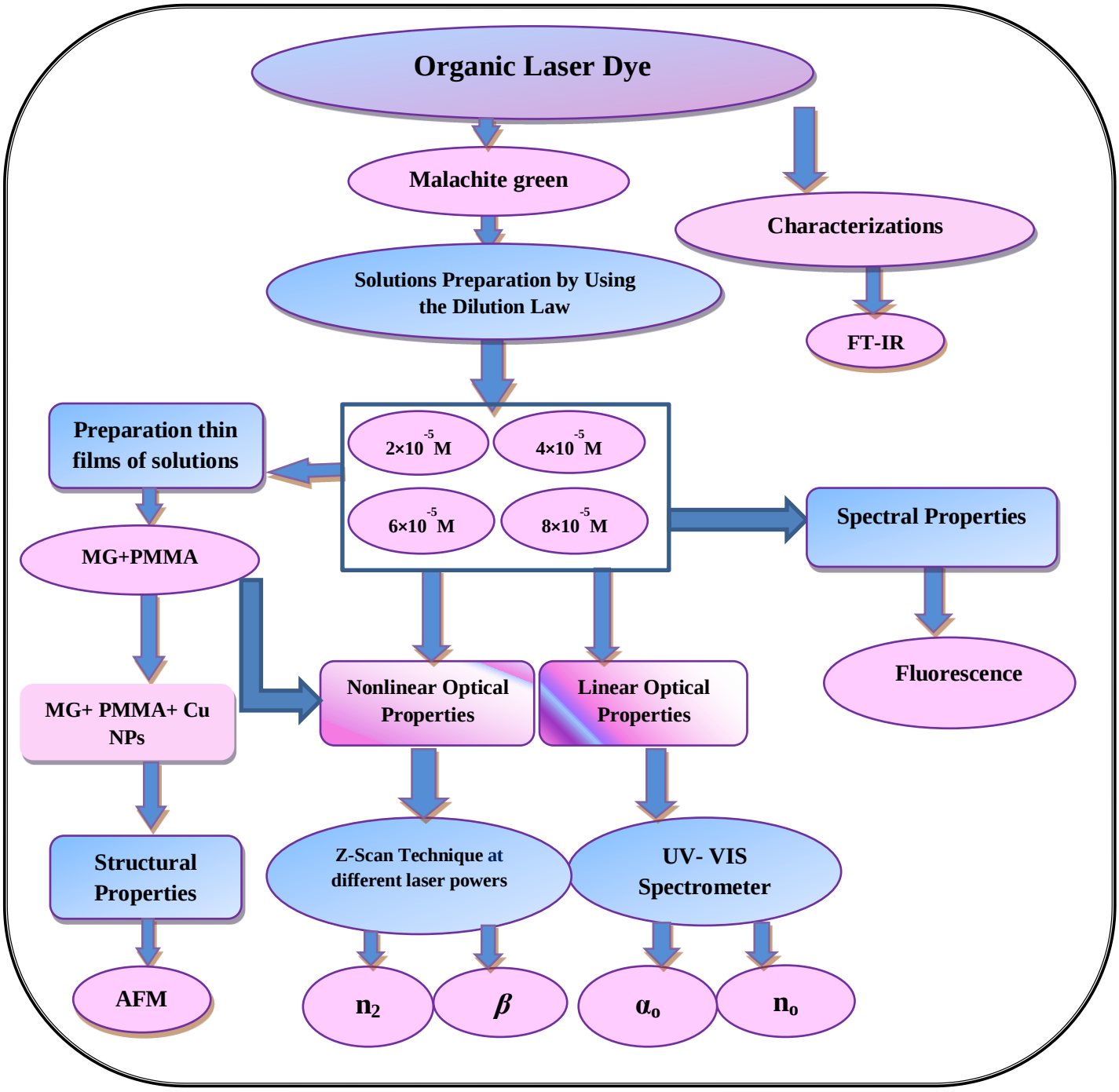

Figure (3.4): Main steps of the experimental work.

3.4 Samples Preparation

3.4.1 Solutions Preparation

Solutions of concentration (10^{-3} M) of Malachite green organic dye in chloroform solvent were prepared. The powder was weighted by using an electronic balance type (BL 210 S), Germany, having a sensitivity of four digits. (0.0182) g from this dye were dissolved in (50 ml) of chloroform solvent according to the following equation [111]:

$$W = \frac{M_W \times V \times C}{1000} \qquad (3.1)$$

Where, W: Weight of the dissolved in material (g), Mw: Molecular weight of the material (g /mol), V: Volume of the solvent (ml) and C: The concentration (M). The prepared solutions were diluted according to the following equation [111]:

$$C_1V_1 = C_2V_2 \qquad (3.2)$$

Where: C_1: Primary concentration, C_2: New concentration.V_1 is the volume before dilution, V_2 is the volume after dilution. In this work, (2×10^{-5} ,4×10^{-5} ,6×10^{-5} and 8×10^{-5}) M concentrations were prepared for Malachite green dye. Figure (3.5) shows pure dye solution and dye doped with PMMA polymer and (Cu) nanoparticles at different concentrations.

Figure (3.5) Malachite green organic laser dye at different concentrations.

Figure (3.6) Malachite green organic laser dye doped with PMMA polymer at different concentrations .

Figure (3.7) Malachite green organic laser dye doped with PMMA polymer and Cu NPs at different concentrations.

3.4.2 Preparation of Solid Samples (Thin Films).

The thin films of (Malachite gree) organic laser dye were prepared on a clean glass slide by drop casting method, with solution at a concentration (10^{-3}) M, and dried at room temperature for (2) days, the thickness of these thin films is about (150-200) nm. Dye doped polymer films were fabricated by drop casting method, at concentration (10^{-3}) M. The solution of PMMA polymer is prepared by dissolving the required amount of polymer (3 g in 50 ml of chloroform solvent).

A desired amount of dye solution was added to PMMA polymer solution and stirred by a magnetic stirrer at room temperature to get a uniform mixture. Thin films were shaped by drying the mixed polymer dye solution on a slide at room temperature.(0.03) g of (Cu) nanoparticles powder was added to polymer dye solution and stirred by magnetic stirrer at room temperature to get a uniform mixture. Thin films dye doped with PMMA polymer and (Cu NPs) are framed by allowing the mixture to be dried on a glass block at room temperature. Figure (3.8) shows thin films of Malachite green dye doped with PMMA polymer and (Cu NPs).

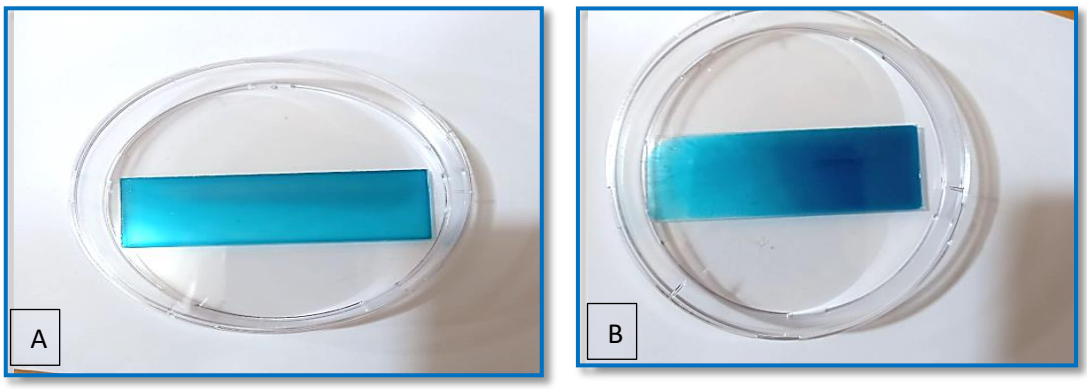

Figure (3.8): Thin Films of : A- Malachite green doped PMMA polymer B- Malachite green doped with PMMA and Cu NPs.

3.4.3 Thickness Measurement

Thickness is one of the most important thin film parameters since it largely determines the properties of thin films. The thickness of thin films is usually measured by monitoring the rate of the deposition during the coating process. However there are several methods used for measuring thickness of thin films, such as weight, optical, electrical and other methods. In our work the thickness of the thin films was measured by optical method it's done by optical thin-film measurement model (LIMF -10, Lambda Scientific Pty Lt). This measured is done in Electro- Optics Laboratory in Babylon University - Science College - Physics department. Figure (3.9) with following specifications .

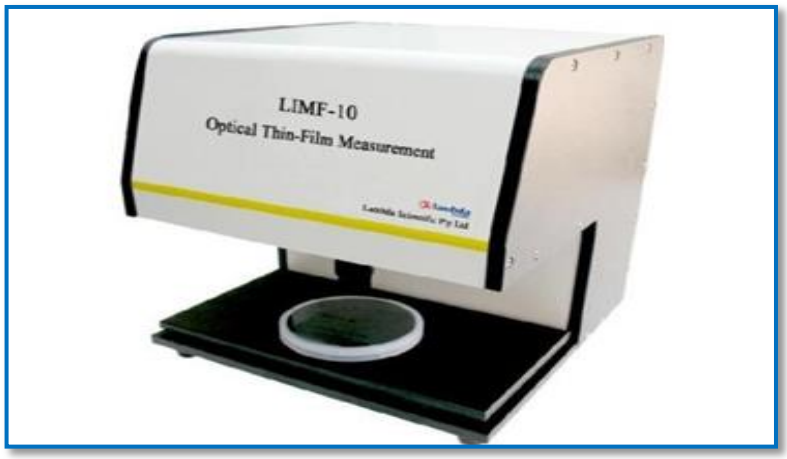

Figure (3.9): Image and specifications for optical thin-film thickness measurement.

3.5 Structural Properties Measurements

The structural properties are examined using (FT-IR) transmission.

3.5.1 Fourier Transforms Infrared Spectrometer (FT-IR)

Infrared spectra of Malachite green organic dye as powder have been taken by using infrared spectrophotometer, at the laboratories of department of chemistry, college of science, university of Kufa. Figure (3.10) shows FT-IR spectrometer.

Figure (3.10): FT-IR spectrometer .

3.5.2 Optical Microscope

Thin films of Malachite green dye doped with PMMA polymer and (Cu NPs) were examined by using an optical microscope, which is supplied from Olympus name (Toupview) type (Nikon -73346) and equipped with light intensity automatic controlled camera. Under magnification (100x), this measurement was implemented in the(University of Babylon / College of education for pure sciences/Department of physics), as shown in Figure (3.11).

Figure (3.11): Optical Microscope.

3.5.3 Atomic Force Microscopy Measurement (AFM)

In order to observe the surface roughness and topography of deposited thin films, AFM micrographs were obtained using digital instruments. AFM images

data include root mean square (r.m.s) roughness and grain size. It has three main modes of mapping topography: contact(which is used in our morphology investigation), non-contact and intermittent contact or tapping. The most important part of an AFM is the tip with its nanoscale radius of curvature .The tip is attached to a micron scale which reacts to the Van der Waals interaction and other forces between the tip and sample, The device was used to determine the morphology of the recorded nano composite , grain size and the statistical distribution that shown in Figure (3.12).

(Model :CSPM AA3000) produced from Angstrom company. The test is done in the central laboratories of the University of Tehran.

Figure (3.12) : Atomic force microscope.

3.6 Linear Optical Properties

3.6.1 UV-Visible Spectrophotometer

The absorbance spectra were measured using a UV-Visible Spectrophotometer type (Shimadzu-1800). This device has two light sources Deuterium Lamp (190-360) nm and Tungsten Lamp (360-1100), so it covers a wide range of the electromagnetic spectrum, extending from the ultraviolet to the near infrared region. The idea of operating the device depends on the separation of the incoming beam into two parts, one of which passes through the sample solution to be studied, while the second beam in the solvent that represents the reference beam. The device then subtracts the reference beam and registers the absorption spectrum of the sample alone. All samples were examined in the laboratory of thin films (University of Babylon / College of Education for Pure Sciences / Department of Physics), as shown in Figure (3.13).

Figure (3.13): UV – Visible spectrophotometer.

3.6.2 Fluorescence Measurements

Fluorescence spectra were measured for all prepared samples using spectrophotometer type (Fluoro Mate FS-2). The samples were mounted cubic cell of quartz dimensions (1×1×5) cm^3 perpendicularly with incident beam. All samples were examined in the laboratory of thin film (University of Babylon /

College of Education for Pure Sciences / Department of Physics), as shown in Figure (3.14).

Figure (3.14): The Fluorescence Spectrometer.

3.7 Nonlinear Optical Properties

Nonlinear optical properties of all samples will be explained in details in the following paragraph:

3.7.1 Z- Scan Technique

The Z-scan measurements were divided into two types: closed aperture and open aperture. Each part was employed by a continuous wave (CW) diode pump solid state laser with a wavelength of (457) nm and different laser power of (84) mW. The nonlinear refractive index was measured using a closed-aperture Z-scan, whereas the nonlinear absorption coefficient was measured using open-aperture Z-scan. The beam was focused by using a convex lens (f =15 cm). The sample was moved along the Z-axis. The transmittance through the sample is recorded as a function of sample position. Figure (3.15) shows the open-aperture and closed-aperture Z-scan setup.

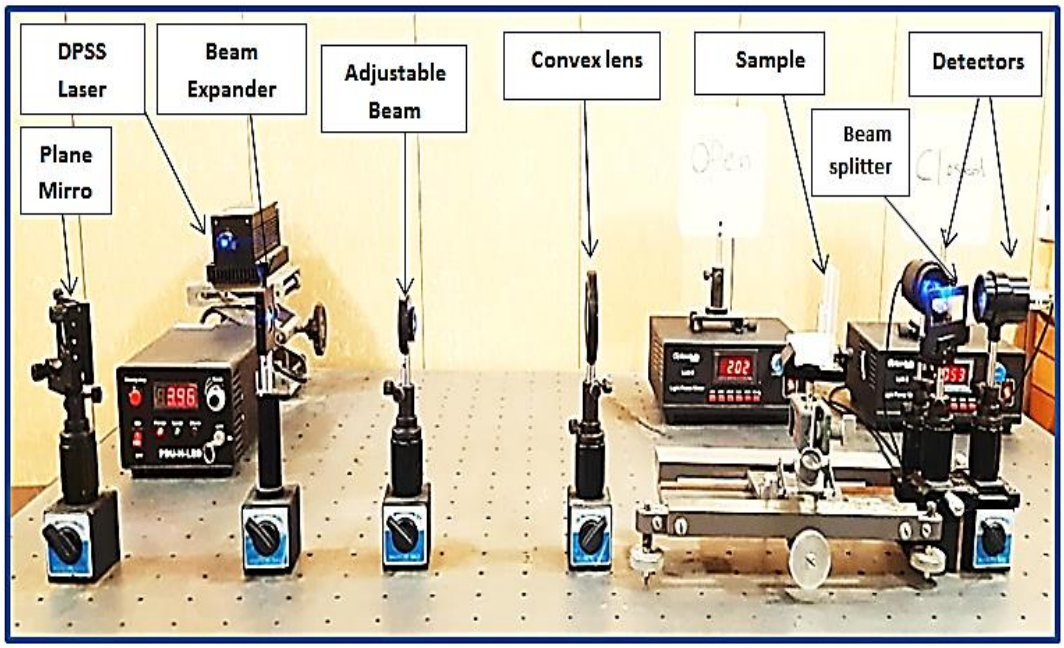

Figure (3.15): Z-Scan set-up.

3.7.2 Diode Pumped Solid-State Laser (DPSS)

CW (457) nm DPSS laser is used. Table (3.5) shows the characteristics of the laser, which used in this research.

Table (3.5): Specifications of 457 nm (DPSS) laser.

Model	**MBL-457 nm**
Wavelength (nm)	457nm
Output power (mW)	142.5mW
Transverse mode	TEM_{00}
Operating mode	CW
Power stability (rms, over 4 hours)	5.71%
Beam divergence, full angle (m rad)	1. 8
Beam diameter at $1/e^2$ (mm)	X:1.883nm Y:1.285nm
Power supply	(100-240)Volt

3.7. 3 Detector

The third element in the Z-Scan is the optical power meter detector type (LLM-2), which is used to measure the output power of the laser. The detector was placed at the far field of a Gaussian laser beam.

3.7.4 Aperture

The aperture is an important parameter in Z-Scan system to measure complex refractive index (n_2) in the closed-aperture technique, and its diameter is (1mm). The aperture was aligned with the lens in the same axis.

3.7.5 The Sample

All solutions are filled into the glass cuvette (1) mm thickness. The cuvette was hand made in the laboratory, which consists of five slides of glass as shown in Figure (3.16). The geometry of a sample cuvette can be shown in Figure (3.17), which is represented engineering drawing of sample cuvette.

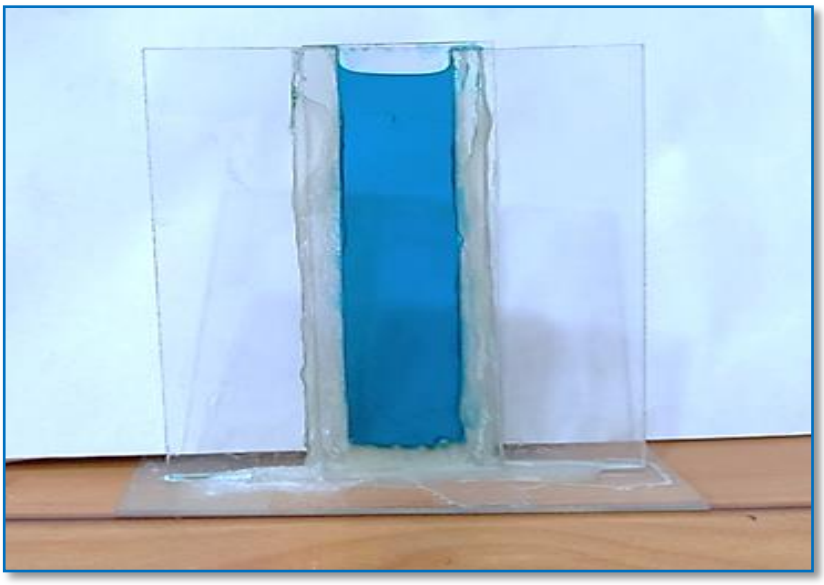

Figure (3.16): Photograph of a sample cuvette.

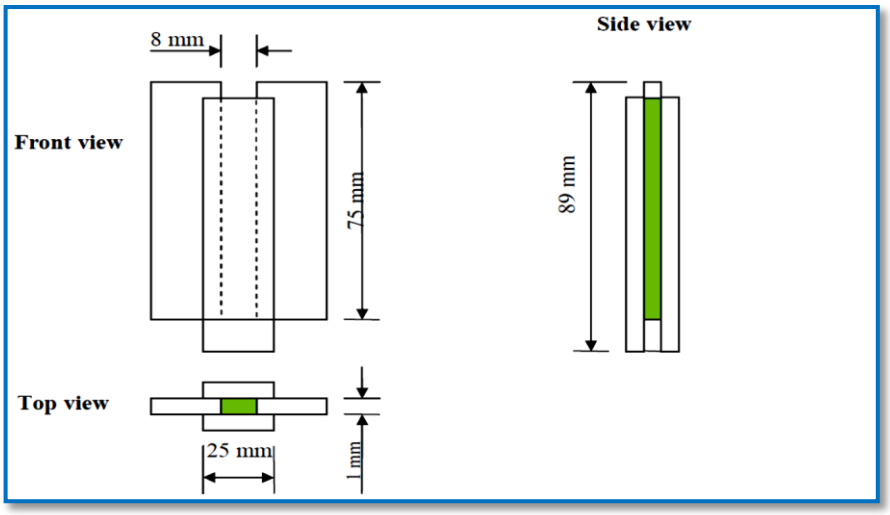

Figure (3.17): Geometry of sample cuvette.

3.8 Reference Beam Measurements

In order to measure the reference power of a CW laser, the detector was placed directly in front of the (457 nm) DPSS laser. The normalized transmission as a function of sample position is given by [111]:

$$T(z) = \frac{P(I)}{P(I)_{ref}} \qquad (3.3)$$

Where, (P) is the power of the transmitted laser beam, when the cuvette is filled by dye solution, and (P_{ref}) is power of the reference laser beam.

Chapter Four

Results , Discussion, Conclusions and Suggestions

4.1 Introduction

In this chapter, the results of all prepared samples of Malachite green organic laser dye at concentrations (2, 4, 6 and 8) $\times 10^{-5}$ M in chloroform solvent as pure and after doped with PMMA polymer and Cu nanoparticles (as solutions) and thin films at (10^{-3}) M were presented, the structural properties which including charts of infrared (FT-IR) and atomic force microscopy (AFM) were investigated. The spectral, linear and non-linear optical properties for all prepared samples were discussed. Z-scan technique using for two cases, closed and open aperture utilized CW diode pump solid state laser operating at a wavelength (457) nm at constant and different powers (70, 84 and 102) mW. The optical limiting behavior of all samples are also discussed.

4.2 Structure Properties

Structural properties of all prepared samples of Malachite green organic laser dye have been determined by study (FT-IR) and (AFM) will be explain in detail in the following paragraph:

4.2.1 FT-IR Spectra

FT-IR spectra of Malachite green dye as powder was measured at room temperature as shown in Figures (4.1), this Figure shows the bond of stretching represented by the range (3738-2854) cm^{-1} is for bond of (N-H). The peak at (1711) cm^{-1} indicate a carbon–nitrogen bond is a covalent bond

between carbon and nitrogen (C=N), the peak at (1572) cm^{-1} indicate (C = C). the peak at (1345) cm^{-1} indicate Carbon-NH_2 bond (C-NH_2),the peak at (1137) cm^{-1} indicate (C-N), its agreement with [19].

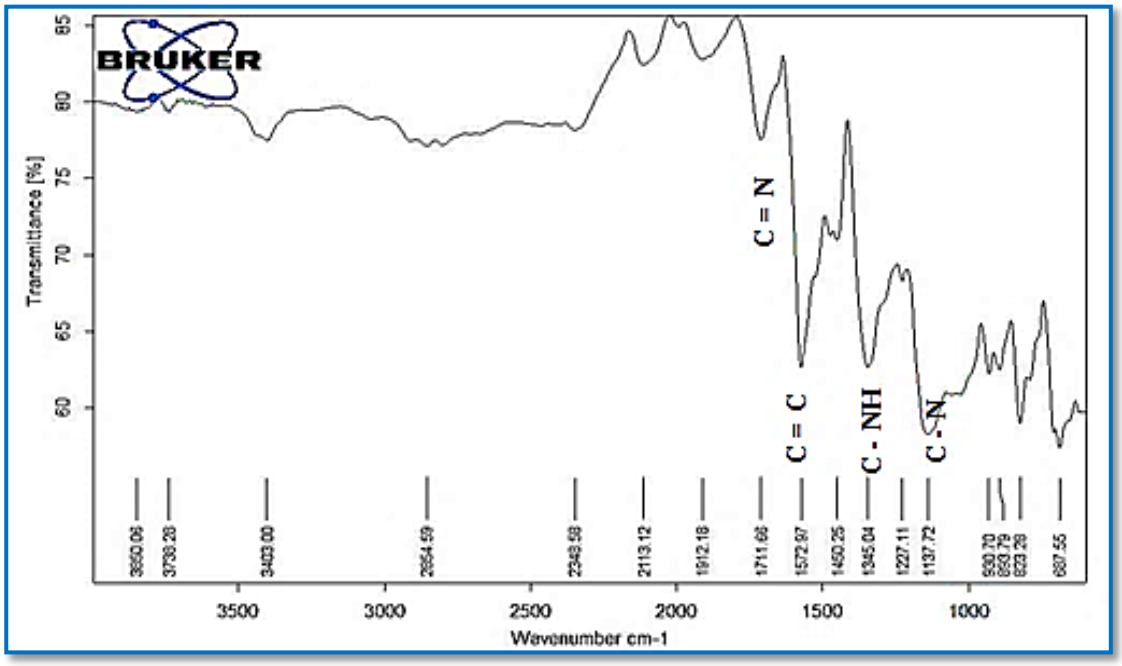

Figure (4.1): FT-IR spectrum for Malachite green dye as powder.

4.2.2 Atomic Force Microscope (AFM)

The 3-D AFM images and granularity accumulation distribution charts for thin films of Malachite green dye with PMMA polymer and (Cu NPs) ,deposited on glass substrate by drop-casting method at room temperature, with the ability to depiction and analysis of these surfaces and give the statistical values with high accuracy about surface roughness values depending on the root mean square (r.m.s) of the average roughnes .Can study through microscopic analysis (AFM) effect of (thickness, concentration, temperature, method of preparation , etc.) ,on the properties

of the deposited film material to the fact that the study of the surfaces of film materials important to recognize how the distribution and arrangement of atoms on surfaces, and to identify the differences or homogeneity properties or attributes relating to each atom separately and illustrative image about the distribution rate of the crystalline size onto surfaces. Figures (4.2 and 4.3) show 2-D and 3-D images of AFM for thin films of Malachite green dye doped with PMMA polymer and (Cu) nanoparticles at (10^{-3}) M, a diagram of distribution of growth granular groups on the surfaces of the deposited films. Table (4.1) shows that the average diameters (grain size) of thin films .It is found that the grain size and the (r.m.s) of surface roughness increases when thickness increases [119].

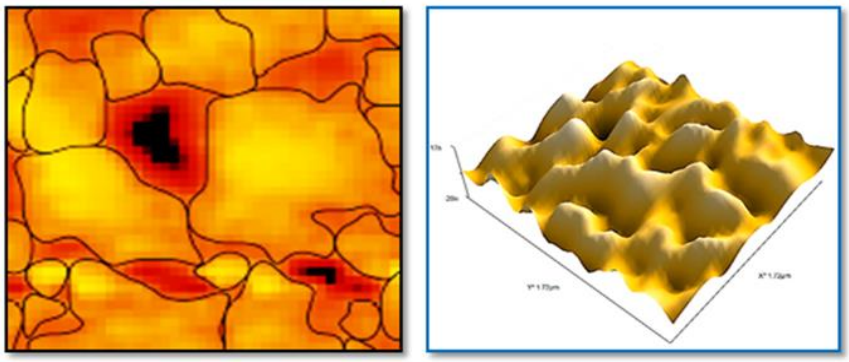

Figure (4.2): 2-D and 3-D AFM images for thinfilm of Malachite green dye doped with PMMA polymer.

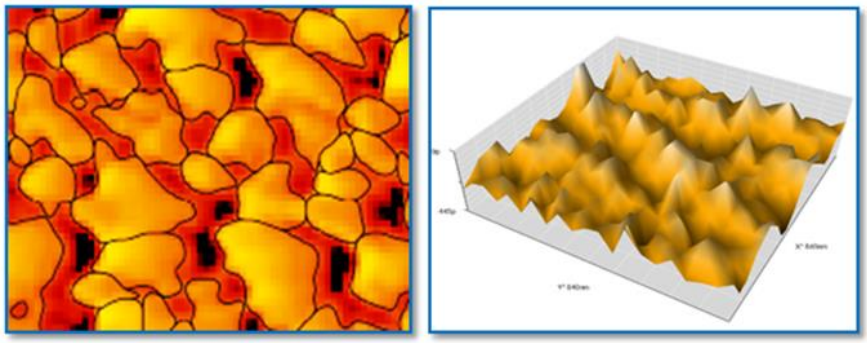

Figure (4.3): 2-D and 3-D AFM images for thinfilm of Malachite green dye doped with PMMA polymer and (Cu Nps).

Table (4.1): AFM parameters of thin films of Malachite green dye doped with PMMA polymer and (Cu Nps).

Material	root mean square (nm)	Roughness (nm)	Average Grain Size (nm)	Thickness (nm)
MG+PMMA	**39.20**	**0.598**	**30**	**160**
MG+PMMA+ (Cu NPs)	**55.30**	**0.791**	**41.41**	**182**

4.2.3 Optical Microscope

Figure (4.4:A and B) show the optical microscope images of thin films for Malachite green dye in two cases : one doping with PMMA and the other case doping with PMMA polymer and (Cu NPs) at magnification power (100 X). Those Figures illustrate spreading dye molecules on the glass substrate with (PMMA) polymer .Thin films exhibit uniform distribution of dye at surface morphology. Thin films in Figure (4.4:A) have exhibited slightly better interference between dye and polymer than thin films were shown in Figure (4.4: B). Figure (4.4:B) shows distribution of (Cu NPs) and form paths of network inside the (Dye-PMMA) blend. Nanoparticles are aggregates as a cluster of dye doped PMMA and (Cu NPs) samples . This behavior is agreement with [25].

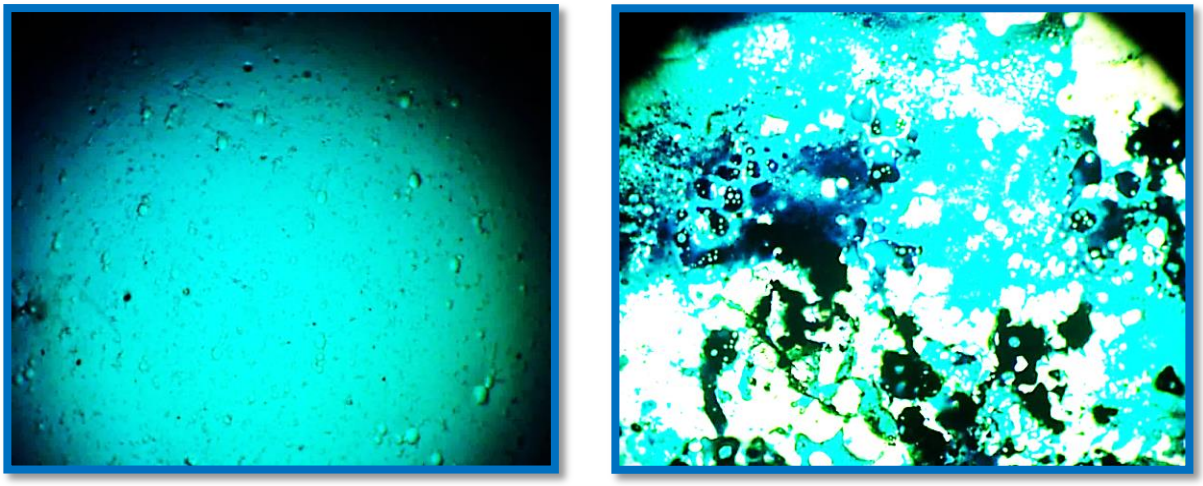

A B

Figure (4.4): Photomicrographs (100x) for thin films of A: Malachite green dye doped with PMMA polymer , B: Malachite green dye doped with PMMA polymer and (Cu) nanoparticles.

4.3 Optical Properties

The optical testing included the linear, spectral and nonlinear optical properties of Malachite green organic laser dye pure and doped with PMMA polymer and (Cu) nanoparticles at concentrations (2, 4, 6, and 8) $\times 10^{-5}$ M as solutions and thin films .

4.3.1 Linear Optical Properties

The linear optical properties consisted of absorption and transmission spectra,as well as measurement of linear refractive index and linear absorption coefficient.

4.3.1.1 Absorbance Spectra of Malachite green dye pure and doped with PMMA polymer and (Cu) nanoparticles (as Solutions)

The absorbance spectra of Malachite green dye pure and doping at different concentrations as solutions were recorded in the region (400-700) nm as shown in Figures (4.5- 4.7) respectively.These Figures show that the four spectra have two bands, the absorbance in visible region which is called Q-band at the range about (420-620) increases strongly with concentrations increases according Beer-Lambert law, it agree with reference [24].

These two bands belongs to transition of ($n \rightarrow \pi^*$) that referred to the neighboured active azomethine groups, which acted as an electron-receptor where the free lone pair of electron was available at each nitrogen atom (has ability for sharing at resonance phenomena). These two bands in visible region which is called Q-band this is suggested to take place because of Xanthene family. It was observed that the intensity of absorption is reduced by reducing the concentration and increase strongly with concentrations increases according Beer- Lambert law, it agree with reference [109]. The absorption spectra for Malachite green dye after adding PMMA polymer a solutions with ratio (1:1) ml shown in Figure (4.6). The absorption spectra of dye doped with PMMA polymer at the same concentrations is similar to the dye alone where it have two band also but the intensity of absorbance is increased. This behavior was in agreement with [16]. The absorption spectra of Malachite green dye solution doped with PMMA and (Cu) nanoparticles were shown in Figure (4.7).The results show that the absorption peaks shifted toward the longer wavelengths after adding PMMA polymer and (Cu) Nanoparticles. This shift was overall obtained due to the increasing

number of molecules per unit volume, this in turn lead to change in energy levels result in effect of vibration field on molecules, its agree with [17].

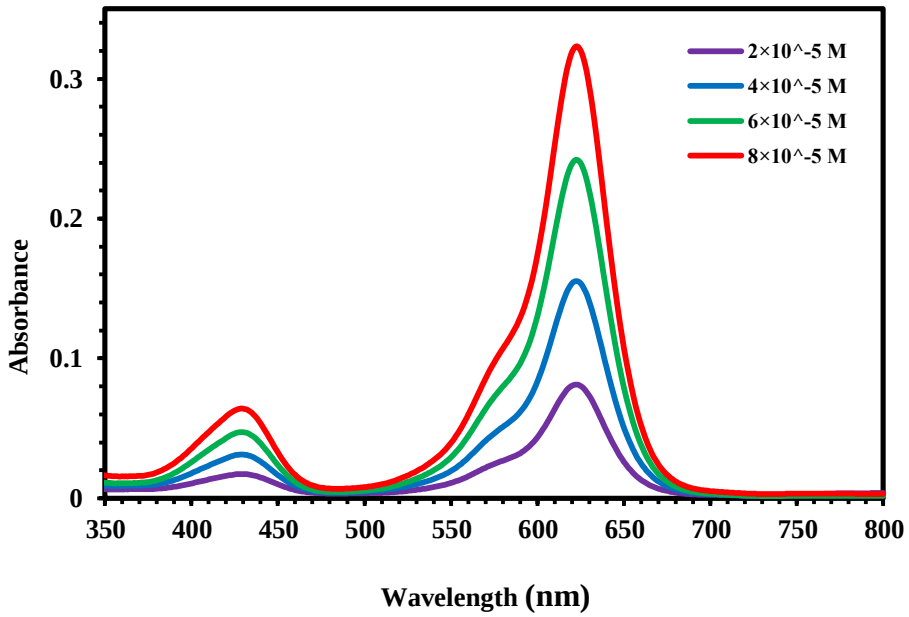

Figure (4.5): Absorbance spectra of Malachite green pure dye at different concentrations.

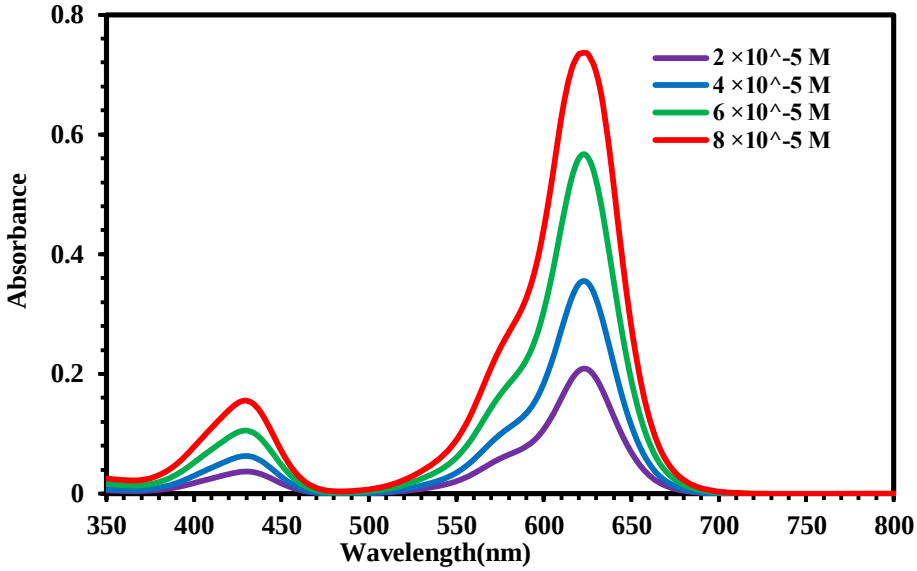

Figure (4.6): Absorbance spectra of Malachite green dye doped with PMMA polymer at different concentrations .

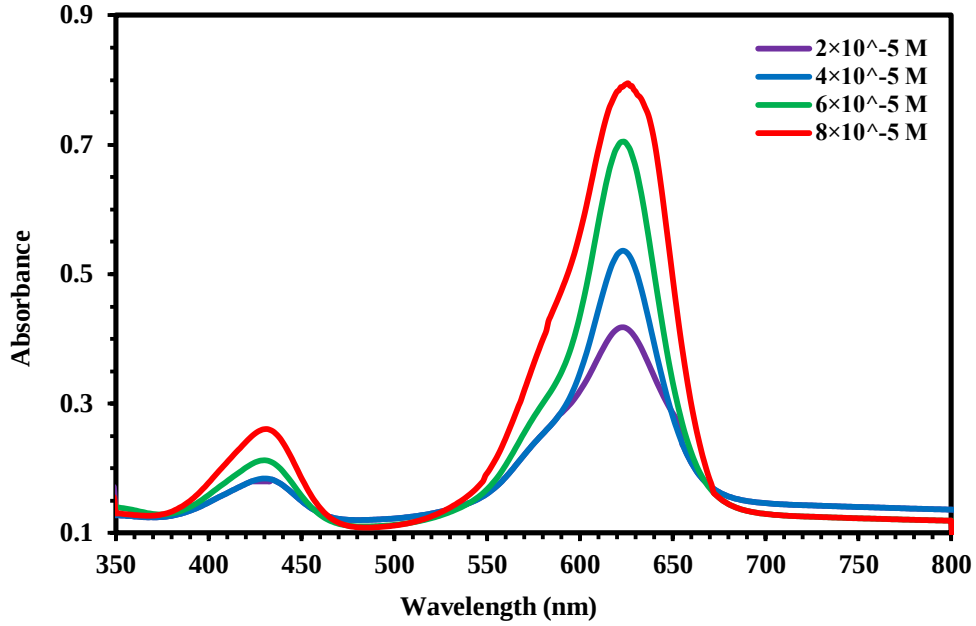

Figure (4.7): Absorbance spectra of Malachite green dye doped with PMMA polymer and (Cu) nanoparticles at different concentrations .

4.3.1.2 The Absorbance Spectra of Malachite green dye doped with PMMA polymer and (Cu) nanoparticles as(Thin Films)

The linear absorbance spectra of thin films of Malachite green dye at concentration (10^{-3}) M doped with PMMA and (Cu) nanoparticles are shown in Figure (4.8). The present results show that the absorption peaks were shifted toward the longer wavelengths after addition PMMA polymer and Cu nanoparticles to pure dyes. This shift obtain due to electronic and vibrational states of interfacial molecules, which is lead to increasing absorption for all samples of nanocomposites, this is suggested to take place because of the excitations of high occupation molecular orbital (HOMO) electrons to the lowest inoccupation molecular orbital (LUMO).

Fundamental absorption of absorption spectra refers to band or excitation transition, at visible and near infrared regions, the absorption of all samples for nanocomposites has high values, this behavior attributed to the energy of incident photons doesn't enough energy to interact with atoms, thus the photons will be transmitted when the wavelength increases, ie, when the amount of energy required for transmission decreases [30].

The linear absorption coefficient (α_o) and linear refractive index (n_o) of all samples obtained from Equations (2.16 and 2.17) respectively as shown in Table (4.3). The values of (α_o) and (n_o) for dye doped with PMMA polymer and (Cu) nanoparticles are larger than values for pure dye, as well as, the values of (α_o) and (n_o) for thin films are larger than those values for same materials as solutions.This behavior agrees with references [27].The results showed that the absorbance of the thin films with nanoparticles (Cu) is higher than that of the thin films without nanoparticles.

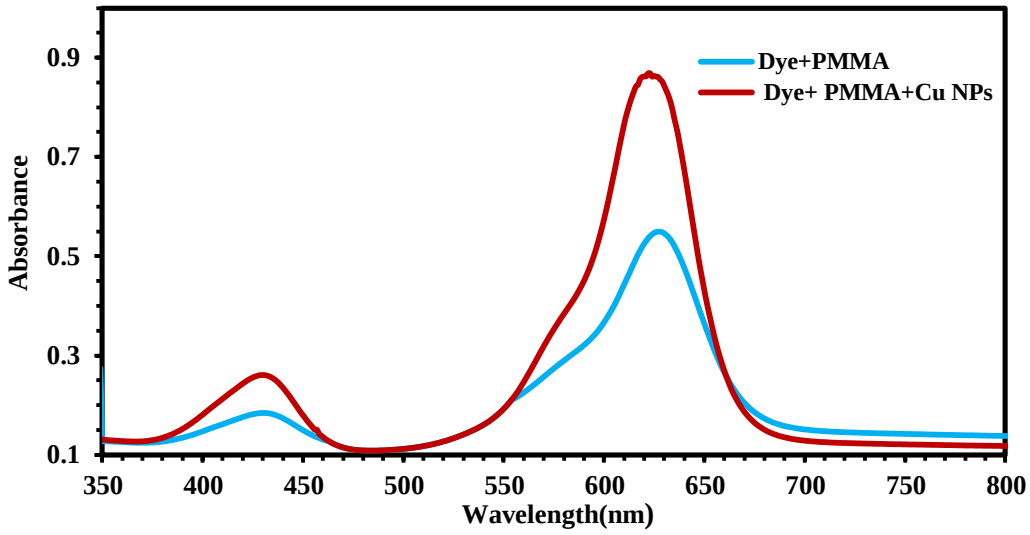

Figure (4.8): Absorbance spectra of thin films of Malachite green dye doped with PMMA polymer and (Cu) nanoparticles.

4.3.1.3 The Transmittance Spectra of Malachite green dye pure and doped with PMMA polymer and (Cu) nanoparticles (as Solutions)

The transmission spectra of Malachite green dye doped with PMMA polymer and (Cu) nanoparticles at different concentrations were analyzed using UV-Vis spectrophotometer as shown in Figures (4.9- 4.11) respectively.The optical transmission curve of all samples showed a variable behavior of the transmission as a function of the incident wavelength ,this behavior agrees with [9].The transmittance decreases with increases concentrations at the same wavelength. The transmittance intensity of nano composite was lower than intensity of pure dye and dye doped with PMMA polymer .Transmittance decreases, this is suggested to take place because of (Cu) nanoparticles contain electrons which can be the absorption of electromagnetic energy of the incident light and travel to higher energy levels. This process is not accompanied by emission of radiation because the traveled electron to higher levels have occupied vacant positions of energy bands, thus part of the incident light is absorbed by the substance and does not penetrate through it, on the other hand, the pure samples have a little transmittance than doping samples this is suggested to take place because of no free electron (i.e. electrons are linked to atoms by covalent bonds),this is because the breaking of electron linkage and moving it to the conduction band need to photon with high energy [113].

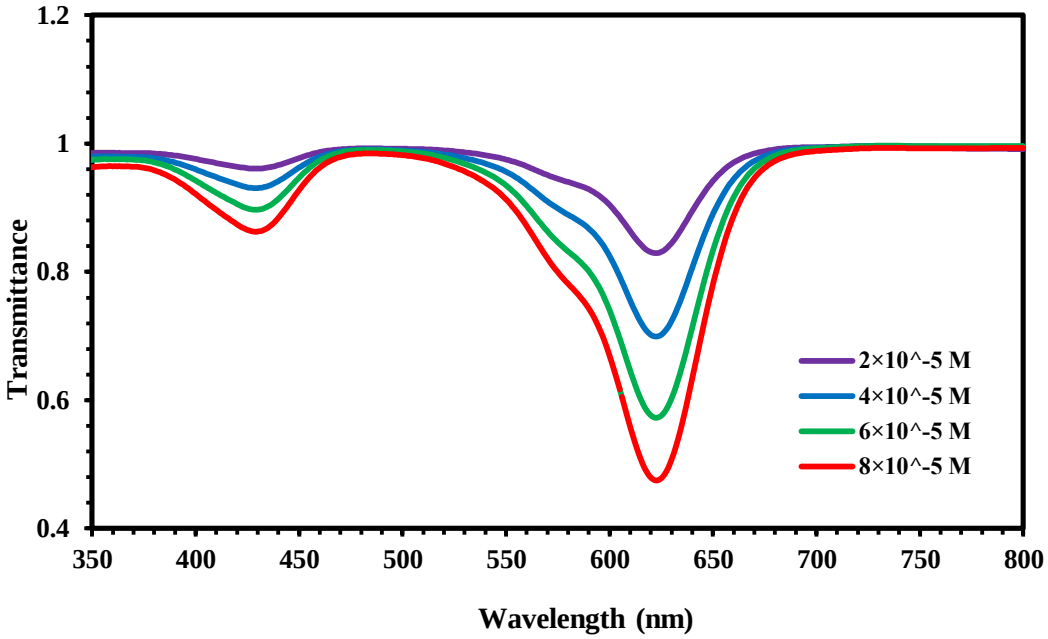

Figure (4.9): Transmittance spectra of Malachite green pure dye at different concentrations.

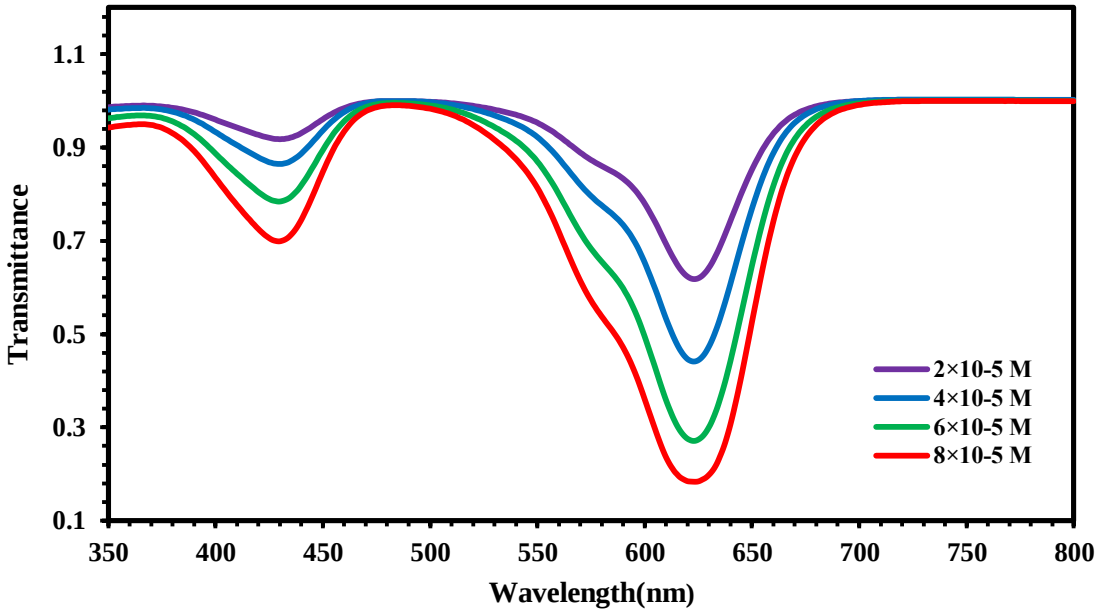

Figure (4.10): Transmittance spectra of Malachite green dye doped with PMMA polymer at different concentrations .

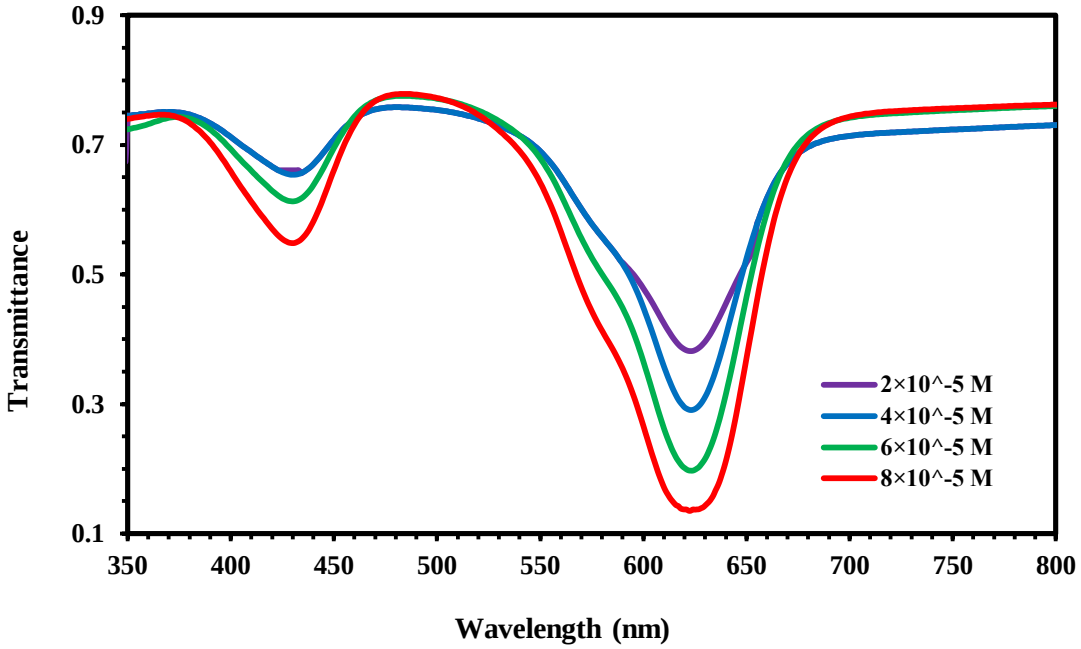

Figure (4.11): Transmittance spectra of Malachite green dye doped with PMMA polymer and (Cu) nanoparticles at different concentrations .

4.3.1.4 The Transmittance of Malachite green dye doped PMMA polymer and (Cu) nanoparticles as (Thin Films)

Transmission spectrum of thin films of Malachite green dye doped with PMMA polymer and (Cu) Nanoparticles at (10^{-3} M), as shown in Figure (4.12).The optical transmission curve of the samples show a variable behavior of the transmission as a function of the incident wavelength. The transmittance intensity of nanocomposite was lower than intensity of dye with adding PMMA.Transmittance decreases, this is suggested to take place because of (Cu) nanoparticlecontain electrons which can be the absorption of electromagnetic energy of the incident light and travel to higher energy levels. This process is not accompanied by emission of radiation because the traveled electron to higher levels have occupied vacant positions of energy bands, thus part of the incident light is absorbed by the substance and does not penetrate

through it. This behavior agrees with [16]. The results showed that intensity of transmittance for thin films are less than those values for same materials as solutions.

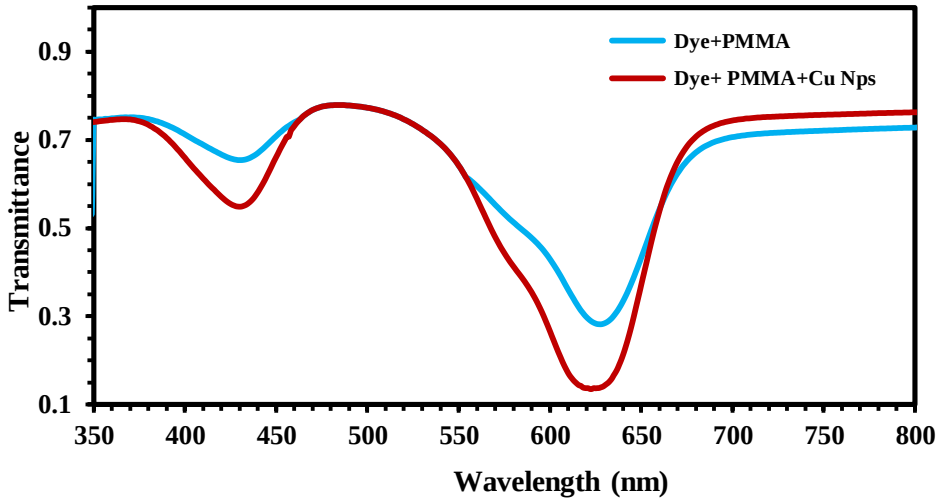

Figure (4.12): Transmittance spectra of thin films for Malachite green dye doped with PMMA polymer and (Cu) nanoparticles .

4.3.2.1 Fluorescence Spectra of Malachite green dye pure and doped with PMMA polymer and (Cu) nanoparticles (as Solutions)

Figures (4.13- 4.15) shows fluorescence intensity for Malachite green organic laser dye at different concentrations (2, 4, 6 and 8) $\times 10^{-5}$ M as pure dye and doping with PMMA polymer and (Cu) nanoparticles, the wavelength of excition is (620) nm. From these Figures it noticed that the fluorescence intensity at higher concentrations reaches a limiting value and then decreases with further increase in concentration, it agree with references [25].

Several factors are responsible for this behavior occurring to stern equation. This can be related to the phenomenon of re-absorption and re-emission, which ultimately reduces fluorescence emission [16].With

increasing dye concentration the formation of dimmers and higher aggregates decreases the fluorescence emission by a combination of monomer-dimer, higher aggregates energy transfer and absorption of radiation by non-fluorescent dimmers and higher aggregates. This transfer of energy between molecules by collisional mechanism makes the nonradioactive processes prominent and hence fluorescence decreases.

The fluorescence spectra of many organic dyes in liquid solution depend on the local electric field which is induced by the surrounding polar solvent molecules, so this effect is a result of intermolecular solute-solvent interaction forces (such as dipole-dipole or dipole-induced dipole) that tend to stretch the molecular bonds and shift the charge distribution on molecules and thus altering the energy difference between the ground and excited states of the solute molecules. This shift is not special case for fluorescence spectra but in the same principles in absorption spectra where the fluorescence represents a mirror image for the absorption [112].

From the Figures (4.13-4.15) show fluorescent spectra of Malachite green dye doped with PMMA polymer and (Cu NPs) it was observed that maximum value was at about (5298) at concentrations (2×10^{-5}) M. The intensity fluorescent of Malachite green dye doped with PMMA polymer and (Cu) nanoparticles is larger than intensity fluorescent of dye as pure and doped PMMA polymer. This behavior of fluorescent spectra is opposites to the behavior of absorbance spectra and this agreement with [114].

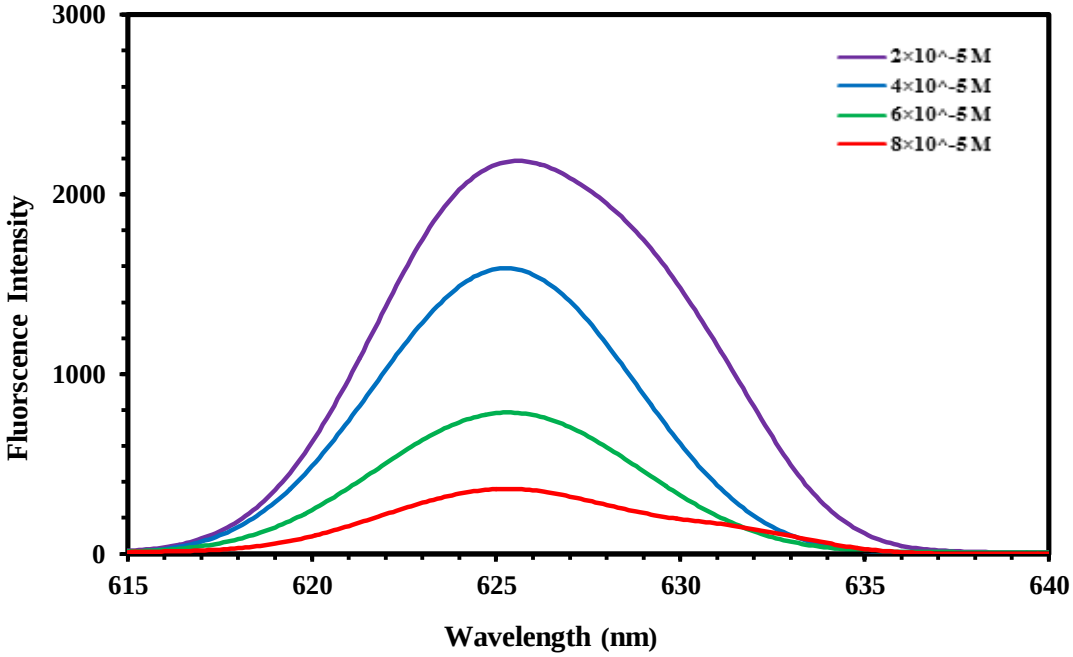

Figure (4.13): Fluorescence spectra of Malachite green pure dye at different concentrations.

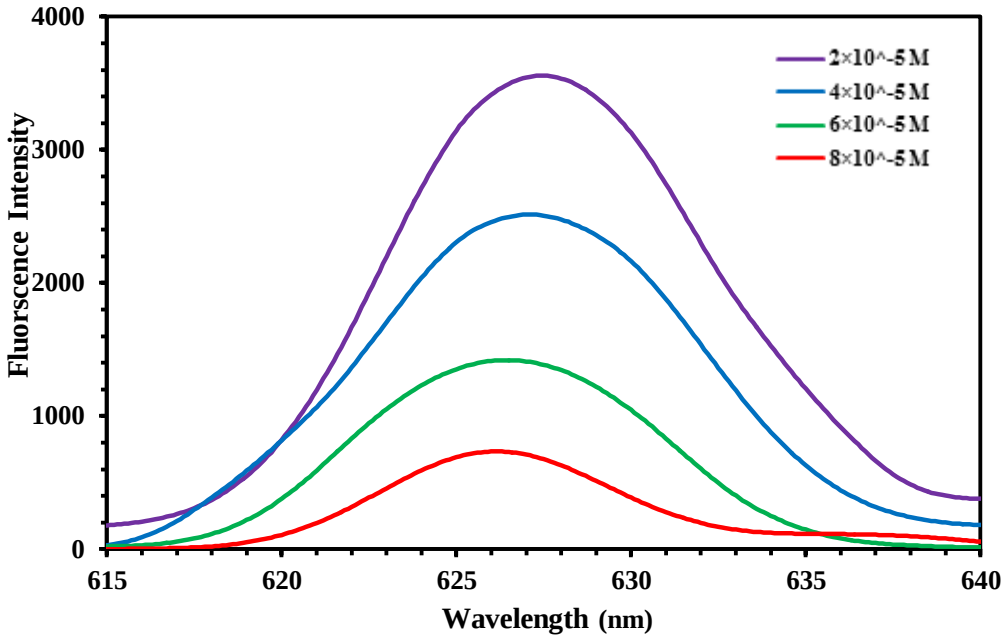

Figure (4.14):Fluorescence spectra for Malachite green dye doped with PMMA polymer at different concentrations.

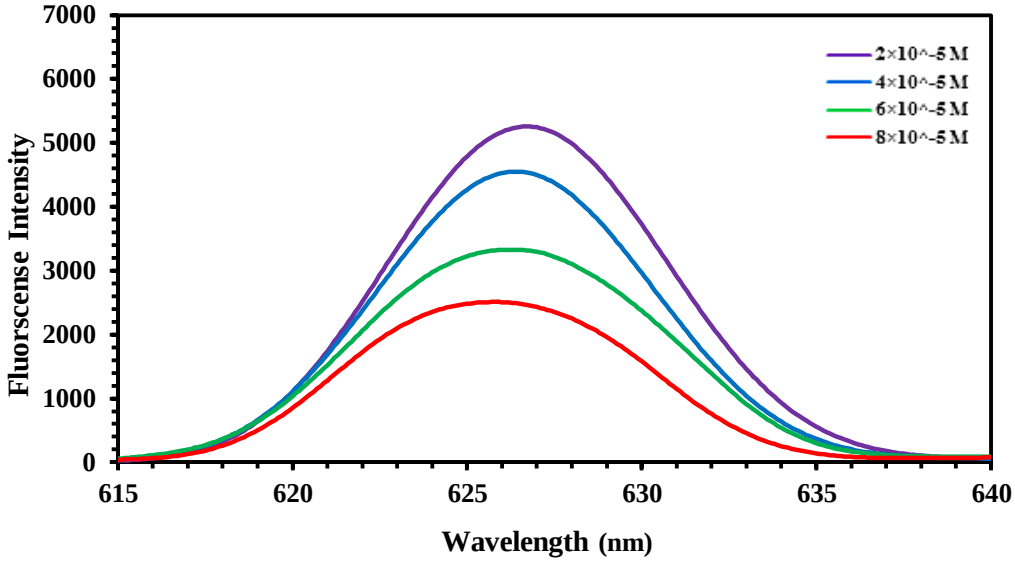

Figure (4.15): Fluorescence spectra of Malachite green dye doped with PMMA polymer and (Cu) nanoparticles at different concentrations.

4.3.2.2 Fluorescence Spectra of of Malachite green dye pure and doped with PMMA polymer and (Cu) nanoparticles (as Thin films)

Fluorescence spectra of thin films for Malachite green dye doped with PMMA polymer and (Cu) nanoparticles at (10^{-3})M prepared by drop-casting method , are shown in Figure (4.16). From this Figure observed that have narrower band width than samples as solutions its agreement with [31].

There are many factors that effect on fluorescence of dye such as concentration, impurities and self-absorption, that could affect directly the fluorescence quantum yield and consequently the energy yield of the fluorescence [115]. One of the most important characteristics of the dye doped in solid matrix is the Stokes shift. In addition, the values of the Stokes shift were increased by increasing the concentration. Fluorescence spectra of

all samples of Malachite green dye doped with PMMA polymer and (Cu NPs) were shifted towards long wavelengths.

Thin films of dye doped with PMMA polymer and (Cu) NPs showed the effect of the existence of nanoparticles on the fluorescence spectra. Thin films showed narrow band width of the emission peaks , also increase intensity agreement with[17].

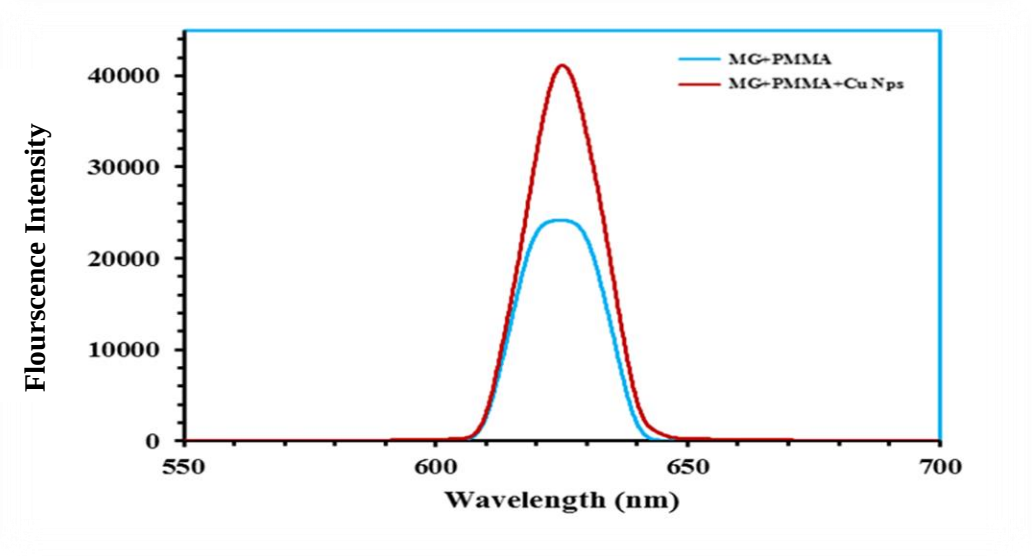

Figure (4.16): Florescence spectra of thin films of Malachite green dye doped with PMMA polymer and with PMMA and (Cu) nanoparticles.

4.4 Calculation of Quantum Efficiency and Life Time

The values of time-life and quantitative efficiency of all the prepared samples are shown in the Table (4.2). The time-life and quantitative efficiency were calculated from the equations (2.5) and (2.8) and the measurement is done by calculating the area under the fluorescence curve over the area under the absorbance curve using a computer program (GEUP 9). It is noted from the Table that the increase in concentration leads to an

increase in the lifespan of time and a decrease in quantitative efficiency, and that the highest quantitative efficiency is in the case of the dye doped with PMMA polymer and (Cu) nanoparticles. Therefore, the fluorescence energy is less than absorption and increased dye concentration leads to the displacement of the fluorescence to long wavelengths with low energies [116].

The explanation is to increase the concentration of the dye solution, the local electric field in the solution will be enhanced and the charges will be rearranged due to the electron transfer of the molecule. It became dipole of excited state more the ground than level its due to increase of solvent solution with more stability of excited state ,its reduce energy level . The following displacement position peak of the fluorescence spectrum to the longer wavelength (red shift) agree with [37] .

Table (4.2): Fluorescence intensity at maximum wavelength, quantum efficiency and life time parameters of Malachite green dye as solutions .

Material	Concentration (Mol/L)	λ_{max} (Absorbance)	λ_{max} (Fluorescence)	Fluorescence intensity	τ_F(ns)	Φ_F
MG	2×10^{-5}	616	626	2357	0.116	86%
	4×10^{-5}	616	626	1616	0.117	85%
	6×10^{-5}	616	626	783	0.119	82%
	8×10^{-5}	616	626	361	0.121	80%
MG + PMMA	2×10^{-5}	617	627	3682	0.118	92%
	4×10^{-5}	617	627	2329	0.120	90%
	6×10^{-5}	617	627	1189	0.122	88%
	8×10^{-5}	617	627	537	0.123	87%
MG +PMMA + (Cu NPs)	2×10^{-5}	618	628	5298	0.126	95%
	4×10^{-5}	618	628	4896	0.128	93%
	6×10^{-5}	618	628	3144	0.129	90%
	8×10^{-5}	618	628	2561	0.130	89%

4.5 Nonlinear Optical Properties

The nonlinear optical properties were calculated for Malachite green (MG) organic laser dye at different concentrations (2, 4, 6 and 8) $\times 10^{-5}$ M in chloroform solvent as pure and after doped with PMMA polymer and (Cu) nanoparticles and thin films doped with PMMA polymer and (Cu) nanoparticles at concentration (10^{-3}) M using Z-scan technique for two cases, closed and open aperture using CW diode pump solid state laser operating at a wavelength (457 nm) and power (84 mW) for all samples then using different powers (70 and 102) mW for concentration (8×10^{-5}) M as solution and for thin films.

4.5.1 Nonlinear Refractive Index for All Samples of Malachite Green Organic Laser Dye

Closed-aperture of Z-scan technique is used to investigated the nonlinear refractive index of all samples of Malachite green organic laser dye as pure and after doped with PMMA polymer and (Cu) nanoparticles as solutions and thin films.

The normalized transmittances of Z-scan measurements as a function of distance is shown in Figures (4.17- 4.20) for solutions and thin films the nonlinear effect region is extended from (-2) cm to (2) cm.

The peak followed by a valley transmittance curve obtained from the closed aperture Z-scan data indicates that the sign of the refraction nonlinearity is negative ($n_2 < 0$), leading to self-defocusing lensing in these samples [118].

In order to describe the Z-scan behavior in the previous Figures, when the sample moves far from the focus, the transmitted beam intensity is low and the transmittance remains relatively constant. As the sample approaches the

beam focus, intensity increases, leading to self-lensing in the sample tend to collimate the beam on the aperture in the far field, increasing the measured transmittance at the iris position. If the beam experiences any nonlinear phase shift due to the sample as it is translated through the focal region, then the fraction of light falling on the detector will vary due to the self-lensing generated in the material by the intense laser beam. In this case, the signal measured by detector will exhibit a peak and valley as the sample is translated [24].

The position of the peak and valley, relative to the z-axis, depends on the sign of the nonlinear phase shift .Where the change in the normalized transmittance from the peak of the curve to the valley (ΔT_{p-v}) is directly proportional to the nonlinear phase shift imparted on the beam. Moreover, if the beam is transmitted through the nonlinear medium the induced phase shift can also be either negative or positive accordingly when the medium is self-defocusing or self-focusing, respectively [28].

The magnitude of the phase shift can be determined from the change in transmittance between peak and valley. After the focal plane, the self-defocusing increases the beam divergence, leading to a widening of the beam at the focus and thus reducing the measured transmittance. Far from focus (Z >0),again the nonlinear refraction is low resulting in a transmittance Z-independent . The behavior of Z-scan curves was in good agreement with reference [119].The nonlinearity of dye doped with PMMA and (Cu) nanoparticles is larger than those for pure dye. As well as thin films possess very large nonlinearity as compared with dye as solutions. The relation between the nonlinear refractive index and the nonlinear phase shift is a linear increasing relation [120].Z-scan measurements indicated that pure

and dye doped and their thin films exhibited negative nonlinear refractive index , it agree with reference [20].

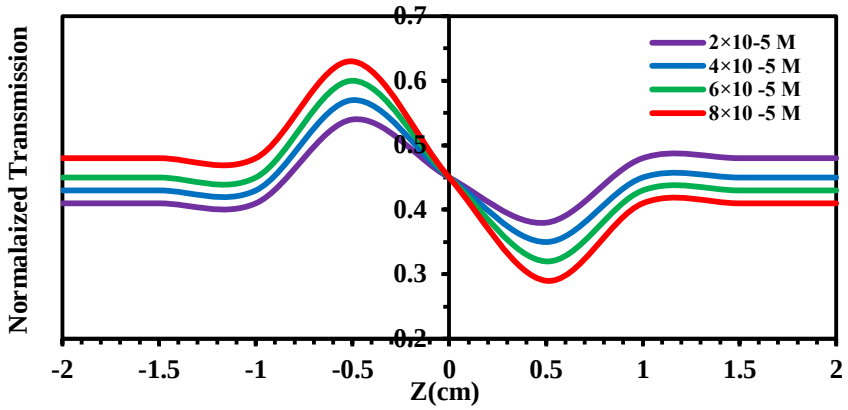

Figure (4.17): Close - aperture Z-Scan data of Malachite green pure dye at different concentrations.

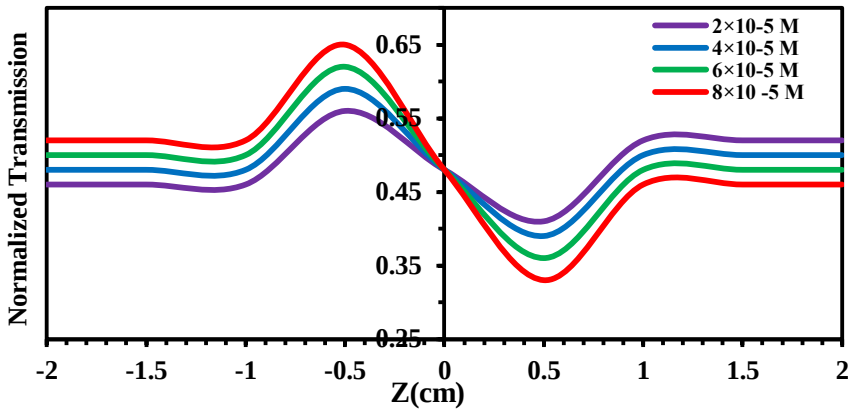

Figure (4.18): Close - aperture Z-Scan data of Malachite green dye doped with PMMA polymer at different concentrations.

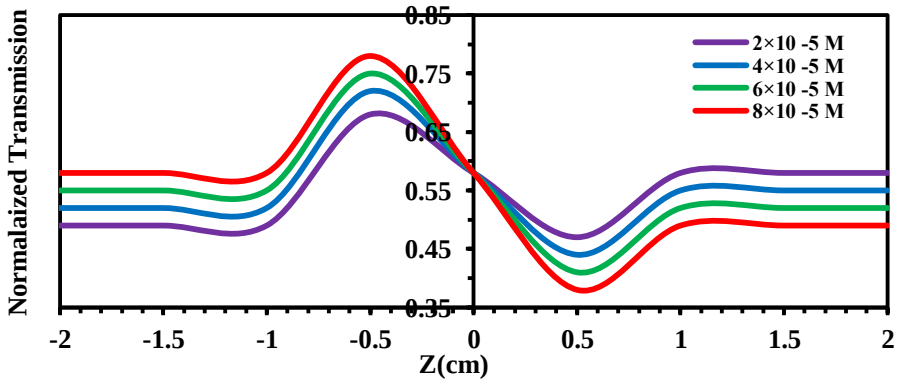

Figure (4.19):Close -aperture Z-Scan data of Malachite green dye doped with PMMA polymer and (Cu) nanoparticles at different concentrations.

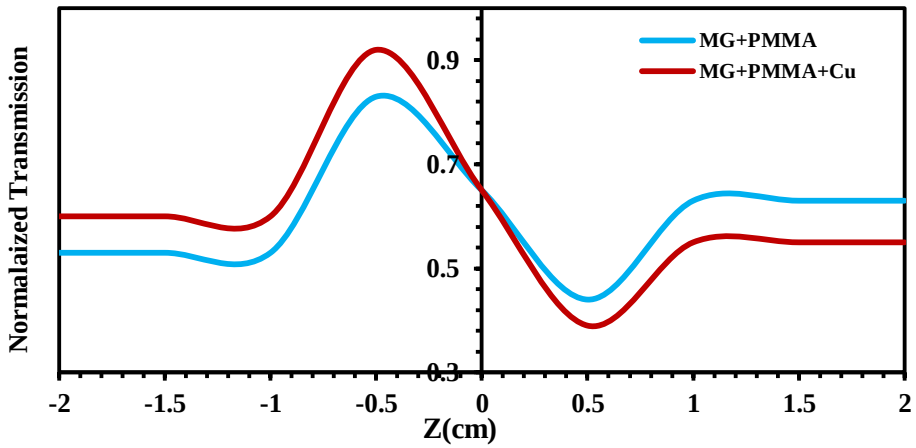

Figure (4.20): Close - aperture Z-scan data of thin films of Malachite green dye doped with PMMA polymer and (Cu) nanoparticles.

4.5.2 Nonlinear Absorption Coefficient for All Samples of Malachite Green Organic Laser Dye

The nonlinear absorption coefficient investigated for all of the prepared samples in different concentrations as solutions and thin films were measured by open-aperture Z-scan technique. The performed open aperture Z-Scan exhibits an increasing in the transmission about the focus of the lens. Open-aperture Z-scan of all samples as solution and thin films at power (84) mW are shown in Figures (4.21- 4.24).

The behavior of transmittance starts linearly at different distances from the far field of the sample position (-Z). At the near field, the transmittance curve begins to decrease until it reaches the minimum value (T_{min}) at the focal point, where (Z= 0 mm). The transmittance begins to increase towards the linear behavior at the far field of the sample position (+Z).The change of intensity, in this case, is caused by two photon absorption phenomena when in the sample travels through beam waist as shown in Figures (4.21- 4.23) respectively, its agree with [118].

The open-aperture Z-scan defines variable transmittance values, which was used to determine absorption coefficient.(Saturable Absorption) phenomenon were observed for open-aperture Z-scan of thin films under study as shown in Figure (4.24). The behavior of transmittance curves starts linearly at different distance from the far field of the sample position (-Z).

At the near field the transmittance curve begins to increase until it reaches the maximum value (T_{max}) at the focal point, where Z=0 mm. Afterwards, the transmittance begins to decrease toward the linear behavior at the far field of the sample position (+Z).The transmittance is sensitive to the nonlinear absorption as a function of input power intensity. The change in intensity is caused by saturation absorption phenomena in the sample as it travels through the beam waist. In the focal plane where the intensity is greatest, the largest nonlinear absorption is observed. At the far field of the Gaussian beam, where , the beam intensity is too weak to elicit nonlinear effects. A symmetric peak value is contributed to the negative nonlinear absorption coefficient, indicates that the sample shows a bleaching-like behavior (saturation of absorption) [119].

From the results its it observed that samples of dye doped with PMMA polymer and (Cu) nanoparticles have high nonlinearity than those which it without nanoparticles and thin films of the prepared samples were exhibited better nonlinearity than liquid samples. This is suggested to be take place due to the $\pi-\pi^*$ stacking in super molecular interactions between delocalized electrons in solid samples. In addition, in the case of thin films, the molecule orientation is crucial where molecules can be arranged either by hemitropic alignment or columnar stacking on the substrate as almost organic dyes are self-organized materials [120].As well as thin films possess very large

nonlinearity as compared with dyes as solution. This is due to increasing number of molecules per volume unit at high concentrations, it agree with [20].The closed-aperture Z-Scan defines variable transmittance values, which used to determine the nonlinear phase shift ΔΦ using equation (2.22) and the nonlinear refractive index (n_2) using equation (2.21),nonlinear absorption coefficient (β) using equation (2.25).The nonlinear parameters are calculated ,as tabulated in Table (4.3).

This Table show that non-linear refractive increased but nonlinear absorption coefficient decreased with increasing the concentrations, as increasing the values of linear parameters (α_o and n_o). This is due to decreasing number of molecules per volume unit at low concentrations. The results showed that the nonlinear optical properties for all samples of Malachite green dye doped with PMMA polymer and (Cu) nanoparticles as (solutions and thin films) were higher as compared with pure dye.

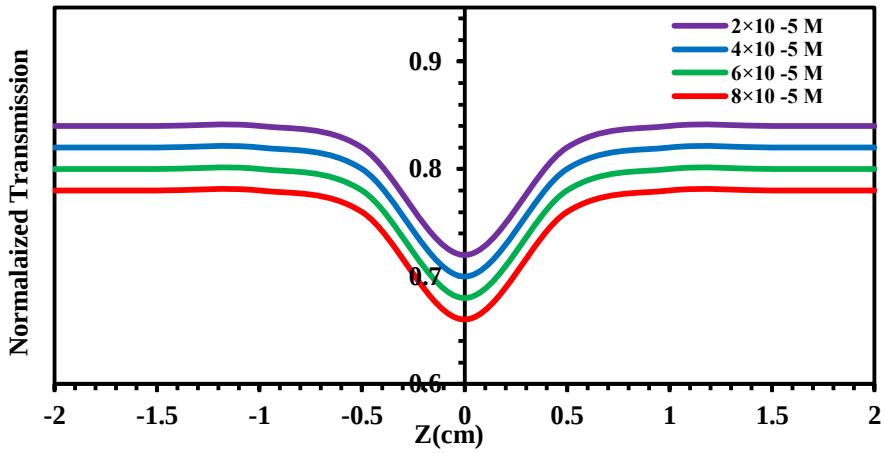

Figure (4.21): Open-aperture Z-Scan data of Malachite green pure dye. at different concentrations.

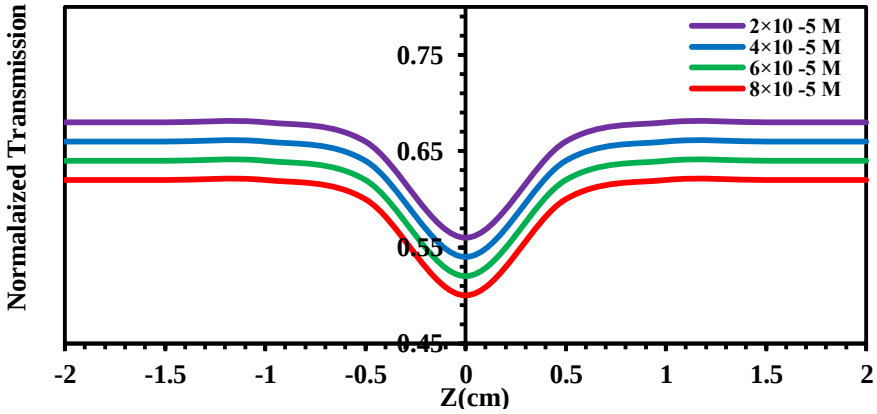

Figure (4.22): Open-aperture Z-Scan data of Malachite green dye doped PMMA polymer at different concentrations.

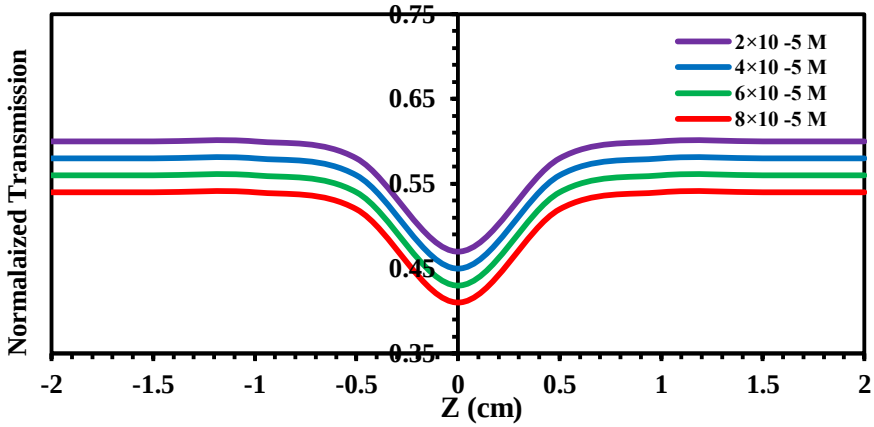

Figure (4.23): Open-aperture Z-Scan data of Malachite green dye doped PMMA polymer and (Cu) nanoparticles at different concentrations

.

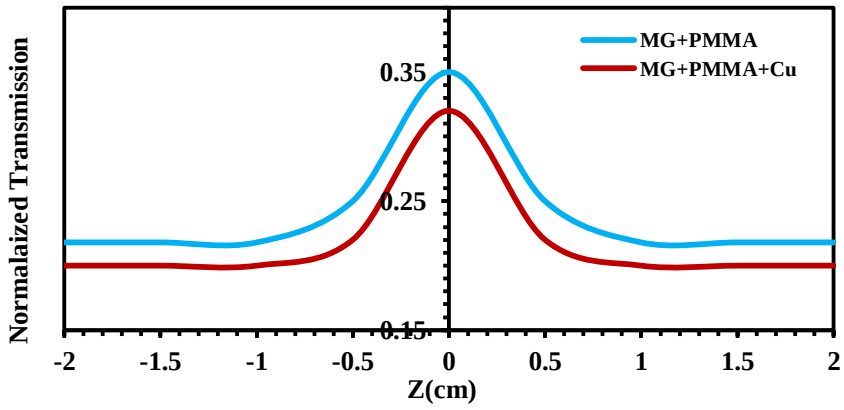

Figure (4.24): Open-aperture Z-Scan data of thin films for Malachite green dye doped with PMMA polymer and (Cu) nanoparticles .

Table (4.3): Linear and nonlinear optical parameters for different concentrations of Malachite green dye as solutions and thin films at (λ=457nm).

Material	Concentration (Mol/L)	T%	($\alpha_\circ$) cm^{-1}	$n_\circ$	ΔT_{P-V}	n_2 (cm^2/mW)	T(z)	β (cm/mW)
MG (solutions)	2×10^{-5}	0.978	0.0155	1.19	0.18	4.233×10^{-10}	0.73	1.699×10^{-3}
	4×10^{-5}	0.966	0.0247	1.229	0.26	5.102×10^{-10}	0.71	1.558×0^{-3}
	6×10^{-5}	0.941	0.0333	1.25	0.34	7.081×10^{-10}	0.69	1.421×10^{-3}
	8×10^{-5}	0.913	0.0472	1.54	0.42	8.078×10^{-10}	0.66	1.235×10^{-3}
MG+ PMMA (solutions)	2×10^{-5}	0.984	0.0213	1.29	0.24	5.121×10^{-10}	0.54	2.190×10^{-3}
	4×10^{-5}	0.975	0.0339	1.45	0.32	6.132×10^{-10}	0.52	2.088×10^{-3}
	6×10^{-5}	0.967	0.0604	1.59	0.41	7.802×10^{-10}	0.50	1.749×10^{-3}
	8×10^{-5}	0.953	0.0909	1.66	0.49	9.371×10^{-10}	0.48	1.582×10^{-3}
Thin Film of (MG+PMMA	10^{-3}	0.644	1680.83	2.30	0.55	10.453×10^{-3}	0.6	2.612
MG+PMMA + Cu NPs (solutions)	2×10^{-5}	0.731	0.3120	2.29	0.28	7.6869×10^{-10}	0.51	3.322×10^{-3}
	4×10^{-5}	0.727	0.3183	2.31	0.37	9.110×10^{-10}	0.49	3.290×10^{-3}
	6×10^{-5}	0.722	0.3247	2.33	0.48	10.822×10^{-10}	0.47	3.177×10^{-3}
	8×10^{-5}	0.713	0.3373	2.38	0.59	11.121×10^{-10}	0.44	3.008×10^{-3}
Thin Film of (MG+PPMA +Cu NPs)	10^{-3}	0.708	1680.92	2.73	0.64	12.861×10^{-3}	0.56	3.541

4.6 Optical Limiting Behavior of Organic Dye

The optical limiting behavior, was performed by closed-aperture Z-Scan with the same laser used in Z-scan technique. Figures (4.25- 4.28) respectively give the optical limiting characteristics at room temperature for all samples of Malachite green organic laser dye as solutions and thin films doped with PMMA polymer and Cu nanoparticles were dissolved in Chloroform solvent respectively. The samples show very good optical limiting behavior arising from nonlinear refraction[117].

The output power rises initially with the increasing in input power, but after a certain threshold value, the sample starts defocusing the beam resulting in a greater part of the beam cross-section being cut off by the aperture. Thus, the transmittance recorded by the photodetector remained reasonably constant showing a plateau region.

Thin films samles give optical power limiting threshold and limiting amplitude less as compared with the dye as solutions, therefore, the properties of optical limiting for thin films of organic laser dye are better than of dye as solutions,due to increasing number of molecules per unit volume which is lead to increasing the nonlinear absorption ,as listed in Table (4.4).This behavior agree with [118].

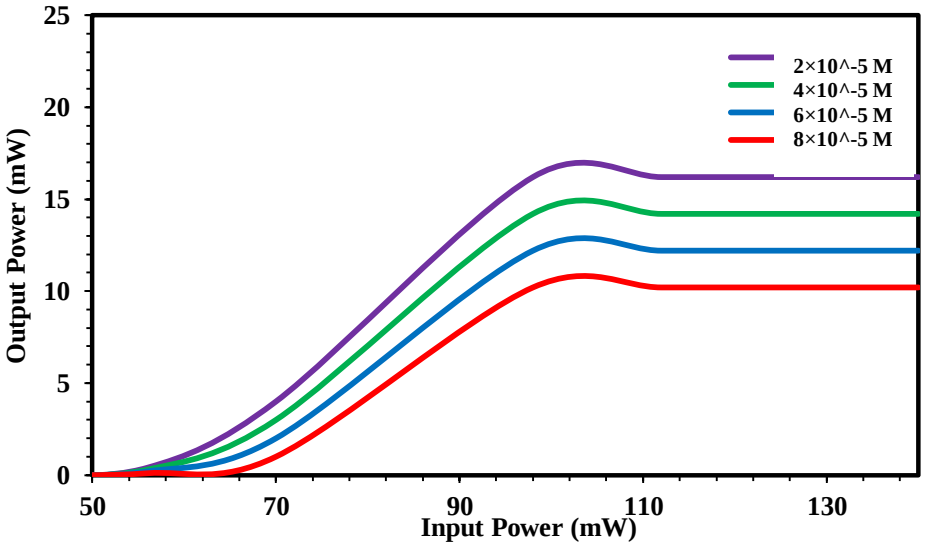

Figure (4.25): Optical limiting response of Malachite green pure dye at different concentrations.

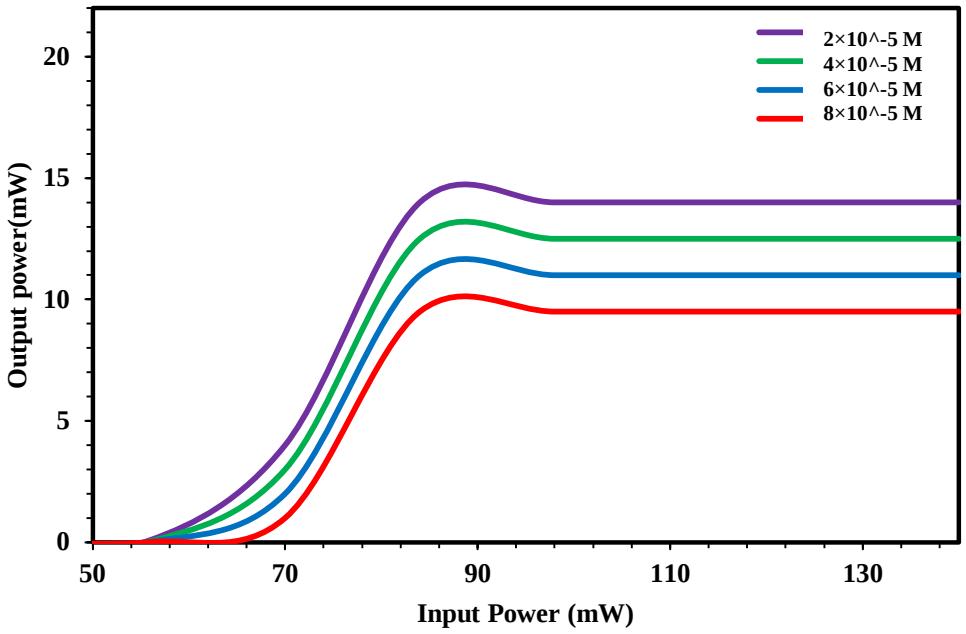

Figure (4.26): Optical limiting response of Malachite green dye doped PMMA polymer at different concentrations.

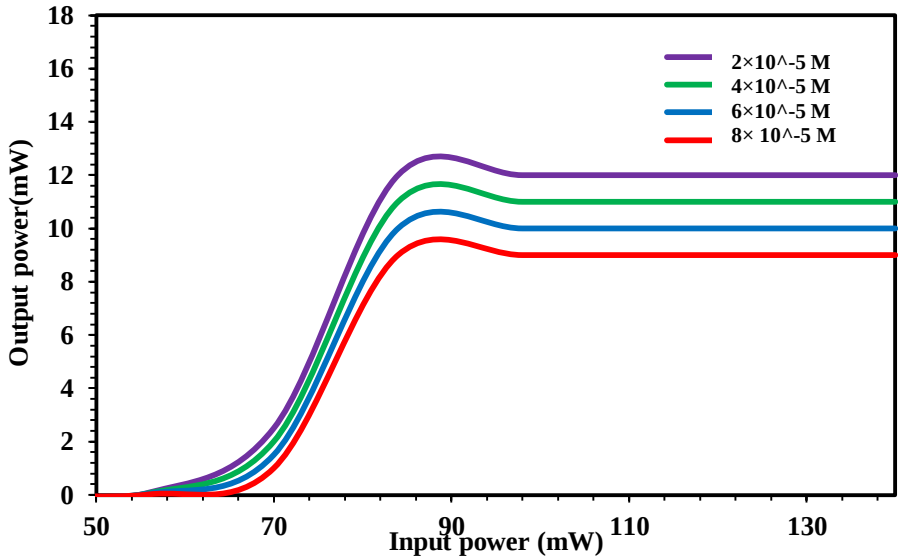

Figure (4.27): Optical limiting response of Malachite green dye doped PMMA polymer and (Cu) nanoparticles at different concentrations.

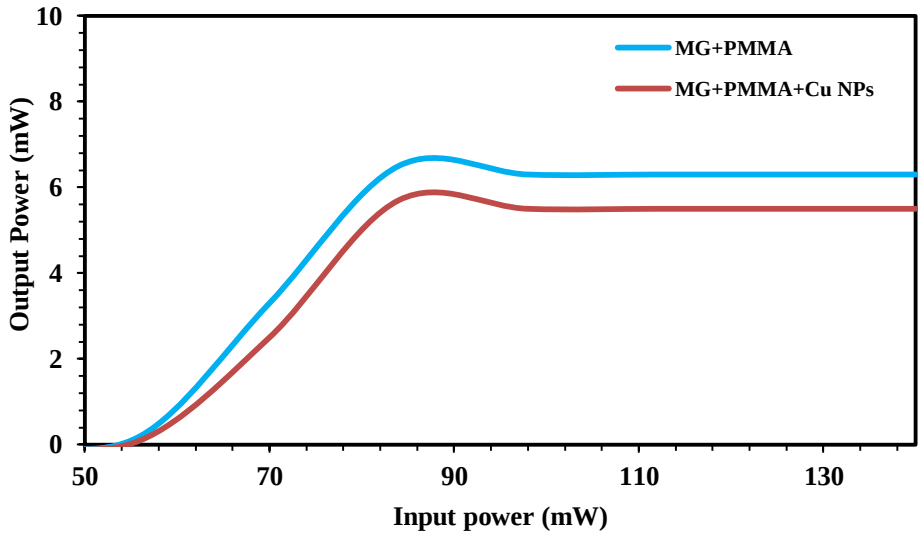

Figure (4.28): Optical limiting response for thin films of Malachite green dye doped PMMA polymer and (Cu) nanoparticles .

Table (4.4): The Optical limiting response of Malachite green dye pure and doped PMMA polymer and (Cu) nanoparticles as Solutions and thin films.

Material	Concentration (Mol/L)	Limiting Amplitude	Limiting Threshold
MG (Solutions)	2×10^{-5}	16	104
	4×10^{-5}	14.2	103
	6×10^{-5}	12.3	102
	8×10^{-5}	10.2	102
MG+PMMA (Solutions)	2×10^{-5}	14	89
	4×10^{-5}	12.5	88
	6×10^{-5}	11	88
	8×10^{-5}	9.5	87
Thin Film MG+PMMA	10^{-3}	12.5	83
MG+ PMMA+ Cu NPs (Solutions)	2×10^{-5}	11	86
	4×10^{-5}	10	85
	6×10^{-5}	9.3	85
	8×10^{-5}	5.8	84
Thin Film MG +PMMA+ Cu NPs	10^{-3}	5.7	82

4.7 Nonlinear Optical Properties at Different Laser powers

The nonlinear parameters (nonlinear refractive index and nonlinear absorption coefficient) for all samples at concentration (8×10^{-5})M as solutions and thin films at (10^{-3}) M are calculated in different laser power (70,84 and 102) mW as shown in Figures (4.29- 4.38) . The results was tabulated in Table (4.5), from this Table it can be seen that the values of nonlinear refractive index (n_2) increased with increasing laser powers, but the values of nonlinear absorption coefficient (β) decreased with increasing laser powers .

The nonlinearity of thin films of doped dye is larger than those for pure dye as solutions due to adding PMMA polymer and (Cu) NPs, and increasing number of molecules per volume unit ,as well as thin films have thickness smaller than liquid dye which is lead to increasing the nonlinear phase shift, its agreement with [48]. The transmittance is sensitive to the nonlinear absorption as a function of input power intensity. The change in intensity is caused by saturation absorption in the sample as it travels through the beam waist. In the focal plane where the intensity is the greatest, the largest nonlinear absorption is observed.

At the far field of the Gaussian beam, where , the beam intensity is too weak to elicit nonlinear effects. A symmetric peak value is contributed to the negative nonlinear absorption coefficient (β), indicates that the sample shows a bleaching-like behavior (saturation of absorption). This behavior agrees with[17].The variation of nonlinear absorption coefficient is inversely proportional to the input power, the nonlinear absorption showed the power dependence. As the power increase there is a significant decreasing in the nonlinear absorption coefficient [119].

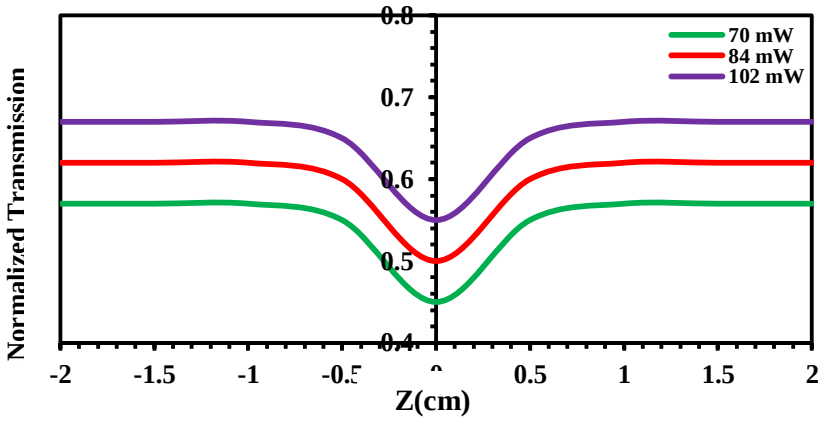

Figure (4.29): Open-aperture Z-scan data for Malachite green pure dye as solutions at concentration (8×10^{-5} M) at different laser powers .

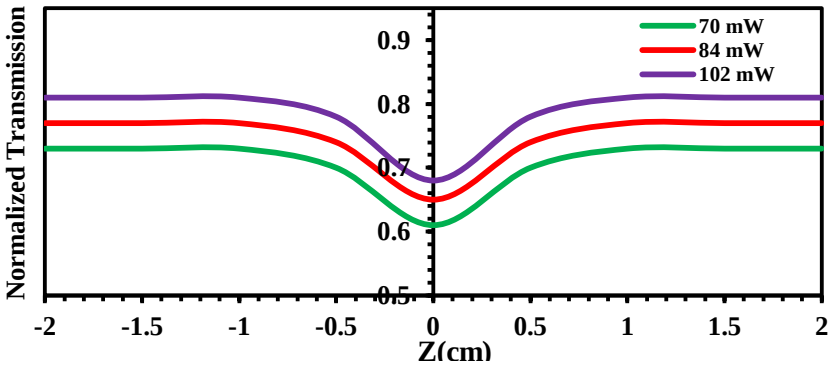

Figure (4.30): Open-aperture Z-scan data for Malachite green dye doped PMMA polymer as solutions at concentration (8×10^{-5} M) at different laser powers .

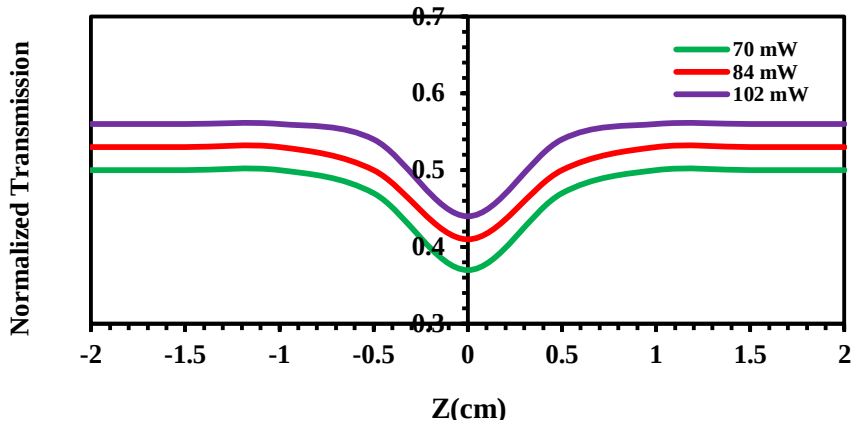

Figure (4.31): Open-aperture Z-scan data for Malachite green dye doped PMMA polymer and Cu NPs as solutions at concentration (8×10^{-5} M) at different laser powers .

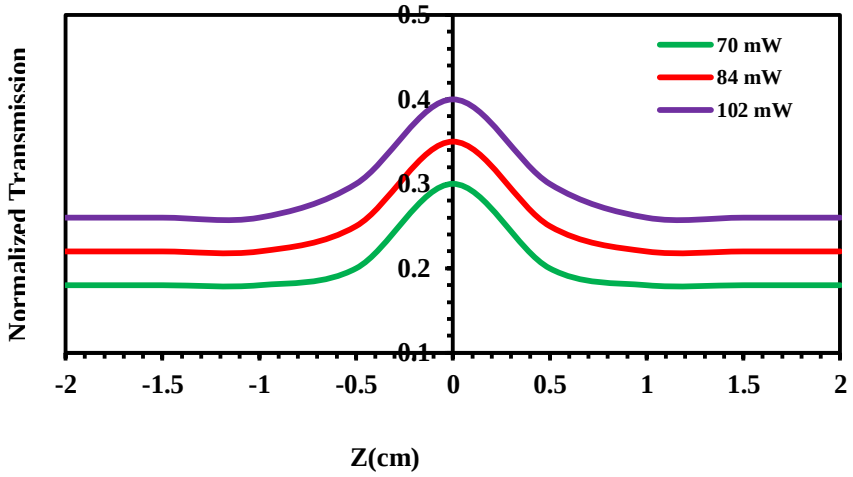

Figure (4.32): Open-aperture Z-scan data for thin film for (MG) dye doped PMMA polymer at different laser powers .

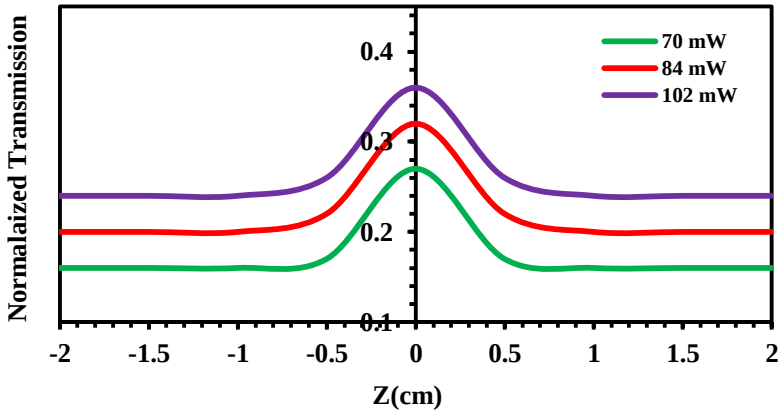

Figure (4.33): Open-aperture Z-scan data of thin film for (MG) dye doped PMMA polymer and Cu NPs at different laser powers .

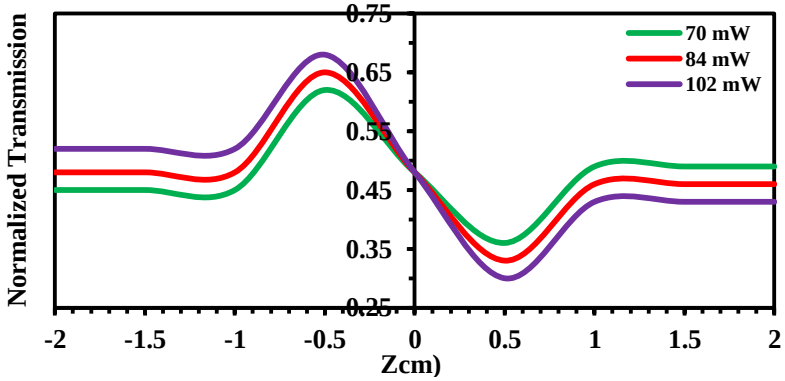

Figure (4.34): Close-aperture Z-scan data of Malachite green pure dye as solution at concentration (8×10^{-5} M) at different laser powers .

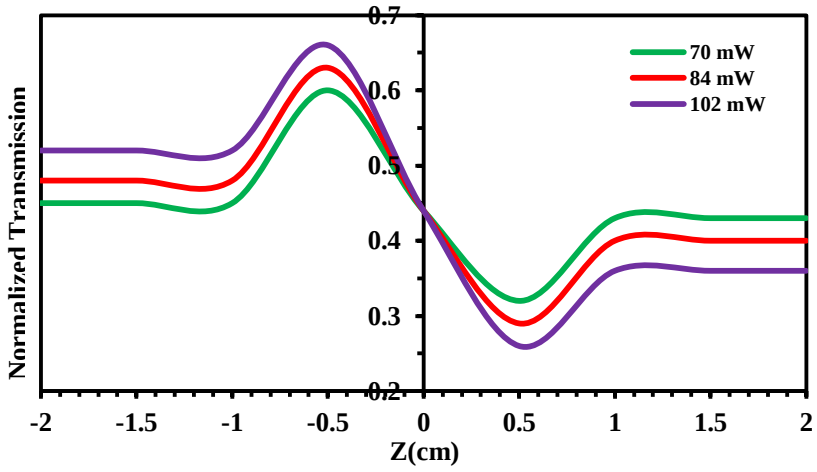

Figure (4.35): Close-aperture Z-scan data of Malachite green dye doped PMMA polymer as solution at concentration (8×10^{-5} M) at different laser powers .

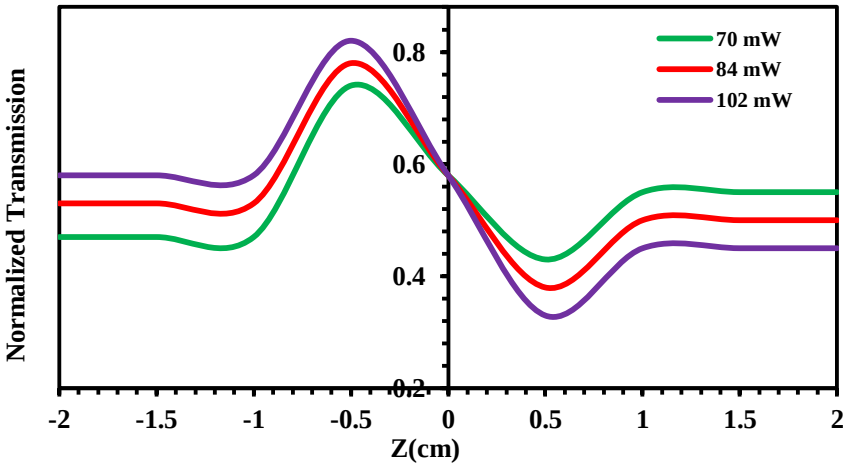

Figure (4.36): Close-aperture Z-scan data of Malachite green dye doped PMMA polymer and Cu NPs as solution at concentration (8×10^{-5} M) at different laser powers .

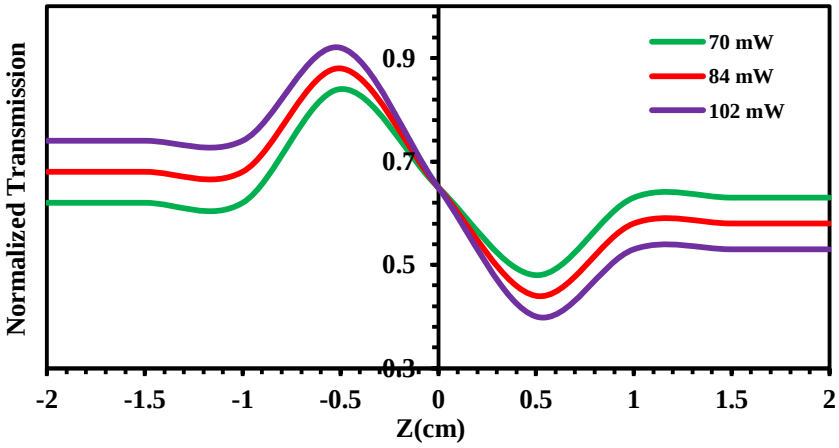

Figure (4.37): Close- aperture Z-scan data of thin film for Malachite green dye doped PMMA polymer at different laser powers .

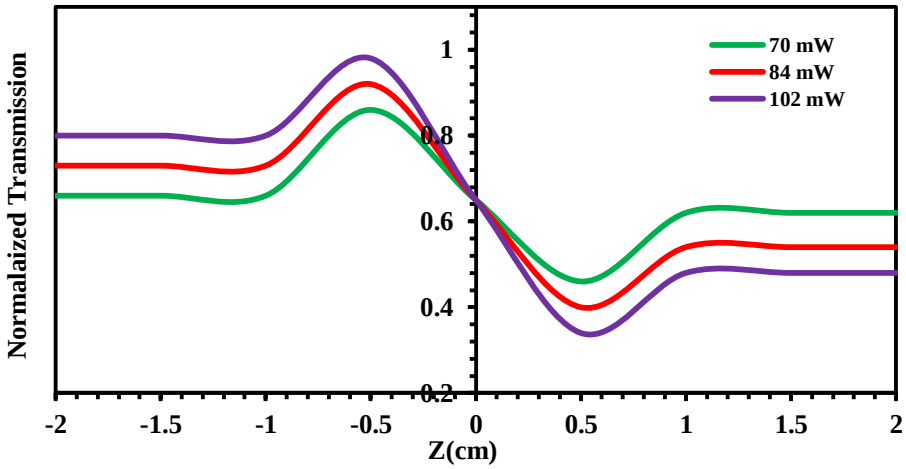

Figure (4.38): Close-aperture Z-scan data of thin film of Malachite green dye doped PMMA polymer and Cu NPs at different laser powers .

Table (4.5): The nonlinear optical parameters for Malachite green dye pure and doped PMMA and with Cu NPs as solutions and thin films at (λ= 457nm) at different laser powers.

Material	Powers (mW)	ΔT_{P-V}	$\Delta\Phi_o$	n_2 (cm^2/mW)	T(z)	β (cm/mW)
MG (Solutions)	70	0.26	0.64	6.024×10^{-10}	0.61	1.316×10^{-3}
	84	0.32	0.78	8.078×10^{-10}	0.65	1.235×10^{-3}
	102	0.38	0.93	9.083×10^{-10}	0.68	1.152×10^{-3}
MG +PMMA (Solutions)	70	0.28	0.68	7.13×10^{-10}	0.45	1.632×10^{-3}
	84	0.34	0.83	9.371×10^{-10}	0.5	1.582×10^{-3}
	102	0.4	0.98	10.231×10^{-10}	0.55	1.471×10^{-3}
Thin Film MG +PMMA	70	0.31	0.76	9.138×10^{-3}	0.3	2.713
	84	0.4	0.98	10.453×10^{-3}	0.35	2.612
	102	0.49	1.20	11.610×10^{-3}	0.4	2.432
MG+PMMA+ Cu NPs (Solutions)	70	0.36	0.88	10.358×10^{-10}	0.37	2.13×10^{-3}
	84	0.44	1.08	11.121×10^{-10}	0.4	2.008×10^{-3}
	102	0.52	1.28	12.581×10^{-10}	0.44	1.931×10^{-3}
Thin Film of MG+PMMA+ Cu NPs	70	0.4	0.98	11.791×10^{-3}	0.27	3.583
	84	0.52	1.28	12.861×10^{-3}	0.32	3.322
	102	0.64	1.57	13.997×10^{-3}	0.36	3.117

4.8 Conclusions

The main conclusions that are obtained in this work:

1. Preparation thin films of Malachite green organic laser dye have been successfully by drop-casting method on glass substrate.
2. The grain size of thin films, calculated from atomic force microscope (AFM) in the range of (30 - 41) nm.
3. All samples of Malachite green organic laser dye doped with PMMA polymer and (Cu) nanoparticles possess large linear optical properties as compared with samples of pure laser dyes, as a result it can be used as optical and photonic devices.
4. The linear refractive index (n_o) and linear absorption coefficient (α_o) of Malachite green organic laser dye doped with PMMA polymer and (Cu) nanoparticles (solutions and thin films) are larger than those for pure dye.
5. Fluorescence intensity of all solutions of Malachite green organic laser dye doped with PMMA polymer and (Cu) nanoparticles decreasing linearly with increasing of concentrations.
6. Fluorescence intensity of thin film Malachite green dye doped with PMMA and (Cu) nanoparticles is higher than these for thin film of the dye doped of PMMA polymer only, as a result it can be used as active laser medium.
7. Decreasing the value of quantum efficiency with increasing in concentration for all prepared samples.
8. The nonlinear optical properties of all samples of Malachite green organic laser dye doped with PMMA polymer and (Cu) nanoparticles (solutions and thin films) are larger than those for pure dye.
9. The nonlinear refractive index for all samples shows the behavior self-defocusing, and two photon absorption in nonlinear absorption coefficient.

10. The nonlinear absorption coefficient for all thin films of laser dye and doped dye show saturable absorption phenomena.
11. The nonlinear optical properties of thin films of Malachite green organic laser dye with (Cu) nanoparticles are higher than the thin film without adding nanoparticles.
12. The nonlinear refractive index of all samples of Malachite green organic laser dye increases when increasing laser powers but the nonlinear absorption coefficient of all samples decreases when increasing laser powers.
13. Optical limiting properties increase with decreasing concentrations for all samples.
14. Optical limiting properties of Malachite green organic laser dye with (Cu) nanoparticles (solutions and thin films) are better than those for pure dyes as a result it can be used as better optical limiting in electro-optical devices.

4.9 The Suggestions and Future Works

In this context, a further investigation can be suggested as future works:

1. Study spectral linear and nonlinear optical properties of dye solution with another types of solvents at different concentrations.
2. Study nonlinear optical properties of dye using different types of nanoparticles at different ratios.
3. Study effect for adding another types of polymers on spectral, linear and non-linear of the dye.

References

[1] R. Menzel, ***"Photonics : Linear and Nonlinear Interactions of Laser Light and Matter"***, 2nd Edition, Springer, Berlin, ISBN: 978-3-662-04521-3, (2001).

[2] R. Boyd, ***''Nonlinear Optics''***, 2nd Edition Academic press, London, (2003).

[3] P. Brwee, ***"Organic Chemistry"***, 2nd. Ed., prentice Hall New Jersey, (1998).

[4] U. Brackmann***,"Laser Dyes",*** 3rd Edition, Lambda Physik, Gottingen, (2000).

[5] A. Kurian and N. George, "***Laser Chemistry"***, Vol. 20 (2-4), 99-110, (2002).

[6] U. Gubler, C. Bosshard and K. Lee, ***"Polymers in Photonics Applications"***, (2002).

[7] F. Mauro, "***Thermo-Optical Effects in Z-Scan Measurements Using High-Repetition-Rate Lasers"***, Journal Optics, Pure Applied, Optics, 1,6,662- 667, (1999).

[8] S. Singh, V.Kanetkar , G.Sridhar, V. Muthuswamy and K. Raja, ***" Solid-State Polymeric Dye Lasers"***, Journal of Luminescence, 1 , 285–291, (2003).

[9] D. Yan, S. You and W. Pei, ***"Effect of Ag Nanoparties on Optical Properties of R6G Doped PMMA Films"***, Chemical Physics Letters, 24, 4, 954 - 956 (2006).

[10] Y. Wenhui, W. Hongcai, O. Masanori and Y. Katsumi , ***"Enhancement of Third- Order Optical Nonlinearities By Conjugate Polymer-Bonded Carbon Nanotubes"***, Journal Applied Physics, 98, 3, 034301- 034307,(2005).

[11] F. Amal ***"A Comparative Study of Third-Order Electronic and Thermally Induced Optical Nonlinearity in Rodamin 610 Doped PMMA Thin Film"***, Al-Mustansiriyah Journal of Science 24.2 (2013).

[12] B. Ulrich,***"Lambdachrome Laser Dyes",*** 3rd Edition, D-37079 Goettingen,Germany, (2000).

[13] F. Radhi, ***" Nonlinear Responses and Optical Limiting Behavior of 2-Chloro-5-Nitroanisole Dye Under CW Laser Illumination"*** ,Journal of Kerbala University,10, 4,181 – 186, (2012).

[14] H. Shaaker , H. Badran and W. Hussain, ***"Linear and nonlinear optical properties of I and $NaBH_4$ doped Malachite green thin films***", Archives of Applied Science Research, 4(4), 1804-1810, (2012).

[15] R. Manshad and Q. Hassan, ***"Nonlinear Characterization of Orcein Solution and Dye Doped Polymer Film For Applicaion in Optical Limiting"***, Journal of Basrh Researches, 38(4), pp.125-136, (2012).

[16] V. Sukumarana and A. Ramalingamb, ***"Nonlinear studies of malachite green polymer***", Optik-International Journal for Light and Electron Optics, 124 (17), 3001-3003, (2013).

[17] M. Rusal, F. Zainab and A. Rawaa, " ***Nonlinear Optical Properties of PMMA Composite using Z-Scan Technique***", University of Baghdad Institute of Laser for Postgraduate Studies, 12, 27-35 (2013).

[18] H. Kitching, A. Kenyon, and I. Parkin, "***The interaction of gold and silver nanoparticles with a range of anionic and cationic dyes"***, Physical Chemistry Chemical Physics, *16*(13), 6050-6059, (2014).

[19] L. Guru, ***"Malachite green doped PVA film for nonlinear optical applications"***, Journal of Chemical and Pharmaceutical Sciences, ISSN: 0974-2115 (2015).

[20] J. Worood, ***"A Study of Optical Properties of Acridine Dye and Alumina Nanoparticles Doped in PMMA Polymer''***, M.sc. Thesis, University of Babylon, (2015).

[21] I. Hussein and S. Abdulkareem***,"Nonlinear optical properties and optical power limiting effect of Giemsa dye"***, Optics Laser Technology, 82, 150-156, (2016).

[22] K. Lamyaa ***"The study of nonlinear optical properties of rhodamine B dye and TiO2 nanoparticles doped in PMMA polymer."*** *Iraqi Journal of Physics* 15.33 : 96-100, (2017).

[23] H. Imad Al-Deen , A. Ali and R. Jaber, ***"Third-Order Nonlinear Optical Properties and Optical Limiting Behavior of Celestin Blue B Dye Doped Polymer Films",*** *Journal of Photonic Materials and Technology*, *4*(1), 1-7, (2018)

[24] R. Mohammad, L. Aboud and A. Jassim, ***"Study of molecular electronic energy levels of malachite green dye",*** AIP Conference Proceedings, 2144, 1, 030022, (2019).

[25] T. Noor Al-huda, ***''Spectroscopic Study of Some New Prepared Organic Dyes as Optical Limiting''***, Ph.D. Thesis, College of Science, University of Babylon, (2019).

[26] A. Jassim, L. Aboud and R. Mohammad, ***"Study the Optical Properties of ($C_{52}H_{54}N_4O_{12}$) Dye"***, IOP Conference Series: Materials Science and Engineering (928, 7, 072004), (2020).

[27] S. Bashair, ***"Spectroscopic Study of Some Organic Dyes as Laser Active Medium"***, Ph.D. Thesis, College of Science, University of Babylon, (2020).

[28] J. Shymaa, ***"Utilizing of Rhodamine B dye as a laser active medium"***, Ph.D. Thesis, College of Science, University of Babylon, (2021).

[29] O. Muller , C. Hege , M. Guerchoux and L. Merlat ***,"Synthesis, characterization and nonlinear optical properties of polylactide and PMMA based azophloxine nanocomposites for optical limiting applications"***, Materials Science & Engineering, 276,(2022).

[30] S. Jeyaram, ***"Nonlinear optical responses in organic dye by Z-scan method"***, *Journal of Optics*, 1-6, (2022).

[31] F. Duarte, ***"Tunable Laser Optics"***, Elsevier Academic, New York, Appendix of Laser Dyes ,(2003).

[32] K. Shanshal, ***"Study of The Effect of Concentration on The Quantum Efficiency of Copper Phthalocyanine Dye (CuPc)"***, Ms.c Thesis, University of Al-Mustansiriya, (2005).

[33] Z. Sadik and A. Jaffar, ***"Third Order Optical Nonlinearities of C450 Doped Polymer Thin Film Investigated by The Z-Scan "***, Advances in Materials Physics and Chemistry, 2,43-49, (2012).

[34] J. Khawla and F. Tawil. ***"Study the optical properties of Fluorescein sodium dye doped in polymer Poly Polyvinyl alcohol for different thickness"***, Journal of Karbala university ,14.1, 4-19, (2018).

[35] M. Abdullah, ***"Study Spectroscopic for Dyes R101 and CV670 in Liquid and Solid Media"***, M.sc. Thesis, University of Baghdad,(2005).

[36] U. Raikar, V.Tangod, B .Mastiholi and S. Sreeni Vasa, ***" Solvent Effects and Photo Physical Studies of ADS 560 EI Laser Dye"***, M.sc. Thesis, Department of Physics , Karnatak University , (2010).

[37] A. Raducan, A. Olteanu, M. Puiu, and D. Oancea, ***"Influence of surfactants on the fading of malachite green"***, Central European Journal of Chemistry, *6*(1), 89-92, (2008).

[38] R. Sundari and P.Palanisamy ***"Optical nonlinearity of a triphenylmethane dye as studied by Z-scan and self-diffraction techniques"***, *Modern Physics Letters B*, *20*(15), 887-897, (2006).

[39] J.Schuhz, ***"Polymer Material Science "***, Englewood Cliffs, New Jersey (1974).

[40] D. Margerison and G. Eust, ***"An Introduction to polychemistry"***, pergamon Press Ltd New York (1964).

[41] A. Ledwith, ***"Molecular Behavior and Development of Polymer Material "***, Chenpoint and Hall, London (1975).

[42] J. Fink, "***Reactive Polymers Fundementals and applications"***, William Andrev, Inc. U.S.A (2005).

[43] P. Ang, M. Čehovski, F. Lompa, C. Hänisch, D. Samigullina, S. Reineke and H. Johannes, ***"Organic Dye-Doped PMMA Lasing***", Polymers, *13*(20), 3566, (2021).

[44] R. Manshad and Q. Hassaen***, "Optical Limiting Properties of Magenta Doped PMMA Under CW Laser Illumination"***, Pelagia Research Library, 3, 6, 3696-3702, (2012).

[45] Z.Tadmor and G.Gogos, ***"Principles of Polymer Processing"***, 2nd ed, Wiley&Sons. Inc.(2006).

[46] B. Bhushan, ***''Nanotechnology"***, Hand Book, Springer Heidelberg Dordrecht London New York, Nanoprobe Laboratory for Bio- and Nanotechnology and Biomimetics (NLB2) Ohio State University, ISBN: 978-3-642-02524-2, (2010).

[47] I. Kareem,***"Optical Properties of Prepared Nanostructure Palladium"***, Thesis, University of Baghdad Institute of Laser for Postgraduate Studies,(2014).

[48] P. Khanna, S. Gaikwad, P. Adhyapak, N. Singh and R. Marimuthu ***"Synthesis and characterization of copper nanoparticles"***, Materials Letters, 61(25), 4711-4714, (2007).

[49] M. Gawande, B. Goswami, A. Felpin, F. Asefa, T. Huang, X. Silva, R and R.Varma, ***"Cu and Cu-based nanoparticles: synthesis and***

applications in catalysis". Chemical reviews, 116(6), 3722-3811, (2016).

[50] C. Dudley,***"Absorption, Fluorescence and Amplified Spontaneous Emission of Blue-Emitting Dyes"***, M.sc Thesis, Washington State University, (2004).

[51] J. Lakowicz, ***"Principles of Fluorescence Spectroscopy"***, Plenum Press, New York. (1983).

[52] D. Robert ***"Introduction to Instrumental"***, Mc Graw Hill , INC , (1987).

[53] D.Elson, J.Siegel, K. Lauritsen, M. Wahl, and R. Erdmann, ***"Fluorescence Lifetime System for Microscopy and Multiwell Plate Imaging with a Blue Picosecond Diode Laser"***, Optics Letters , 27, 16,(2002).

[54] A. Rodnyi and I. V. Khodyuk, ***"Optical and Luminescence Properties of zinc oxide"***, 111, 5, 776-785,(2011).

[55] R. J. Keyes, ***"Optical and infrared detectors"***, Springer Verlag Berlin, 19, (1980).

[56] H. Ali, ***"Non-linear Properties for Membranes of Rhodamine Tincture by Using Z-Scan Technique",*** International Journal of Application or Innovation in Engineering and Management, 4, 9, 2319 – 4847, (2015).

[57] K. Wasan, ***"A Study of Linear and Nonlinear Optical Properties of Composite Poly Vinyl Cloride – B by Using Z-Scan Technique"***, Journal of Babylon of pure and applied science, 23, 1, 368-377, (2015).

[58] J.R. Mannekutla, B.G. Mulimani and S.R. Inamdar, ***"Solvent Effect on Absorption and Fuorescence Spectra of Coumarin Laser Dyes: Evaluation of Ground and Excited State Dipole Moments"***, Spectrochimica Acta Part A, 69, 419-426, (2008).

[59] H. Ali, A. Al-Hamdani, and A. Al-Khafaj,*" Investigation of the Non-linear Properties of Hybrid Chlorophyll a doped TiO_2 Nano Particles "*, International Journal of Computation and Applied Sciences, 2, 2399-4509, 27-32, (2017).

[60] Z. Xiaoqiang,C. Wang, and Y. Zeng, *"Nonlinear Optical Properties of a Series of Azobenzene Liquid-Crystalline Materials",* Optik, 123, 26–29, (2012).

[61] Y.Feng ., C.Sung., S.Chen, and S.Sun, *"Relationship Between the Photoluminescence and Conductivity of Undoped ZnO Thin Films Grown with Various Oxygen Pressures"*, Appl. Surf. Sci., (2009).

[62] D.Elson, J.Siegel, K. Lauritsen, M. Wahl, and R. Erdmann, *"Fluorescence Lifetime System for Microscopy and Multiwell Plate Imaging with a Blue Picosecond Diode Laser"*, Optics Letters , 27, 16,(2002).

[63] D. Avnir , D. Levy and R. Reisfeld, *"The Nature of the Silica Cage As Reflected by Spectral Changes and Enhanced Photostability of Trapped Rhodamine 6G"*,Journal of Physics and Chemistry ,88, 5956-5959, (1984).

[64] C. Ostela, *" Spectral-luminescent and lasing properties of laser active media based on distyrylbenzene derivatives in various media"*, J. Appl. Phys ,80, 6, 3167-3173, (1996).

[65] B. A.Lenkil, "***Lasers***", Mosul University, (1984).

[66] Y .Ahmad, M. Palanichant, and P.Palanisamy ,*"Influence of Solvents Polarity on NLO Properties of Fluorone Dye"*, International Journal of Nonlinear Science, 7, 3, 290-300, (2009).

[67] H. Muncheryan, "***Principles and Practices of Laser Technology***", TAB Books Inc., USA, (1983).

[68] H. Nasser and O. Ali, "***Effect of molecular weight and illumination on optical constants of PMMA thin films***", Iranian Polymer Journal 19 (1) , 57-63, (2010).

[69] A. Maslyukov, S. Kaivola, M. Nyholm, and S. Popov, " ***Solid-state dye laser with modified poly (methyl methacrylate)-doped active elements***", Appl. Optics, 34(9), (1516-1518), (1995).

[70] W. Demtroder***,"Laser Spectroscopy"***, Springer, Verlag, (1981).

[71] G. Turrell and J. Corset, **" Raman Microscopy"**, Academic Press, London, (1996).

[72] J. Alda,***"Laser and Gaussian Beam Propagation and Transformation"***, Encyclopedia of optical engineering, Marcel Dekker (INC), PP.999- 1013,(2003).

[73] V. Millar***,"New Extended Methine Dyes for Application in Laser Technology"***, Ph.D. Thesis, Leeds University, (1993).

[74] A. Ban, A. Asim, A.Alhak, and O. Abdulazeez,*" **Study of the Nonlinear Optical Properties of New Diarylethene Perfluorocyclopentene Derivative by Using Z-Scan Technique"***, Journal of Engineering and Applied Sciences,18, 1816-949,(2018).

[75] N. Al-Huda and S.Yakop and H.A. Badran, "***Single-Beam Z-Scan Measurement of the Third-Order Nonlinearities of Ethidium Bromide"***, Journal of Engineering Research and Applications, 4, 3, 727-731, (2014).

[76] R. Ahmad Al-Saady,*" **Investigation of Some Optical Properties for Prepared Silver Nanoparticles embedded in polymer film"***, Thesis, University of Baghdad Institute of Laser for Postgraduate Studies,(2009).

[77] M. William, ***"Laser Material Processing"***, Springer, Verlag London , 3th, (2003).

[78] M. Fox, ***"Optical Properties of Solids"***, 2th ed., Oxford University Press, (2006)

[79] C. Kittel, ***"Introduction to solid state physics"***, 8th ed., Wiley, (2005).

[80] R. Manshad, ***"Studing Of Nonlinear Optical Properties for Organic Dye"***, Thesis, University of Basrah,(2013).

[81] A. Jawad , ***"Study Of the Nonlinear Optical and Optical Limiting Proerties Of New Structres Of Organic _Inorganic Materials for Photoinc Applications"***, University of Basrah,(2012).

[82] A. Faisal,***"expermentel stuied of doped polymer thin films by using Z-Scan technique"***, Thesis, University of Baghdad,(2009).

[83] R. Mohamed,***" Nonlinear Optical Properties of PMMA Composite using Z-Scan Technique"***, Thesis, University of Baghdad Institute of Laser for Postgraduate Studies, (2008).

[84] A. Abdul-Zahra ***," Investigation of nonlinear optical properties for laser dyes-doped polymer thin film"***, Thesis, University of Baghdad Institute of Laser for Postgraduate Studies,(2008).

[85] J. Loicq, Y.Renotte, J. Delplancke and Y.Lion***," Nonlinear optical measurements and crystalline characterization of CdTe nanoparticles produced by the 'electropulse' technique "***, New Journal of Physics , 6 ,No. 32 , (2004).

[86] F. Radhi, ***" Nonlinear responses and optical limiting behavior of 2-Chloro-5-nitroanisole dye under CW laser illumination"***, Journal of Kerbala University ,10, 4 ,181 – 186, (2012).

[87] E . Bahaa ***" Fundamentals of Photonics "***, Ch.19,Wiley and Sons, Inc, ISBNs:0-471-8396 5-5, (1991).

[88] Y. Andy**,** H. Lin, C. Mo, and C. Chen, ***"Nonlinear Optical Property of Azo-Dye Doped Liquid Crystals Determined by Biphotonic Z-Scan Technique"***, Optics Express, 13,26,10634-10641, (2005).

[89] S. Patil, S. Rao, and S. Dharmaprakash, ***"Crystalline Perfection, Third-Order Nonlinear Optical Properties and Optical Limiting Studies Of 3,4-Dimethoxy-4-Methoxy Chalcone Single Crystal"***, Optics and Laser technology, 81, 70-76, (2016).

[90] L. Yong, and L. Dan, "***Fabrication and Application of 1-D Micro-Cavity Film Made by Cholesteric Liquid Crystal and Reactive Mesogen"***, *Optical* Materials Express 466, 6,2,691-696, (2016).

[91] G.Saini, "***Spectroscopic studies of rhodamine 6G dispersed in polymethyl cyanoacrylate"***, Spectro chimica Acta Part A .61, 653–658, (2005).

[92] V. Roman, M. Gamernyk, S. Malynych, and O. Zaichenko, ***" Spatial Coherency of Light and Nonlinear Optical Properties of Colloidal Gold Studied by CW Z- ScanTechnique"***, Nano World Journal , 2,1,5-9, (2016).

[93] Z. Fryad and S. Patil,*"* ***Nonlinear Optical Properties and Optical Limiting Measurements of (1Z) (Dimethylamino) Phenyl] Methylene}4-Nitrobenzocarboxy Hydrazone Monohydrate under CW Laser Regime****", Photonics Journal*, 4,182-188, (2014).

[94] A. Ketamm and A. Hussain, "***The Study of the Nonlinear Optical Properties of Solutions under CW Laser Illumination***", Journal of Basrah Researches Sciences 38,4 ,73-79, (2012).

[95] A. Hussain, Y. Alaa, and F. Mohammad, *"****Study of The Linear and Nonlinear Optical Properties of Neutral Red Doped Polyvinylpyrrolidone Film****",* Journal of Basrah Researches (Sciences), 37,2 ,57-63, (2011).

[96] Z. N. Razook,*"* ***Study of Spectral Properties of Eosiny Dye Dope Polymer PMMA****",* M.Sc. thesis , AL-Mustansiriyah University, college of science , (2011).

[97] H. Muncheryan, "***Principles and Practices of Laser Technology***", TAB Books Inc., USA, (1983).

[98] A. Maslyukov, S. Kaivola, M. Nyholm, and S. Popov, " ***Solid-state dye laser with modified poly (methyl methacrylate)-doped active elements***", Appl. Optics, 34(9), (1516-1518), (1995).

[99] C.Ladoulis, and T. Gill, "***Physical chemical studies on the specific interaction of an acriflavine - phosphotungstic acid complex with double-stranded nucleic acids***", Journal of Cell Biology, 47(2), 500-511, (1970).

[100] B. Bhushan," ***Hand Book of Nanotechnology***", 3rd. Editio, ISBN: 978-3-642-02524-2,Springer-Verlag Berlin Heidelberg,(2010).

[101] C.Winter, R.Manning, S.Oliver and C.Hill, ***"Measurment of the Large Optical Nonlinearity of Nickel Dithioene Doped Polymers"***, Journal of Elsevier Science,90, 139-143, (1992).

[102] X. Li, Q. Zhai, and M. Zou, ***"Optical properties of (nanometer MCM-41)–(malachite green) composite materials"***, Applied Surface Science, *257*(3), 1134-1140, (2010).

[103] A. Jaffar. ***"Nonlinear optical characteristics of Nile blue films doped with the polymers PMMA, PVC and their blend by using z-scan technique"***, *Iraqi Journal of Science*, 1839-1848, (2017).

[104] S. Zongo, A. Kerasidou, B. Sone, A. Diallo, P. Mthunzi, K. Iliopoulos, and B. Sahraoui, ***"Nonlinear optical properties of poly (methyl methacrylate) thin films doped with Bixa Orellana dye"***, Applied Surface Science, 340, 72-77, (2015).

[105] W. Khilkhal, G. Al-Dahashand S. A.Wahid, ***"Study the effect of the aqueous media on the properties of produced copper nanoparticles colloidal by using laser ablation technique"***, *J. Eng.* Technol, 33(5), 830-837, (2015).

[106] M. Afrah and A. Ban, ***"Non-linear optical properties of organic laser dye"***, Annals of the Romanian Society for Cell Biology, 25(6), 11556-11567, (2021).

[107] S. Sreeja, S. Sreedhanya, N. Smijesh, R. Philipc and C. Muneera ,***"Organic Dye Impregnated Poly (Vinyl Alcohol) Nanocomposite as an Efficient Optical Limiter: Structure, Morphology and Photophysical Properties"***, Journal of Materials Chemistry C 1.24, 3851-3861, (2013).

[108] H. Joakim,*" **Atomic Force and Scanning Tunneling Microscopy Studies of Single Walled Carbon Nanotubes"***, Ph.D., Thesis, Karlstad's university, (2006).

[109] Shaymaa, O. Abdulazeez, and M. Talib, ***"Linear Optical Characterization of Rhodamine B and Malachite Green Organic Laser Dyes Mixture Solutions"***, Design Engineering : 2546-2557, (2021).

[110] Y. Sadoon, ***"Effect of adding Poly Methyl Methacrylate on the optical and Spectral Properties of organic lasers dyes",*** Diploma. Thesis , University of Bagdad,2004.

[111] Q. Ali, ***"Photobleaching Spectroscopic Studies and Lifetime Measurements of Fluorescent Organic Dyes"***, M.sc. Thesis, University of Baghdad, College of Science, (2013).

[112] I. Slafa and H. Majid, ***"Optical Spectral Study of Rhodamin Mixture Solution in Chloroform"***, Journal of Engineering and Technology, 31(4), (2013).

[113] B.Herman, V.Centonzen, J.Lakowicz and D.Murphy, ***"Basic Concepts in Flouresncence"***, Microscopy Resurce Center , (2012).

[114] A. Ketamm and A. Hussain, "***The Study of the Nonlinear Optical Properties of Solutions under CW Laser Illumination***", Journal of Basrah Researches Sciences 38,4 ,73-79, (2012).

[115] M. Afrah, ***"Effect of Laser Power on Non-Linear Optical Properties for Laser Dyes in Liquid and Solid Media "***, M.sc. Thesis, University of Babylon, College of Science, (2021).

[116] H. Fadhil , ***"Study the Non-Linear Optical Properties of Organic Dyes and its Optical - Medical Applications"***, Ph.D. Thesis, College of Science, University of Babylon, (2022).

[117] C.Winter, C. Manning, R. Oliver, and C. Hill, "***Measurement of the large optical nonlinearity of nickel dithiolene doped polymers***", Optics communications, 90,1-3, 139-143, (1992).

[118] O. Shaker and Shafeeq, "***Nonlinear optical properties of polymer [PMMA] thin films doped with dye lasing compounds, Rhodamine 6G and Acriflavine in chloroform solvent by using dip coating method***" , Iraqi Journal of Physics *(IJP)* 15.35, 125-132, (2000).

[119] R. Manshad, and M.Qusay "***Surface morphology and optical limiting properties of azure B doped PMMA film***", Optical Materials ,92, 22-29, (2019).

[120] S. Ola ***"Synthesis and Study of Optical Properties of Aniline Blue Dye and Its Applications"***, Ph.D. Thesis, College of Science, University of Babylon, (2021).

الخلاصة

يتضمن البحث الحالي دراسة الخصائص الطيفية والبصرية الخطية واللاخطية لصبغة الميليكات الخضراء العضوية المطعمة ببوليمر بولي ميثيل ميثاكريليت (PMMA) وجسيمات النحاس النانوية (Cu NPs)، وذلك للإستفادة منهما في مجال البصريات اللاخطية.

في هذا العمل تم تحضير محاليل من الصبغة الليزرية المذابة في مذيب الكلوروفوم بتراكيز مختلفة $M\ ^{-5}10\times$ (2, 4, 6 and 8) في درجة حرارة الغرفة ، وحضرت اغشية رقيقة. تم دراسة تأثير قدرة الليزر على الخصائص البصرية اللاخطية لجميع النماذج المحضرة. تم تشخيص صبغة الميليكات الخضراء باستخدام مطياف الاشعة تحت الحمراء FT-IR.

تم دراسة الخصائص البصرية الخطية لجميع النماذج المحضرة وكذلك طيفي الامتصاصية والنفاذية باستخدام مطياف الاشعة المرئية - الفوق البنفسجية لتراكيز مختلفة مذابة في مذيب الكلوروفورم. تبين من خلال النتائج انه كلما زاد التركيز ازدادت الامتصاصية لنفس الطول الموجي بينما يحدث العكس بالنسبة لطيف النفاذية . تم دراسة الخصائص البصرية الطيفية لجميع النماذج المحضرة باستخدام مطياف الفلورة.

تضمنت الفحوصات اللاخطية استخدام تقنية (Z-scan) لحالتي الفتح (Open-aperture) و الغلق(Closed-aperture)، للحصول على معامل الانكسار اللاخطي (n_2) ومعامل الامتصاص اللاخطي (β) على التوالي، انجزت القياسات باستخدام (CW) ليزر الحالة الصلبة ذو الطول الموجي (457 nm) عند قدرات ليزرية مختلفة mW (70,84,102) .

أظهرت النتائج زيادة في معامل الانكسار اللاخطي وانخفاض معامل الامتصاص اللاخطي مع زيادة القدرات الليزرية لجميع النماذج المحضرة. أظهرت النتائج ايضا ان زيادة التركيز تؤدي الى زيادة معاملي الانكسار اللاخطي (n_2) ، و انخفاض معامل الامتصاص اللاخطي (β) لكل نماذج الصبغة الليزرية العضوية المحضرة.

تمتلك الاغشية الرقيقة خصائص بصرية طيفية خطية ولا خطية أفضل بالمقارنة مع المحاليل. وان النماذج المحضرة من الصبغة المطعمة ببوليمر ومواد نانوية تمتلك خصائص بصرية طيفية ،خطية و لا خطية أفضل مقارنة مع النماذج المحضرة من الصبغة النقية.

اظهرت النتائج ان عتبة محدد القدرة البصرية تتناسب عكسيا مع تركيز المحلول لكل النماذج. ان الاغشية المحضرة من الصبغة الليزرية والمطعمة ببوليمر وجسيمات النحاس النانوية اعطت اعلى معاملات بصرية ، طيفية خطية ولا خطية مقارنة بالصبغة النقية. اعلى قيمة للكفاءة الكمية كانت (95%) واعلى قيمة لكل من معامل الانكسار اللاخطي (13.997×10^{-3} cm^2/mW) ومعامل الامتصاص اللاخطي (3.583 cm/mW) على التوالي.

بينت النتائج امكانية استخدام كل نماذج الصبغة المطعمة والنقية (المحاليل والاغشية) كأوساط جهد لمختلف التطبيقات الكهروبصرية كمحددات بصرية وأوساط ليزرية فعالة في الليزرات السائلة .